Integrated Planning of Drone-Based Disaster Relief: Facility Location, Inventory Prepositioning, and Fleet Operations under Uncertainty

Yuyang Ma, Karmel S. Shehadeh*, Man Yiu Tsang

[a] *Daniel J. Epstein Department of Industrial and Systems Engineering, University of Southern California*
[b] *Department of Industrial, Manufacturing, and Systems Engineering, Texas Tech University*

Abstract

We introduce a two-stage robust optimization (RO) framework for the integrated planning of a drone-based disaster relief operations problem (DDROP). Given sets of demand points, candidate locations for establishing drone-supported relief facilities, facility types, drone types, and relief items types, our first-stage problem solves the following problems simultaneously: (i) a *location problem* that determines the number of facilities to establish and where to establish them, (ii) an *inventory prepositioning problem* that decides the quantity of relief items to store at each established facility, (iii) a *fleet sizing problem* that decides the number of drones to deploy, and (iv) an *assignment problem* that assigns drones to established facility and demand points. In the second stage, the model determines a relief distribution plan and enables the reassignment of drones to demand nodes. We equip the RO model with an uncertainty set that captures the relationship between facility disruptions, demand for relief items, drone operational status, and the remaining usable fraction of pre-positioned supplies after the disaster. Additionally, we explicitly model the dependency of post-disaster drone functionality on the pre-disaster assignment decisions. To address the challenges of integer recourse, we derive a K-adaptability approximation of the RO model and develop a column-and-constraint generation (C&CG) algorithm to solve it. Moreover, we introduce several strategies to enhance the computational performance of C&CG, including an efficient warm-starting mechanism, symmetry-breaking constraints, and valid inequalities. We present extensive numerical experiments that demonstrate the computational efficiency of our framework and provide valuable insights.

Keywords: Drone; Endogenous uncertainty; Facility location; Humanitarian logistics; Last-mile logistics; Robust optimization

*Corresponding author.
Email address: kshehade@usc.edu (Karmel S. Shehadeh)

1. Introduction

The United Nations Office for the Coordination of Humanitarian Affairs (OCHA) projects that approximately 305 million people worldwide will require humanitarian assistance in 2025 (UN-OCHA, 2024). The three major drivers of the surge in humanitarian needs are conflicts, disasters, and economic factors. Disasters, such as earthquakes, often strike communities with little to no warning, resulting in devastating impacts for both residents and the infrastructure of the affected areas. In 2024 alone, 393 natural-hazard-related disasters resulted in 16,753 deaths, affected over 167 million people, and caused nearly $242 billion in damages (CRED, 2024).

The timely and efficient distribution of essential supplies (e.g., blood, food, and water) following a disaster is often critical for saving lives (Dönmez et al., 2021; Kovács and Spens, 2009). However, designing an effective prepositioning and distribution plan is a complex task. A key challenge is the unpredictability of the scale and impact of disasters, leading to significant variability in relief demand and uncertainty about the extent of damage to transportation networks. Disruptions to transportation networks—especially road infrastructure, which may be partially functional or destroyed in many disaster scenarios—are among the most significant barriers to the effective delivery of aid packages (Akbari et al., 2021). For instance, the recent Noto Peninsula earthquake, which struck Japan's Hokuriku region on January 1, 2024, caused severe disruptions to the ground transportation network due to strong tremors, landslides, and tsunamis. It led to the closure of 40 roads, damage to two national highways at 409 locations, and the shutdown of Noto Airport. These damages significantly hindered the delivery of essential supplies to the affected areas (Ishiwatari, 2024; Itatani et al., 2024). Another example is Hurricane Dorian, which severely damaged transportation infrastructure in the Bahamas in 2019, including roads, airports, and seaports, leaving affected communities without access to transportation, food, water, and medical care for days (OCHA, 2019; Ghelichi et al., 2022).

Drones, also known as unmanned aerial vehicles (UAVs), are pilotless aircraft that have the potential to improve disaster response operations. In particular, there are several potential advantages to using drones for delivering aid packages over the traditional last-mile delivery methods, such as crewed ground transportation (e.g., trucks). Drones do not require ground infrastructure for travel or delivery and thus can enable the delivery of critical relief supplies to hard-to-reach and isolated regions, as well as those with destroyed ground infrastructure (Rejeb et al., 2023; Zhu et al., 2022). Additionally, drones offer lower operational costs, partly because they consume less energy and eliminate the need for drivers or delivery personnel. They can deliver urgently needed aid quickly by flying at higher speeds, taking more direct routes than ground vehicles, and avoiding road traffic congestion (Agatz et al., 2018; Wang and Sheu, 2019).

Advances in drone technology, along with their demonstrated benefits, have facilitated their testing and adoption across various commercial and civil sectors (Hassanalian and Abdelkefi, 2017; Otto

et al., 2018), including humanitarian relief operations. For example, Zipline—a leading drone delivery company—has been deploying drones to deliver medical supplies to remote regions in Ghana, enabling timely diagnostics and treatment, and is developing drones for post-disaster delivery operations (Dean and Entsie, 2020). Another notable example is the United Nations International Children's Emergency Fund, which has incorporated drones into several humanitarian initiatives. These include the establishment of a drone corridor in Malawi for transporting lightweight medical and diagnostic supplies and delivering vaccines across Vanuatu (UNICEF, 2017, 2018). Drones also played a crucial role in delivering essential supplies to isolated areas after the 2024 Noto Peninsula earthquake (Ishiwatari, 2024).

Optimizing drone deployment and operations involves simultaneously solving several complex stochastic integer programming problems, including fleet sizing (determining the number and types of drones to deploy), facility location (determining the number and locations of drone-supported relief facilities), and drone allocation to facilities and demand nodes. Integrating these decisions often results in a large-scale optimization model that is computationally challenging to solve. However, adopting solutions from a non-integrated approach can lead to adverse outcomes, such as high operational costs, shortages, inefficient resource utilization, and delayed emergency responses. One should also consider the characteristics of drones, such as payload capacity and limited flight range, which vary across different types. Moreover, as noted in Snyder et al. (2016), disasters often cause partial or complete damage to relief facilities. The proportion of usable relief items and functional drones after a disaster depends directly on the extent of damage to the facility. Thus, it is crucial to model the relationship between disaster severity, usable fraction of relief items, and drone operability. An additional complicating factor often overlooked in the related literature is the uncertainty in drone functionality after a disaster, which depends on their pre-disaster assignment to facilities. For example, drones stored at facilities that suffer greater damage are more likely to become non-functional. Such decision-dependent uncertainty makes predicting the outcome of different drone assignment decisions challenging, further complicating the decision-making process.

Current stochastic optimization models for drone-based relief logistics assume that the probability distributions of uncertain factors are known or can be estimated. However, obtaining accurate estimates is challenging, especially since decision-makers often have limited information about the uncertain factors before a disaster. Thus, their distributions are hard to characterize and subject to ambiguity. Within the limited literature on FL for drone delivery under uncertainty, studies have overlooked the risks of facility and drone disruption and have focused on exogenous uncertainty; see Dukkanci et al. (2023b) for a survey. Furthermore, no study has yet considered the impact of disruptions on drone functionality or the possibility of reassigning drones to demand points after the disaster. Our paper addresses these fundamental gaps.

1.1. Contributions

We introduce a two-stage robust optimization (RO) approach for the integrated planning of *drone-based disaster relief operations problem* (DDROP). Our main contributions are as follows.

- We propose a new two-stage RO model for the DDROP. Specifically, given sets of demand (or gathering) points, candidate locations for establishing drone-supported relief facilities, facility types, drone types, and relief items, our first-stage formulation aims to solve the following decision-making problems simultaneously: (i) a *location problem* that determines the number of drone-supported relief facilities to establish and where to establish, (ii) an *inventory prepositioning problem* that decides the quantity of each relief item to purchase and store at each established facility, (iii) a *fleet sizing problem* that decides the number of drones to use, (iv) an *assignment problem* that assigns drones to established facility and demand points. In the second stage (a mixed-integer programming problem), after the disaster strikes, the model determines the number of relief items to distribute to each gathering point using the prepositioned drones, considering different demand and disruption scenarios. Unlike prior studies, we additionally consider drone reassignment to demand nodes after a disaster. This flexibility allows decision-makers to prioritize the most critical areas by reallocating drones in response to real-time demand and disruptions. The objective is to minimize the pre-disaster planning cost and the random post-disaster operational costs. The planning cost is the sum of costs for establishing facilities and the drone fleet, acquiring relief items, and managing aerial paths. The operational costs comprise expenses associated with drone reassignment, delivery of relief items, unmet demand, and unused inventory. We equip the RO model with a decision-dependent uncertainty set that captures the relationship between facility disruptions, the usable fraction of relief items, and the dependence of drone functionality on their assignments to facilities.
- We derive a K-adaptability approximation of the RO model. In this formulation, we select K candidate reassignment policies in the first stage, before the disaster. Once the values of uncertain factors are observed (after the disaster), the best feasible policy is implemented. We derive an equivalent, solvable reformulation of the K-adaptability problem and propose a column-and-constraint generation (C&CG) algorithm to solve it. We introduce several strategies to enhance the computational performance of C&CG, including an efficient warm-start mechanism, valid inequalities, and symmetry-breaking constraints.
- We construct a diverse set of DDROP instances and conduct extensive computational experiments, demonstrating the computational efficiency of our algorithm and the benefits of the proposed enhancement strategies. Two real-world disaster case studies further demonstrate that our integrated model yields a superior preparedness plan compared with a non-integrated model that prohibits drone reassignment (also demonstrated theoretically in Theorem 1). Importantly, the optimal DDROP plan achieves lower operational cost, mitigate demand shortages, and makes better use of relief items.

The remainder of the paper is organized as follows. In Section 2, we review the relevant literature. In Section 3, we detail our problem setting. In Section 4, we introduce our RO model. In Section 5, we derive a K-adaptability approximation of our RO model as well as methodologies to solve it. In Section 6, we present our numerical insights. We conclude the paper in Section 7.
Notation: For $(a, b) \in \mathbb{Z} \times \mathbb{Z}$, we define $[a] := \{1, 2, \ldots, a\}$ and $[a, b]_{\mathbb{Z}} := \{c \in \mathbb{Z} \,|\, a \leq c \leq b\}$. For a real number c, we define $(c)^+ := \max\{c, 0\}$. We use boldface for vectors.

2. Relevant Literature

Our work is related to the literature on facility location, inventory prepositioning, and drone-supported relief operations under uncertainty. Next, we provide a review of relevant studies.

2.1. Facility location under uncertainty

Facility location problems (FLPs) have received significant attention from the operations research and management science communities. We refer to Ahmadi-Javid et al. (2017), Daskin and Dean (2005), Daskin (2011), Eiselt and Marianov (2011), and Revelle et al. (2008) for comprehensive surveys on FL models, solution methods, and applications. We refer to Correia and Saldanha-da Gama (2019), Shehadeh and Snyder (2023), Snyder (2006) for surveys on FLP under uncertainty.

The literature on FLP under uncertainty and logistics network design is strongly interconnected. As noted in Dönmez et al. (2021), although these research streams grew independently, there has been a significant increase in research that integrates elements from both, addressing complex problems at their intersection. One specific area that has received significant attention is humanitarian logistics—the efficient and cost-effective planning, implementation, and control of the storage and distribution of relief items from supply facilities to affected populations. Dönmez et al. (2021) provides a comprehensive review of the literature on FLP under uncertainty in humanitarian contexts. Next, we review relevant work on stochastic optimization models for location and inventory prepositioning of disaster relief supplies.

Two-stage stochastic programming (SP) has been widely adopted to model and solve such problems. The first stage of these models typically involves facility location and inventory planning, while the second stage entails decisions regarding transportation and distribution. For example, Döyen et al. (2012) proposed a two-stage SP model to determine the location of regional rescue centers, the number of relief items to be stocked at each, the amount of relief item flows at each echelon, and the amount of relief item shortage. The objective is to minimize the total cost of facility location, inventory holding, transportation, and shortage. Rawls and Turnquist (2010) proposed a two-stage SP model to determine the location and quantities of various types of emergency supplies to be pre-positioned. They considered uncertainty in demand for stocked supplies and uncertainty regarding the availability of the transportation network after a disaster. The objective

is to minimize the sum of the fixed cost and the expected costs resulting from unmet demand penalties and holding costs for unused material. Noyan (2012) proposed a two-stage SP model for determining the locations of response facilities and the inventory levels of disaster relief supplies. The second-stage decision variables concern distributing supplies to demand nodes. Uncertain factors considered include demand, usable fraction of pre-positioned supplies, and arc capacity. Other SP models include Rath et al. (2016), Paul and Zhang (2019), Klibi et al. (2018), and references therein.

These pioneering models assume perfect knowledge about post-disaster conditions. However, it is unlikely that decision-makers can predict the exact post-disaster conditions (Anaya-Arenas et al., 2014; Comes et al., 2020; Sabbaghtorkan et al., 2020). Moreover, as noted in Shehadeh and Tucker (2022), historical data on past disasters are often insufficient for accurately estimating the underlying uncertainty distributions. To address this challenge, recent studies have proposed various robust optimization (RO) and distributionally robust optimization (DRO) approaches. For example, Zokaee et al. (2016) proposed an RO approach for designing humanitarian relief chains. Ni et al. (2018) proposed an RO model for location and emergency inventory prepositioning. They equipped the model with a budget uncertainty set for the demand, usable fraction of supplies, and arc capacity. Ni et al. (2018) derived a reformulation of the model and utilized off-the-shelf solvers to solve small instances and Benders' decomposition to solve larger instances. Velasquez et al. (2020) proposed a two-stage RO model for prepositioning disaster relief supplies. In the first stage, the model determines the location and number of prepositioned relief supplies. In the second stage, the model determines the number of additional items to procure and allocates them to disaster-affected areas. The objective is to minimize the total cost of prepositioning and distributing relief supplies. Shehadeh and Tucker (2022) proposed the first DRO approach for the location and inventory prepositioning of disaster relief supplies. Their model incorporates a larger set of uncertain factors than Velasquez et al. (2020) and Ni et al. (2018).

Our work is also related to the reliable FL under the risk of disruption. Classic FLP models select facility locations and customer assignments to balance the trade-off between initial setup and transportation costs. However, some of the constructed facilities may become unavailable due to disruptions caused by, for example, natural disasters. When a facility failure occurs, customers may need to be reassigned to alternative facilities, which often results in higher transportation costs. Drezner (1987) is one of the early works that addresses unreliable p-median and p-center problems. Snyder and Daskin (2005) introduced the first reliability-based formulation for the uncapacitated fixed charge FLP (UFLP) and p-median location problem. Cui et al. (2010) considered a reliable UFLP assuming each facility has site-dependent failure distribution and proposed a mixed-integer programming model and a continuum approximation model. Shen et al. (2011) proposed a two-stage SP model for the reliable UFLP and several heuristics to solve the proposed model. Li and Ouyang (2010) considered the spatial correlation among facility disruptions in the UFLP. Xie et al.

(2019) is another study that considered correlated facility disruption. They modeled this correlation via virtual supporting stations and quasi-probabilities.

Cheng et al. (2021) proposed a two-stage RO model for a fixed charge location problem under uncertain demand and facility disruptions. They solved the proposed model using the C&CG algorithm. An et al. (2014) proposed a two-stage RO approach for the reliable p-median FLP and employed the C&CG algorithm to solve their models. Cheng et al. (2018) proposed three two-stage RO models for reliable logistics network design and employed the C&CG algorithm to solve their models. We refer to Snyder et al. (2016) for a comprehensive survey on reliable FL. As detailed in the next section and highlighted in recent surveys, the limited literature on FL for drone operations under uncertainty has largely overlooked facility disruptions, and no study has examined the impact of such disruptions on drone functionality.

2.2. Drone-supported relief operations

Drone optimization problems have garnered significant attention in recent years (Shakhatreh et al., 2019; Otto et al., 2018). A rapidly growing body of literature focuses on FL decisions for drone delivery and combined drone-truck operations; see Chung et al. (2020), Dukkanci et al. (2023a), and Dukkanci et al. (2024) for comprehensive surveys. One stream of this literature that is relevant to our work focuses on optimizing drone-supported relief operations. Drones are anticipated to play a significant role in saving lives during disasters and enhancing the speed of recovery efforts (Ishiwatari, 2024). They offer valuable support in disaster management and risk mitigation through various means, including early warning systems, real-time monitoring, rapid damage assessment, and the delivery of critical relief items in the immediate aftermath. We refer to Rejeb et al. (2021) for the capabilities, performance outcomes, and barriers associated with drones in humanitarian logistics. Recent studies have investigated truck–drone delivery systems, in which a truck operates as a mobile base for drones, enabling battery recharging, replacement, and reloading, while both vehicles collaboratively perform delivery tasks (see, e.g., Murray and Chu, 2015; Murray and Raj, 2020; Dukkanci et al., 2024). In this paper, we focus solely on drone deliveries and do not consider truck routing, as in certain disaster situations, such as earthquakes, road infrastructure may be severely damaged, making drone delivery the only practical method for transporting relief supplies. Next, we review studies relevant to our work.

Ghelichi et al. (2022) studied a drone location and scheduling problem for delivering aid packages to disaster-affected areas under demand uncertainty. They proposed a chance-constrained SP model to select a set of platform locations, assuming the demand distribution is known. Ghelichi et al. (2022) proposed a decomposition approach that solves the formulations in three stages. Kim et al. (2019) proposed a chance-constrained SP model to determine the locations and capacities of drone facilities for disaster response, accounting for uncertainty in drones' flight ranges. They solved the proposed model using a heuristic algorithm based on Benders' decomposition. Wang

et al. (2023) proposed a multi-objective drone-supported queueing-location model for delivering aid packages that incorporates uncertain demands and congestion effects. The model jointly determines the locations of selected service facilities, their storage capacities for drones, and the corresponding demand assignments. They employed chance-constrained, second-order cone, fuzzy, and weighted goal-programming approaches to reformulate the model as a mixed-integer second-order conic program. Zhu et al. (2022) proposed a two-stage RO model for a short-term post-disaster humanitarian relief application, where drones must deliver first-aid products to demand points. In the first stage, the model determines the warehouse locations and allocates drones to them. In the second stage, the model assigns customers to warehouses and drones to customers. Zhu et al. (2022) employed C&CG and Benders' decomposition algorithms to solve the model.

Jin et al. (2024) proposed a two-stage DRO approach for a closely related problem to the DDROP. In the first stage, the model decides on the locations of drone-supported relief facilities, the inventory prepositioning of relief items, the assignment of drones to the opened facilities, and the allocation of drones to disaster demand sites. Decisions related to delivery quantities are made in the second stage. The objective of the first stage is to minimize the sum of facility opening costs, inventory prepositioning costs, and drone aerial path management costs. The objective of the second stage is to minimize the sum of the delivery cost, the penalty cost of unsatisfied demand, and the cost of unused inventory. Key differences between our work and Jin et al. (2024) are the following. First, Jin et al. (2024) assumed that demand is the only (exogenous) uncertain factor and did not consider facility disruptions or their impact on drone functionality and the inventory of relief items. Other studies, including those above, did not consider these elements. In contrast, our uncertainty set captures the relationship between facility disruptions, the usable fraction of relief items, and the functionality of drones. Additionally, we explicitly model the dependency of post-disaster drone functionality on the pre-disaster assignment decisions. Second, Jin et al. (2024) assumes a fixed fleet of drones and does not incorporate decisions related to determining fleet size. Third, Jin et al. (2024) model and other models for drone delivery under uncertainty assume that drone-to-customer assignments are fixed and cannot be adjusted. In contrast, our model is the first to enable the reassignment of functional drones to demand nodes in the aftermath of a disaster, which, as we later show, could significantly enhance post-disaster operations.

Fourth, our second-stage problem is a mixed-integer linear program (MILP), and the uncertainty set is decision-dependent. As a result, classical reformulation techniques and solution algorithms developed for RO problems with exogenous uncertainty and continuous recourse are not applicable. Stochastic optimization problems with decision-dependent uncertainty and/or integer recourse, such as our DDROP, are known to be computationally challenging (Zhao and Zeng, 2012; Küçükyavuz and Sen, 2017). To address this challenge, we approximate our two-stage RO problem by its corresponding K-adaptability problem. In this framework, we select K candidate second-stage reassignment policies in the first stage. After observing the uncertain parameters, the most cost-

effective feasible policy is implemented. The K-adaptability approach, originally proposed by Hanasusanto et al. (2015), has been widely adopted for solving two-stage robust optimizations with integer recourse problem (Vayanos et al., 2020; Zheng et al., 2022; Ren et al., 2024). We propose a new C&CG algorithm to solve the K-adaptability formulation and introduce several enhancement strategies tailored for the DDROP, including a warm starting mechanism, valid inequalities, and symmetry-breaking constraints.

3. Problem Settings

We start by introducing our DDROP settings. We suppose there is a set $\mathcal{I}$ of gathering points (demand nodes), a set $\mathcal{J}$ of candidate locations for establishing facilities, a set $\mathcal{L}$ of facility types, a set $\mathcal{T}$ of relief item types, and a set $\mathcal{D} = \bigcup_{r\in\mathcal{R}} \mathcal{D}_r$ of drones, where $\mathcal{R}$ is the set of drone types and $\mathcal{D}_r$ is the set of drones of type $r \in \mathcal{R}$. We use non-negative parameters c_l^{f}, c_t^{a}, and c_r^{d} to respectively represent the cost of establishing a facility of type $l \in \mathcal{L}$, the unit acquisition cost of relief item of type $t \in \mathcal{T}$, and the cost of purchasing or renting a drone of type $r \in \mathcal{R}$. Each facility of type $l \in \mathcal{L}$ can store W_l^{d} drones and W_l^{r} relief items, respectively. Each drone of type $r \in \mathcal{R}$ has a maximum payload weight limit P_r (i.e., how much it can carry) and a battery capacity B_r. We use non-negative parameter $b_{i,j,d}$ to represent the battery consumption of drone $d \in \mathcal{D}$ during a trip between a facility $j \in \mathcal{J}$ and demand point $i \in \mathcal{I}$ (Figliozzi, 2017a; Chauhan et al., 2019); we refer to Appendix A for details on how to compute this parameter. Drones of the same type are identical, i.e., they have the same purchasing or renting cost, payload capacity, battery capacity, and other operational characteristics and cost parameters.

In the pre-disaster phase (first-stage problem in our formulation), we make the following planning decisions: how many facilities to establish and where to establish them (*facility location*), the number and type of drones to deploy (*fleet sizing*), the number of relief items of each type to store in each facility (*inventory prepositioning*), the assignment of drones to established facilities and demand locations (i.e., decide the set of demand points that each drone will serve). We use the following decision variables and parameters to formulate our first-stage problem. For each $j \in \mathcal{J}$, we define a binary decision variable $y_{j,l}$ that equals 1 if a facility of type $l \in \mathcal{L}$ is open at location j, and is 0 otherwise. We define a non-negative continuous variable $w_{j,t}$ to represent the number of relief items of type $t \in \mathcal{T}$ prepositioned at facility $j \in \mathcal{J}$.

For each $d \in \mathcal{D}$, we define a binary decision variable $z_{j,d}$ that equals 1 if drone d is stored in facility $j \in \mathcal{J}$. We consider settings where each drone departs from a drone-supported facility, delivers relief items to a gathering point, and then returns to the same facility. We refer to this delivery operation as a *drone trip*. Furthermore, our model permits each drone to serve multiple demand points if its battery capacity permits. To represent this, we define a binary decision variable $x_{i,j,d}$, which equals 1 if drone $d \in \mathcal{D}$, prepositioned at facility $j \in \mathcal{J}$, is assigned to serve

Table 1: Notation

Sets	
$\mathcal{I}$	Set of gathering points (demand locations)
$\mathcal{J}$	Set of potential facility locations
$\mathcal{T}$	Set of types of relief items
$\mathcal{R}$	Set of types of drones
$\mathcal{D}_r$	Set of drones of type $r \in \mathcal{R}$
$\mathcal{D} = \bigcup_{r \in \mathcal{R}} \mathcal{D}_r$	Set of drones
$\mathcal{L}$	Set of facility types (with different inventory capacities)
Parameters	
W_l^{r}	Capacity for relief items of a facility of type $l \in \mathcal{L}$
W_l^{d}	Capacity for drones of a facility of type $l \in \mathcal{L}$
P_r	Payload limits of drones of type $r \in \mathcal{R}$
c_l^{f}	Cost of opening a facility of type $l \in \mathcal{L}$
c_t^{a}	Unit acquisition cost of the relief item of type $t \in \mathcal{T}$
c_r^{d}	Cost of purchasing a drone of type $r \in \mathcal{R}$
$c_{i,j,d}^{\mathrm{m},1}$ / $c_{i,j,d}^{\mathrm{m},2}$	Cost of managing aerial path from facility $j \in \mathcal{J}$ to gathering point $i \in \mathcal{I}$ for the delivery by drone $d \in \mathcal{D}$ in the pre-disaster/post-disaster stage
$c_{i,j,d}^{\mathrm{t}}$	Unit transportation cost between facility $j \in \mathcal{J}$ and demand location $i \in \mathcal{I}$ using the drone $d \in \mathcal{D}$
c_t^{u}	Penalty per unit of unmet demand of relief item of type $t \in \mathcal{T}$
c_t^{h}	Holding cost per unit of unused inventory of relief item of type $t \in \mathcal{T}$
$b_{i,j,d}$	Energy consumption for drone $d \in \mathcal{D}$ to deliver from facility $j \in \mathcal{J}$ to demand location $i \in \mathcal{I}$
B_r	Battery capacity of a drone of type $r \in \mathcal{R}$
$q_{i,t}$	Demand for relief item $t \in \mathcal{T}$ from gathering point $i \in I$
a_d	Binary value that equals 1 if drone $d \in \mathcal{D}$ remains functioning after the disaster, and is 0 otherwise
$e_{j,t}$	Continuous value in $[0, 1]$ indicating the fraction of relief items of type $t \in \mathcal{T}$ prepositioned in facility $j \in \mathcal{J}$ that remains usable
First-stage decision variables	
$y_{j,l}$	Binary variable that equals 1 if a facility of type $l \in \mathcal{L}$ is open at location $j \in \mathcal{J}$, and is 0 otherwise
$z_{j,d}$	Binary variable that equals 1 if drone $d \in \mathcal{D}$ is assigned to facility $j \in \mathcal{J}$, and is 0 otherwise
$x_{i,j,d}$	Binary variable that equals 1 if drone $d \in \mathcal{D}$ assigned to facility $j \in \mathcal{J}$ is assigned to serve gathering point $i \in \mathcal{I}$ in the pre-disaster stage, and is 0 otherwise
$w_{j,t}$	Number of relief items of type $t \in \mathcal{T}$ prepositioned at facility $j \in \mathcal{J}$
Second-stage decision variables	
$v_{i,j,d}$	Binary variable that equals 1 if drone $d \in \mathcal{D}$ stored in facility j is assigned to serve gathering point $i \in \mathcal{I}$ in the post-disaster stage, and is 0 otherwise
$n_{i,j,d,t}$	Number of relief items of type $t \in \mathcal{T}$ delivered by drone $d \in \mathcal{D}$ from facility $j \in \mathcal{J}$ to gathering point $i \in \mathcal{I}$
$u_{i,t}$	Unmet demand of relief items of type $t \in \mathcal{T}$ at gathering point $i \in \mathcal{I}$
$h_{j,t}$	Unused inventory in facility $j \in \mathcal{J}$ of relief item of type $t \in \mathcal{T}$

demand point $i \in \mathcal{I}$. We also consider the costs associated with managing drone operations and planning aerial paths, such as expenses related to path planning and equipment for monitoring and controlling low-altitude airspace; see Jin et al. (2024) and Haidari et al. (2016) for further discussions. We use a non-negative parameter $c_{i,j,d}^{\mathrm{m},1}$, known as the drone aerial path management cost (Jin et al., 2024), which captures the operational cost associated with pre-disaster decisions involving the use of drone $d \in \mathcal{D}$ to deliver supplies from facility $j \in \mathcal{J}$ to demand location $i \in \mathcal{I}$.

In the post-disaster phase (the second-stage problem in our formulation), we determine the number of relief items to distribute to each gathering point using prepositioned drones, considering different demand and disruption scenarios. We use the following decision variables and parameters in our second-stage formulation. For each $i \in \mathcal{I}$, $j \in \mathcal{J}$, $t \in \mathcal{T}$, and $d \in \mathcal{D}$, we define a non-negative

decision variable $n_{i,j,d,t}$ to represent the number of relief items of type t delivered by drone d to node i. The non-negative decision variable $u_{i,t}$ denotes the unmet demand for relief item $t \in \mathcal{T}$ from $i \in \mathcal{I}$, and the non-negative decision variable $h_{j,t}$ denotes the unused inventory of item $t \in \mathcal{T}$ in facility $j \in \mathcal{J}$.

We use parameter $q_{i,t}$ to represent the uncertain demand for relief item of type $t \in \mathcal{T}$ from gathering point $i \in \mathcal{I}$. As mentioned earlier, the disaster may cause significant damage to the established facilities, and hence, to the stored relief items and drones. We use a parameter $\tau_j \in [0,1]$ to represent the severity of disruption at facility $j \in \mathcal{J}$. A higher value of τ_j indicates a more severe disruption. For each $j \in \mathcal{J}$ and $t \in \mathcal{T}$, we define $e_{j,t} \in [0,1]$ to represent the fraction of relief item of type t prepositioned at a facility opened at location j that remains usable after a disaster. We define a binary random parameter a_d, which takes value 1 if drone $d \in \mathcal{D}$ remains operational after the disaster event and is 0 otherwise. Note that relief items and drones stored in the same facility are potentially subject to the same level of damage. Thus, the remaining usable fraction of relief items and the number of functional drones in facility $j \in \mathcal{J}$ depend on τ_j. We model the relationship between $\boldsymbol{a}$, $\boldsymbol{e}$, and $\boldsymbol{q}$ in Section 4.2, where we also consider the dependency of drone functionality on the assignment decisions to the established facility. For notational convenience, we let $\boldsymbol{\xi} = (\boldsymbol{a}, \boldsymbol{e}, \boldsymbol{q})$ with support $\Xi = \{\boldsymbol{\xi} \,|\, \boldsymbol{a} \in \{0,1\}^{|\mathcal{D}|}, \boldsymbol{e} \in [0,1]^{|\mathcal{J}|\times|\mathcal{T}|}, \boldsymbol{q} \in \mathbb{R}_+^{|\mathcal{I}|\times|\mathcal{T}|}\}$.

Note that if a drone is damaged, it cannot deliver aid packages to the designated gathering points, leaving those locations without timely support. In contrast to prior studies, we allow reassignment of functional drones to demand nodes after a disaster, thereby mitigating the impact of such disruptions. This flexibility allows decision-makers to prioritize the most critical areas by reallocating drones in response to real-time demand and disruptions. In particular, it could lead to better resource utilization and mitigate shortages. We formally demonstrate the benefits of drone reassignment in Section 4.3. For each $i \in \mathcal{I}$, $j \in \mathcal{J}$, and $d \in \mathcal{D}$, we define a binary variable $v_{i,j,d}$ that equals one if drone d stored in facility j is assigned to serve node i after the disaster. We use the non-negative parameter $c^{\mathrm{m},2}_{i,j,d}$ to capture the operational cost associated with reassigning drones. Its interpretation is similar to that of $c^{\mathrm{m},1}_{i,j,d}$. We assume that $c^{\mathrm{m},1}_{i,j,d} < c^{\mathrm{m},2}_{i,j,d}$ for all $i \in \mathcal{I}, j \in \mathcal{J}, d \in \mathcal{D}$ to ensure that drone assignment decisions are not delayed until uncertainty is resolved (see Álvarez-Miranda et al., 2015 for a detailed discussion). The delivery or transportation cost of relief item $t \in \mathcal{T}$ to gathering point $i \in \mathcal{I}$ from facility $j \in \mathcal{J}$ using drone $d \in \mathcal{D}$ is $c^{\mathrm{t}}_{i,j,d}$.

We use non-negative parameters c^{h}_t and c^{u}_t to represent the unit holding cost and unit penalty cost of unmet demand for relief item $t \in \mathcal{T}$, respectively. We assume that the transportation cost, acquisition cost, holding cost, and penalty for unmet demand satisfy the following conditions:

$$\max_{i\in\mathcal{I}, j\in\mathcal{J}, d\in\mathcal{D}} \{c^{\mathrm{t}}_{i,j,d}\} < c^{\mathrm{h}}_t < c^{\mathrm{u}}_t \;\text{ and } c^{\mathrm{a}}_t < c^{\mathrm{u}}_t. \tag{1}$$

The first set of inequalities ensures we always deliver relief items instead of holding them. The

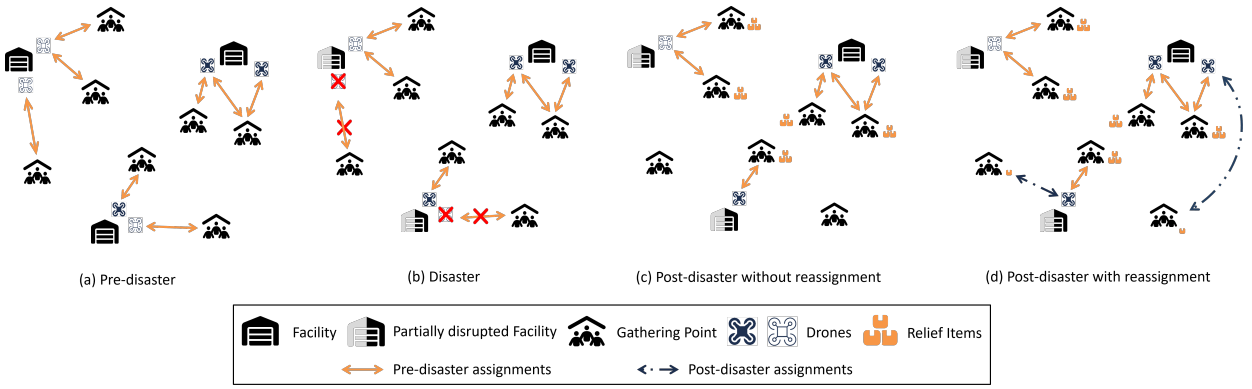

Figure 1: An illustration of the DDROP with and without drone reassignment.

second set of inequalities reflects the realistic assumption that acquiring items in advance is less costly than failing to meet demand after the disaster. The objective is to minimize the pre-disaster planning cost and the random post-disaster operational (second-stage) costs. The planning cost is the sum of the costs associated with establishing facilities, acquiring relief items, establishing the drone fleet, and managing aerial paths. The operational costs comprise expenses associated with drone reassignment, delivery of relief items, shortage, and storage of unused inventory. Table 1 summarizes the main sets, parameters, and variables used in the DDROP.

Example 1. Figure 1 provides an illustrative example of the DDROP. There are seven gathering (demand) nodes, one type of facility, and two types of drones (represented by gray and black). Subfigure (a) represents the planning decisions made before the disaster. Specifically, three facilities are established, and each has two drones. The solid orange arrows in this subfigure represent the pre-disaster assignments of drones to demand nodes. Subfigure (b) illustrates the status of facilities and drones following the disaster. Specifically, two facilities are partially disrupted, and one drone at each of these facilities is damaged (indicated by a red cross). As noted earlier, damaged drones cannot deliver aid packages to the demand nodes they were initially assigned to serve (the links between these damaged drones are removed). If drone reassignment is not allowed, as in existing models, demand nodes initially assigned to damaged drones will not receive any aid packages; see Subfigure (c) for illustration. In contrast, by allowing drone reassignment after the disaster—as proposed in our model—these demand nodes can be served by drones that remain operational; see Subfigure (d) for an illustration where dashed arrows represent drone reassignments.

4. Two-stage RO Formulation and Properties

We are now ready to introduce our two-stage RO model for the DDROP (Section 4.1). In Section 4.2, we present the uncertainty set employed in the model. In Section 4.3, we investigate the value of drone reassignment in the post-disaster phase.

4.1. The RO Formulation

Using the notation introduced in Section 3, we formulate our first-stage problem as follows.

$$\underset{\boldsymbol{y},\boldsymbol{x},\boldsymbol{w},\boldsymbol{z}}{\text{minimize}} \quad \Bigg\{ \sum_{j\in\mathcal{J}}\sum_{l\in\mathcal{L}} c^{\mathrm{f}}_l y_{j,l} + \sum_{j\in\mathcal{J}}\sum_{t\in\mathcal{T}} c^{\mathrm{a}}_t w_{j,t} + \sum_{j\in\mathcal{J}}\sum_{r\in\mathcal{R}}\sum_{d\in\mathcal{D}_r} c^{\mathrm{d}}_r z_{j,d} + \sum_{i\in\mathcal{I}}\sum_{j\in\mathcal{J}}\sum_{d\in\mathcal{D}} c^{\mathrm{m},1}_{i,j,d} x_{i,j,d} + \sup_{\boldsymbol{\xi}\in\mathcal{U}(\boldsymbol{z};\boldsymbol{\kappa},\Gamma)} Q(\boldsymbol{x},\boldsymbol{w},\boldsymbol{z},\boldsymbol{\xi}) \Bigg\} \tag{2a}$$

$$\text{subject to} \quad \sum_{l\in\mathcal{L}} y_{j,l} \le 1, \quad \forall j\in\mathcal{J}, \tag{2b}$$

$$z_{j,d} \le \sum_{l\in\mathcal{L}} y_{j,l}, \quad \forall j\in\mathcal{J},\, d\in\mathcal{D}, \tag{2c}$$

$$\sum_{j\in\mathcal{J}} z_{j,d} \le 1, \quad \forall d\in\mathcal{D}, \tag{2d}$$

$$x_{i,j,d} \le z_{j,d}, \quad \forall i\in\mathcal{I},\, j\in\mathcal{J},\, d\in\mathcal{D}, \tag{2e}$$

$$\sum_{i\in\mathcal{I}} b_{i,j,d}\, x_{i,j,d} \le B_r z_{j,d}, \quad \forall j\in\mathcal{J},\, r\in\mathcal{R},\, d\in\mathcal{D}_r, \tag{2f}$$

$$\sum_{d\in\mathcal{D}} z_{j,d} \le \sum_{l\in\mathcal{L}} W^{\mathrm{d}}_l y_{j,l}, \quad \sum_{t\in\mathcal{T}} w_{j,t} \le \sum_{l\in\mathcal{L}} W^{\mathrm{r}}_l y_{j,l}, \quad \forall j\in\mathcal{J}, \tag{2g}$$

$$y_{j,l}\in\{0,1\}, \quad \forall j\in\mathcal{J},\, l\in\mathcal{L}, \tag{2h}$$

$$z_{j,d}\in\{0,1\},\, x_{i,j,d}\in\{0,1\},\, w_{j,t}\ge 0, \quad \forall i\in\mathcal{I},\, j\in\mathcal{J},\, t\in\mathcal{T},\, d\in\mathcal{D}. \tag{2i}$$

Formulation (2) finds optimal first-stage decisions $(\boldsymbol{y},\boldsymbol{x},\boldsymbol{w},\boldsymbol{z})$ that minimize the sum of the fixed cost of establishing facilities (first term), relief items acquisition cost (second term), cost of establishing the drone fleet (third term), drones' operational cost (fourth term), and the maximum value of the random second-stage function Q (more on this below). Constraints (2b) ensure at most one facility is opened at each potential facility location. Constraints (2c) restrict drone propositioning to open facilities. Constraints (2d) ensure that each drone can be prepositioned at most one facility. Constraints (2e) link variables $\boldsymbol{x}$ and $\boldsymbol{z}$. Specifically, it ensures that drone d can be assigned to serve gathering point i from facility j (i.e., $x_{i,j,d}=1$) only if it is deployed at facility j (i.e., $z_{j,d}=1$). Constraints (2f) enforce battery range constraints on all drones. Constraints (2g) restrict the storage capacity for prepositioning drones and relief supplies.

Given feasible first-stage decisions $(\boldsymbol{x},\boldsymbol{w},\boldsymbol{z})$ and a realization of $\boldsymbol{\xi}=(\boldsymbol{a},\boldsymbol{e},\boldsymbol{q})$, the following second-stage mixed-integer linear program (MILP) computes costs related to drone reassignment, relief items delivery, unmet demand, and unused inventory:

$$Q(\boldsymbol{x},\boldsymbol{w},\boldsymbol{z},\boldsymbol{\xi}) = \underset{\boldsymbol{v},\boldsymbol{n},\boldsymbol{u},\boldsymbol{h}}{\text{minimize}} \quad \Bigg\{ \sum_{i\in\mathcal{I}}\sum_{j\in\mathcal{J}}\sum_{d\in\mathcal{D}} c^{\mathrm{m},2}_{i,j,d} v_{i,j,d} + \sum_{i\in\mathcal{I}}\sum_{j\in\mathcal{J}}\sum_{d\in\mathcal{D}}\sum_{t\in\mathcal{T}} c^{\mathrm{t}}_{i,j,d} n_{i,j,d,t} + \sum_{i\in\mathcal{I}}\sum_{t\in\mathcal{T}} c^{\mathrm{u}}_t u_{i,t}$$

$$+ \sum_{j\in\mathcal{J}} \sum_{t\in\mathcal{T}} c_t^{\mathrm{h}} h_{j,t} \Bigg\} \tag{3a}$$

$$\text{subject to} \quad \sum_{d\in\mathcal{D}} \sum_{j\in\mathcal{J}} n_{i,j,d,t} + u_{i,t} = q_{i,t}, \quad \forall i \in \mathcal{I},\, t \in \mathcal{T}, \tag{3b}$$

$$\sum_{d\in\mathcal{D}} \sum_{i\in\mathcal{I}} n_{i,j,d,t} + h_{j,t} = w_{j,t}\, e_{j,t}, \quad \forall j \in \mathcal{J},\, t \in \mathcal{T}, \tag{3c}$$

$$x_{i,j,d} + v_{i,j,d} \le z_{j,d}, \quad \forall i \in \mathcal{I},\, j \in \mathcal{J},\, d \in \mathcal{D}, \tag{3d}$$

$$\sum_{i\in\mathcal{I}} b_{i,j,d}\,(x_{i,j,d} + v_{i,j,d}) \le B_r z_{j,d}, \quad \forall j \in \mathcal{J},\, r \in \mathcal{R},\, d \in \mathcal{D}_r, \tag{3e}$$

$$\sum_{t\in\mathcal{T}} n_{i,j,d,t} \le P_r\, a_d (x_{i,j,d} + v_{i,j,d}),\ \forall i \in \mathcal{I},\, j \in \mathcal{J},\, r \in \mathcal{R},\, d \in \mathcal{D}_r, \tag{3f}$$

$$v_{i,j,d} \in \{0,1\},\, n_{i,j,d,t} \ge 0,\, u_{i,t} \ge 0,\, h_{j,t} \ge 0, \quad \forall i \in \mathcal{I},\, j \in \mathcal{J},\, d \in \mathcal{D},\, t \in \mathcal{T}. \tag{3g}$$

Constraints (3b) and (3c) compute the unmet demand and unused inventory, respectively. Constraints (3d) ensure that each gathering point may be served either by a drone that was initially assigned to it in the pre-disaster phase or reassigned to it in the post-disaster phase. Constraints (3e) respect the battery capacity of the drones. Constraints (3f) ensure that the total number of relief items a functioning drone (i.e., $a_d = 1$) delivers does not exceed its payload capacity. Finally, constraints (3g) specify the feasible range of the second-stage variables. Note that the two-stage RO model (2) has a complete recourse, i.e., for any feasible first-stage decision $(\boldsymbol{y}, \boldsymbol{w}, \boldsymbol{z}, \boldsymbol{x})$ and $\boldsymbol{\xi} \in \Xi$, the recourse problem (3) is always feasible.

Remark 1. Suppose we adopt a particular distributional belief $\mathbb{P}$ for $\boldsymbol{\xi}$. We formulate the following SP model for the DDROP by replacing $\max_{\boldsymbol{\xi}\in\mathcal{U}(\boldsymbol{z};\boldsymbol{\kappa},\Gamma)} Q(\boldsymbol{x}, \boldsymbol{w}, \boldsymbol{z}, \boldsymbol{\xi})$ with $\mathbb{E}_{\mathbb{P}}[Q(\boldsymbol{x}, \boldsymbol{w}, \boldsymbol{z}, \boldsymbol{\xi})]$,

$$\underset{\boldsymbol{y},\boldsymbol{x},\boldsymbol{w},\boldsymbol{z}}{\text{minimize}} \ \Bigg\{ \sum_{j\in\mathcal{J}} \sum_{l\in\mathcal{L}} c_l^{\mathrm{f}} y_{j,l} + \sum_{j\in\mathcal{J}} \sum_{t\in\mathcal{T}} c_t^{\mathrm{a}} w_{j,t} + \sum_{j\in\mathcal{J}} \sum_{r\in\mathcal{R}} \sum_{d\in\mathcal{D}_r} c_r^{\mathrm{d}} z_{j,d} + \sum_{i\in\mathcal{I}} \sum_{j\in\mathcal{J}} \sum_{d\in\mathcal{D}} c_{i,j,d}^{\mathrm{m},1} x_{i,j,d} + \mathbb{E}_{\mathbb{P}}[Q(\boldsymbol{x}, \boldsymbol{w}, \boldsymbol{z}, \boldsymbol{\xi})] \Bigg\}. \tag{4}$$

4.2. Uncertainty Set

Recall that we consider three key uncertain factors: the demand for relief items ($\boldsymbol{q}$), the remaining usable fraction of each relief item type ($\boldsymbol{e}$), and the operational status of each drone ($\boldsymbol{a}$). As discussed in Sections 1 and 3, the severity of the disaster influences each of these factors. In general, the greater the severity of the disaster, the higher the likelihood that relief items and drones stored at the disrupted facilities will be damaged. Hence, it is important to model the relationship between disaster severity, the usable fraction of relief items, and drone operability. Recall also that the number of drones that remain functional after a disaster depends on the extent of damage

to the facility where they are stored. Hence, uncertainty in drone functionality is influenced by the assignment decisions to established facilities ($\boldsymbol{z}$) and the corresponding disruption levels ($\boldsymbol{\tau}$). Accordingly, we construct the following uncertainty set for $\boldsymbol{\xi}$.

$$\mathcal{U}(\boldsymbol{z};\boldsymbol{\kappa},\Gamma) = \left\{ \begin{array}{l} \boldsymbol{e} \in [0,1]^{|\mathcal{J}|\times|\mathcal{T}|} \\ \boldsymbol{a} \in \{0,1\}^{|\mathcal{D}|} \\ \boldsymbol{q} \in \mathbb{R}_+^{|\mathcal{I}|\times|\mathcal{T}|} \end{array} \middle| \begin{array}{l} \left| \dfrac{1}{T}\displaystyle\sum_{t\in\mathcal{T}}(1-e_{j,t}) - \tau_j \right| \le \kappa_j^{\mathrm{f}}, \quad \forall j \in \mathcal{J} \\ \displaystyle\sum_{d\in\mathcal{D}}(1-a_d)z_{j,d} - \tau_j \sum_{d\in\mathcal{D}} z_{j,d} \le \kappa_j^{\mathrm{d}} \sum_{d\in\mathcal{D}} z_{j,d}, \quad \forall j \in \mathcal{J} \\ q_{i,t} = \bar{q}_{i,t} + \displaystyle\sum_{j\in\mathcal{J}} \tau_j\, \tilde{q}_{i,j,t}, \quad \forall i \in \mathcal{I},\, t \in \mathcal{T} \\ \displaystyle\sum_{j\in\mathcal{J}} \tau_j \le \Gamma,\, \tau_j \in [0,1], \quad \forall j \in \mathcal{J} \end{array} \right\} \tag{5}$$

The first set of constraints in (5) ensures that, for facility $j \in \mathcal{J}$, the difference between the average proportion of damaged relief items and τ_j is at most $\kappa_j^{\mathrm{f}} \in [0,1]$. The second set of constraints bounds the difference between the actual number of disrupted drones assigned to facility j, given by $\sum_{d\in\mathcal{D}}(1-a_d)z_{j,d}$, and the expected number based on the disruption level τ_j, given by $\tau_j \sum_{d\in\mathcal{D}} z_{j,d}$. The tolerance parameter $\kappa_j^{\mathrm{d}} \in [0,1]$ limits this deviation. The third set of constraints defines the uncertain demand. Parameter $\bar{q}_{i,t}$ represents the nominal demand for relief item $t \in \mathcal{T}$ at gathering point $i \in \mathcal{I}$. As in Lu and Cheng (2021), we use parameter $\tilde{q}_{i,j,t}$ to represent the maximum increase in the demand at gathering point $i \in \mathcal{I}$ caused by disruption at facility $j \in \mathcal{J}$. When $\tilde{q}_{i,j,t} = 0$, a disruption at facility j does not impact the demand at gathering point i. This typically happens when the two locations are geographically distant. In contrast, a positive value of $\tilde{q}_{i,j,t}$ indicates that a disruption at location j may cause an increase in demand at gathering point i, reflecting a proximity-based influence. The severity of this increase depends on the disruption level τ_j, where a higher value of τ_j implies more severe disruption and, thus, a potentially larger shift in demand. The fourth set of constraints imposes a bound on the total disruption level across all facilities.

4.3. The Value of Drones Reassignments

In this section, we analyze the value of enabling drone reassignment in the post-disaster phase. Note that the formulations with and without drone reassignment share the same first-stage variables and constraints. However, the second-stage problem without drone reassignment differs from the one that incorporates it (defined in (3)). The RO problem without drone reassignment is as follows.

$$\begin{aligned} \underset{\boldsymbol{y},\boldsymbol{x},\boldsymbol{w},\boldsymbol{z}}{\text{minimize}} \; \Bigg\{ & \sum_{j\in\mathcal{J}}\sum_{l\in\mathcal{L}} c_l^{\mathrm{f}} y_{j,l} + \sum_{j\in\mathcal{J}}\sum_{t\in\mathcal{T}} c_t^{\mathrm{a}} w_{j,t} + \sum_{j\in\mathcal{J}}\sum_{r\in\mathcal{R}}\sum_{d\in\mathcal{D}_r} c_r^{\mathrm{d}} z_{j,d} + \sum_{i\in\mathcal{I}}\sum_{j\in\mathcal{J}}\sum_{d\in\mathcal{D}} c_{i,j,d}^{\mathrm{m},1} x_{i,j,d} \\ & + \max_{\boldsymbol{\xi}\in\mathcal{U}(\boldsymbol{z};\boldsymbol{\kappa},\Gamma)} \widehat{Q}(\boldsymbol{x},\boldsymbol{w},\boldsymbol{z},\boldsymbol{\xi}) \,\Big|\, \text{(2b)–(2i)} \Bigg\} \end{aligned} \tag{6}$$

where for a feasible $(\boldsymbol{x}, \boldsymbol{w}, \boldsymbol{z})$ and realization of $\boldsymbol{\xi}$, the recourse problem $\widehat{Q}(\boldsymbol{x}, \boldsymbol{w}, \boldsymbol{z}, \boldsymbol{\xi})$ is defined as

$$\widehat{Q}(\boldsymbol{x}, \boldsymbol{w}, \boldsymbol{z}, \boldsymbol{\xi}) = \underset{\boldsymbol{n}, \boldsymbol{u}, \boldsymbol{h}}{\text{minimize}} \quad \left\{ \sum_{i\in\mathcal{I}} \sum_{j\in\mathcal{J}} \sum_{d\in\mathcal{D}} \sum_{t\in\mathcal{T}} c^{\mathrm{t}}_{i,j,t} n_{i,j,d,t} + \sum_{i\in\mathcal{I}} \sum_{t\in\mathcal{T}} c^{\mathrm{u}}_{t} u_{i,t} + \sum_{j\in\mathcal{J}} c^{\mathrm{h}}_{t} h_{j,t} \right\} \tag{7a}$$

$$\text{subject to} \quad \text{(3b)–(3c)}, \tag{7b}$$

$$\sum_{t\in\mathcal{T}} n_{i,j,d,t} \le P_r\, a_d\, x_{i,j,d}, \quad \forall i \in \mathcal{I},\, j \in \mathcal{J},\, r \in \mathcal{R},\, d \in \mathcal{D}_r, \tag{7c}$$

$$n_{i,j,d,t} \ge 0,\, u_{i,t} \ge 0,\, h_{j,t} \ge 0, \quad \forall i \in \mathcal{I},\, j \in \mathcal{J},\, d \in \mathcal{D},\, t \in \mathcal{T}. \tag{7d}$$

Let η and $\widehat{\eta}$ denote the optimal objective values of problems (2) and (6), respectively. We define the *value of reassignment* (VoR) as $\texttt{VoR} = \widehat{\eta} - \eta$. In Theorem 1, we derive a lower bound on VoR.

Theorem 1. Let $(\bar{\boldsymbol{y}}, \bar{\boldsymbol{w}}, \bar{\boldsymbol{z}}, \bar{\boldsymbol{x}})$ and $(\hat{\boldsymbol{y}}, \hat{\boldsymbol{w}}, \hat{\boldsymbol{z}}, \hat{\boldsymbol{x}})$ denote the optimal first-stage solutions to the RO problem (2) and its counterpart without reassignment (6), respectively. Let $\boldsymbol{\xi}^* = (\boldsymbol{a}^*, \boldsymbol{e}^*, \boldsymbol{q}^*)$ be an optimal solution to $\max_{\boldsymbol{\xi}\in\mathcal{U}(\hat{\boldsymbol{z}};\kappa,\Gamma)} Q(\hat{\boldsymbol{x}}, \hat{\boldsymbol{w}}, \hat{\boldsymbol{z}}, \boldsymbol{\xi}^*)$. Also, let $(\hat{\boldsymbol{n}}, \hat{\boldsymbol{u}}, \hat{\boldsymbol{h}})$ and $(\bar{\boldsymbol{v}}, \bar{\boldsymbol{n}}, \bar{\boldsymbol{u}}, \bar{\boldsymbol{h}})$ be optimal second-stage solutions to $\widehat{Q}(\hat{\boldsymbol{x}}, \hat{\boldsymbol{w}}, \hat{\boldsymbol{z}}, \boldsymbol{\xi}^*)$ and $Q(\hat{\boldsymbol{x}}, \hat{\boldsymbol{w}}, \hat{\boldsymbol{z}}, \boldsymbol{\xi}^*)$, respectively. Then, we have $\texttt{VoR} \ge \max\{\varphi(\bar{\boldsymbol{n}}, \hat{\boldsymbol{n}}, \bar{\boldsymbol{v}}), 0\}$, where $\varphi(\bar{\boldsymbol{n}}, \hat{\boldsymbol{n}}, \bar{\boldsymbol{v}}) = \sum_{i\in\mathcal{I}} \sum_{j\in\mathcal{J}} \sum_{d\in\mathcal{D}} \sum_{t\in\mathcal{T}} \left(c^{\mathrm{u}}_t + c^{\mathrm{h}}_t - c^{\mathrm{t}}_{i,j,d}\right)\left(\bar{n}_{i,j,d,t} - \hat{n}_{i,j,d,t}\right) - \sum_{i\in\mathcal{I}} \sum_{j\in\mathcal{J}} \sum_{d\in\mathcal{D}} c^{\mathrm{m},2}_{i,j,d} \bar{v}_{i,j,d}$.

Theorem 1 shows that allowing drone reassignment in the post-disaster phase is always beneficial. Specifically, it establishes that the VoR is non-negative and can be positive depending on the relative weights (cost parameters) of the post-disaster performance metrics. Our numerical results in Section 6.4 also demonstrate that the VoR can be substantial in practice.

5. Solution Approaches

The RO formulation (2) is computationally challenging to solve. First, the uncertainty set $\mathcal{U}(\boldsymbol{z}; \boldsymbol{\kappa}, \Gamma)$ defined in (5) is a function of decision $\boldsymbol{z}$. Second, the recourse problem defining $Q(\boldsymbol{x}, \boldsymbol{w}, \boldsymbol{z}, \boldsymbol{\xi})$ in (3) is an MILP with binary decision variables $\boldsymbol{v}$. Thus, we cannot employ traditional reformulation techniques and decomposition algorithms designed to solve RO problems with exogenous uncertainty and continuous recourse to solve problem (2). To address these challenges, we propose a K-adaptability approximation to problem (2) and a C&CG algorithm to solve it. In Section 5.1, we introduce the K-adaptability problem. We present the optimality cuts employed in our algorithm and the algorithm's steps in Sections 5.2 and 5.3, respectively. We present an efficient warm-starting mechanism for C&CG in Section 5.4. In Section 5.5 we propose valid inequalities to strengthen the master problem in C&CG, thereby improving convergence. Finally, in Section 5.6, we derive symmetry-breaking constraints that improve the model's solvability.

5.1. The K-adaptability problem

In the K-adaptability problem, we determine K drone reassignment policies $\{\boldsymbol{v}^k\}_{k\in[K]}$ before observing uncertainty $\boldsymbol{\xi} \in \Xi$. Once the value of $\boldsymbol{\xi}$ is observed, the best reassignment policy among $\{\boldsymbol{v}^k\}_{k\in[K]}$ is implemented. Mathematically, the K-adaptability problem is

$$\begin{aligned}
\underset{\substack{\boldsymbol{y},\boldsymbol{x},\boldsymbol{w},\boldsymbol{z}\\ \boldsymbol{v}^k,\, k\in[K]}}{\text{minimize}} \quad & \left\{ \sum_{j\in\mathcal{J}}\sum_{l\in\mathcal{L}} c^{\mathrm{f}}_l y_{j,l} + \sum_{j\in\mathcal{J}}\sum_{t\in\mathcal{T}} c^{\mathrm{a}}_t w_{j,t} + \sum_{j\in\mathcal{J}}\sum_{r\in\mathcal{R}}\sum_{d\in\mathcal{D}_r} c^{\mathrm{d}}_r z_{j,d} + \sum_{i\in\mathcal{I}}\sum_{j\in\mathcal{J}}\sum_{d\in\mathcal{D}} c^{\mathrm{m},1}_{i,j,d} x_{i,j,d} \right. \\
& \qquad \left. + \max_{(\boldsymbol{a},\boldsymbol{e},\boldsymbol{q})\in\mathcal{U}(\boldsymbol{z};\boldsymbol{\kappa},\Gamma)} \min_{k\in[K]} \widetilde{Q}(\boldsymbol{x},\boldsymbol{w},\boldsymbol{\xi};\boldsymbol{v}^k) \right\} && \text{(8a)} \\
\text{subject to} \quad & \text{(2b)–(2i)}, && \text{(8b)} \\
& x_{i,j,d} + v^k_{i,j,d} \le z_{j,d}, \quad \forall k\in[K],\, i\in\mathcal{I},\, j\in\mathcal{J},\, d\in\mathcal{D}, && \text{(8c)} \\
& \sum_{i\in\mathcal{I}} b_{i,j,d}\,(x_{i,j,d} + v^k_{i,j,d}) \le B_r z_{j,d}, \quad \forall k\in[K],\, j\in\mathcal{J},\, r\in\mathcal{R},\, d\in\mathcal{D}_r, && \text{(8d)}
\end{aligned}$$

where for each feasible $(\boldsymbol{x},\boldsymbol{w})$, a realization of $\boldsymbol{\xi}$, and a reassignment policy $\boldsymbol{v}^k$

$$\begin{aligned}
\widetilde{Q}(\boldsymbol{x},\boldsymbol{w},\boldsymbol{\xi};\boldsymbol{v}^k) = \underset{\boldsymbol{n},\boldsymbol{u},\boldsymbol{h}}{\text{minimize}} \quad & \left\{ \sum_{i\in\mathcal{I}}\sum_{j\in\mathcal{J}}\sum_{d\in\mathcal{D}} c^{\mathrm{m},2}_{i,j,d} v_{i,j,d} + \sum_{i\in\mathcal{I}}\sum_{j\in\mathcal{J}}\sum_{d\in\mathcal{D}}\sum_{t\in\mathcal{T}} c^{\mathrm{t}}_{i,j,d} n_{i,j,d,t} \right. \\
& \qquad \left. + \sum_{i\in\mathcal{I}}\sum_{t\in\mathcal{T}} c^{\mathrm{u}}_t u_{i,t} + \sum_{j\in\mathcal{J}}\sum_{t\in\mathcal{T}} c^{\mathrm{h}}_t h_{j,t} \right\} && \text{(9a)} \\
\text{subject to} \quad & (\boldsymbol{n},\boldsymbol{u},\boldsymbol{h}) \in \mathcal{H}(\boldsymbol{x},\boldsymbol{w},\boldsymbol{\xi};\boldsymbol{v}) := \{(\boldsymbol{u},\boldsymbol{n},\boldsymbol{h}) \ge 0 \mid \text{(3b), (3c), (3f)}\}. && \text{(9b)}
\end{aligned}$$

For each $k\in[K]$, constraints (8c) ensure that each gathering point $i\in\mathcal{I}$ could be served by a drone that was either initially assigned to it in the pre-disaster phase or assigned to it in the post-disaster phase. On the other hand, constraints (8d) ensure that the total energy consumption of a drone does not exceed its battery capacity. When K is sufficiently large (e.g., $K = |\mathcal{I}|\times|\mathcal{J}|\times|\mathcal{D}|$), problems (8) and (2) have the same optimal value (Hanasusanto et al., 2015).

The K-adaptability problem (9) has practical and computational advantages. From a practical perspective, complete flexibility in the second-stage drone reassignments may be too costly and impractical. Instead, decision-makers may prefer a limited set of reassignment plans to implement once a disaster strikes and more information about the uncertain parameters becomes available. In the context of pre-disaster planning, having a predefined set of contingency plans may be more practical than an impromptu solution to the second-stage problem. From a mathematical standpoint, by moving the binary reassignment decisions $(\boldsymbol{v})$ to the first stage, the second-stage problem reduces to the linear program (9), which results in a function that is amenable to decomposition algorithms. To this end, we use the following equivalent representation of (8) to facilitate the

subsequent discussions.

$$\underset{\substack{\boldsymbol{y},\boldsymbol{x},\boldsymbol{w},\boldsymbol{z},\eta\\ \boldsymbol{v}^k,\,k\in[K]}}{\text{minimize}} \quad \left\{ \sum_{j\in\mathcal{J}}\sum_{l\in\mathcal{L}} c^{\mathrm{f}}_l y_{j,l} + \sum_{j\in\mathcal{J}}\sum_{t\in\mathcal{T}} c^{\mathrm{a}}_t w_{j,t} + \sum_{j\in\mathcal{J}}\sum_{r\in\mathcal{R}}\sum_{d\in\mathcal{D}_r} c^{\mathrm{d}}_r z_{j,d} + \sum_{i\in\mathcal{I}}\sum_{j\in\mathcal{J}}\sum_{d\in\mathcal{D}} c^{\mathrm{m},1}_{i,j,d} x_{i,j,d} + \eta \right\} \tag{10a}$$

$$\text{subject to} \quad \text{(8b)–(8d)}, \tag{10b}$$

$$\eta \geq \max_{(\boldsymbol{a},\boldsymbol{e},\boldsymbol{q})\in\mathcal{U}(\boldsymbol{z};\boldsymbol{\kappa},\Gamma)} \min_{k\in[K]} \widetilde{Q}(\boldsymbol{x},\boldsymbol{w},\boldsymbol{\xi};\boldsymbol{v}^k). \tag{10c}$$

The general idea of our C&CG algorithm is to relax constraint (10c) and iteratively solve the resulting relaxation with a finite but increasing number of valid optimality cuts on η. Specifically, in each iteration, we construct new optimality cut(s) and add it (them) to the current relaxation to improve the approximation. Details of the optimality cuts and our C&CG are provided next.

5.2. Optimality cut

In this section, we introduce the optimality cut employed in our C&CG algorithm. We first derive the following equivalent representation of the uncertainty set $\mathcal{U}(\boldsymbol{z};\boldsymbol{\kappa},\Gamma)$.

Proposition 1. For any $\Gamma\in\mathbb{R}_+$, $\boldsymbol{\kappa}^{\mathrm{d}}\in\mathbb{R}_+^{|\mathcal{J}|}$, $\boldsymbol{\kappa}^{\mathrm{f}}\in\mathbb{R}_+^{|\mathcal{J}|}$, and feasible first-stage decisions $\boldsymbol{z}$, we have

$$\mathcal{U}(\boldsymbol{z};\boldsymbol{\kappa},\Gamma) = \bigcup_{\boldsymbol{a}\in\{0,1\}^{|\mathcal{D}|}} \Big(\{\boldsymbol{a}\} \times \mathcal{U}(\boldsymbol{z},\boldsymbol{a};\boldsymbol{\kappa},\Gamma) \Big), \tag{11}$$

where the set $\mathcal{U}(\boldsymbol{z},\boldsymbol{a};\boldsymbol{\kappa},\Gamma)$ equals to the set (5) for a fixed $\boldsymbol{a}\in\{0,1\}^{|\mathcal{D}|}$.

Proposition 1 establishes that the uncertainty set $\mathcal{U}(\boldsymbol{z};\boldsymbol{\kappa},\Gamma)$ can be equivalently represented as a finite union of sets, each corresponding to a fixed drone disruption pattern $\boldsymbol{a}\in\{0,1\}^{|\mathcal{D}|}$ and its associated uncertainty set $\mathcal{U}(\boldsymbol{z},\boldsymbol{a};\boldsymbol{\kappa},\Gamma)$, which defines the feasible values of continuous parameters $(\boldsymbol{e},\boldsymbol{q})$. It follows that we can equivalently rewrite constraint (10c) as

$$\eta \geq \max_{\boldsymbol{a}\in\{0,1\}^{|\mathcal{D}|}} \max_{(\boldsymbol{e},\boldsymbol{q})\in\mathcal{U}(\boldsymbol{z},\boldsymbol{a};\boldsymbol{\kappa},\Gamma)} \min_{k\in[K]} \widetilde{Q}(\boldsymbol{x},\boldsymbol{w},\boldsymbol{\xi};\boldsymbol{v}^k), \tag{12}$$

where the right-hand side of the inequality involves a max–max–min problem. In Proposition 2, we derive an equivalent formulation of (12) that is solvable.

Proposition 2. For any $(\boldsymbol{x},\boldsymbol{w},\boldsymbol{z})$ and $\{\boldsymbol{v}^k\}_{k=1}^K$ satisfying (8b)–(8d), constraint (12) is equivalent to

$$\eta \geq G\left(\boldsymbol{x},\boldsymbol{w},\boldsymbol{z},\boldsymbol{v};\boldsymbol{a},\boldsymbol{\mu},\boldsymbol{\pi},\boldsymbol{\lambda}\right), \quad \forall \boldsymbol{a}\in\{0,1\}^{|\mathcal{D}|},\, (\boldsymbol{\mu}^k,\boldsymbol{\pi}^k,\boldsymbol{\lambda}^k)\in\mathcal{G},\, k\in[K], \tag{13}$$

where

$$\mathcal{G} := \left\{ (\boldsymbol{\mu}, \boldsymbol{\pi}, \boldsymbol{\lambda}) \;\middle|\; \begin{array}{l} \lambda_{i,t} \le c^{\mathrm{u}}_t, \quad \forall i \in \mathcal{I},\, t \in \mathcal{T} \\ \pi_{j,t} \le c^{\mathrm{h}}_t, \quad \forall j \in \mathcal{J},\, t \in \mathcal{T} \\ \lambda_{i,t} + \pi_{j,t} - \mu_{i,j,r,d} \le c^{\mathrm{t}}_{i,j,d}, \quad \forall i \in \mathcal{I},\, j \in \mathcal{J},\, r \in \mathcal{R},\, d \in \mathcal{D}_r, t \in \mathcal{T} \\ \mu_{i,j,r,d} \ge 0, \quad \forall i \in \mathcal{I},\, j \in \mathcal{J},\, r \in \mathcal{R},\, d \in \mathcal{D}_r \end{array} \right\} \tag{14}$$

and $G(\boldsymbol{x}, \boldsymbol{w}, \boldsymbol{z}, \boldsymbol{v}; \boldsymbol{a}, \boldsymbol{\mu}, \boldsymbol{\pi}, \boldsymbol{\lambda})$ is the optimal value of the following problem:

$$\begin{aligned} \underset{\substack{\boldsymbol{\alpha}, \bar{\boldsymbol{\beta}}, \underline{\boldsymbol{\beta}}, \boldsymbol{\gamma}, \\ \boldsymbol{\psi}, \boldsymbol{\phi}, \boldsymbol{\iota}, \sigma}}{\text{minimize}} \quad & \sum_{k\in[K]} \alpha_k \left[\sum_{i\in\mathcal{I}} \sum_{j\in\mathcal{J}} \sum_{d\in\mathcal{D}} c^{\mathrm{m},2}_{i,j,d} v^k_{i,j,d} - \sum_{i\in\mathcal{I}} \sum_{j\in\mathcal{J}} \sum_{r\in\mathcal{R}} \sum_{d\in\mathcal{D}_r} P_r a_d (x_{i,j,d} + v^k_{i,j,d}) \mu^k_{i,j,d} \right] \\ & + \sum_{j\in\mathcal{J}} \underline{\beta}_j (1 + \kappa^{\mathrm{f}}_j) + \sum_{j\in\mathcal{J}} \bar{\beta}_j (\kappa^{\mathrm{f}}_j - 1) + \sum_{j\in\mathcal{J}} \gamma_j \left[\kappa^{\mathrm{d}}_j \sum_{d\in\mathcal{D}} z_{j,d} - \sum_{d\in\mathcal{D}} (1 - a_d) z_{j,d} \right] \\ & - \sum_{i\in\mathcal{I}} \sum_{t\in\mathcal{T}} \iota_{i,t} \bar{q}_{i,t} + \psi \Gamma + \sum_{j\in\mathcal{J}} \phi_j + \sum_{j\in\mathcal{J}} \sum_{t\in\mathcal{T}} \sigma_{j,t} \qquad (15a) \\ \text{subject to} \quad & \sum_{k\in[K]} \alpha_k = 1, \qquad (15b) \\ & w_{j,t} \sum_{k\in[K]} \pi^k_{j,t} \alpha_k - \frac{1}{T} \underline{\beta}_j + \frac{1}{T} \bar{\beta}_j - \sigma_{j,t} \le 0, \quad \forall j \in \mathcal{J},\, t \in \mathcal{T}, \qquad (15c) \\ & \gamma_j \sum_{d\in\mathcal{D}} z_{j,d} - \underline{\beta}_j + \bar{\beta}_j - \sum_{i\in\mathcal{I}} \sum_{t\in\mathcal{T}} \iota_{i,t} \tilde{q}_{i,j,t} - \psi - \phi_j \le 0, \quad \forall j \in \mathcal{J}, \qquad (15d) \\ & \sum_{k\in[K]} \alpha_k \lambda^k_{i,t} + \iota_{i,t} \le 0, \quad \forall i \in \mathcal{I},\, t \in \mathcal{T}, \qquad (15e) \\ & \boldsymbol{\alpha} \ge 0,\, \bar{\boldsymbol{\beta}} \ge 0,\, \underline{\boldsymbol{\beta}} \ge 0,\, \boldsymbol{\gamma} \ge 0,\, \boldsymbol{\psi} \ge 0,\, \boldsymbol{\phi} \ge 0,\, \boldsymbol{\sigma} \ge 0. \qquad (15f) \end{aligned}$$

Since G represents the optimal value of the minimization problem (15), it follows from Proposition 2 that, for any combination $\{\boldsymbol{a}\} \times \{(\boldsymbol{\mu}^k, \boldsymbol{\pi}^k, \boldsymbol{\lambda}^k)\}_{k\in[K]} \subseteq \{0,1\}^{|\mathcal{D}|} \times \mathcal{G}^K$, the optimality cuts in (13) can be equivalently reformulated as the following set of constraints:

$$\begin{aligned} \eta \ge & \sum_{k\in[K]} \alpha_k \left[\sum_{i\in\mathcal{I}} \sum_{j\in\mathcal{J}} \sum_{d\in\mathcal{D}} c^{\mathrm{m},2}_{i,j,d} v^k_{i,j,d} - \sum_{i\in\mathcal{I}} \sum_{j\in\mathcal{J}} \sum_{r\in\mathcal{R}} \sum_{d\in\mathcal{D}_r} P_r a_d (x_{i,j,d} + v^k_{i,j,d}) \mu^k_{i,j,d} \right] \\ & + \sum_{j\in\mathcal{J}} \underline{\beta}_j (1 + \kappa^{\mathrm{f}}_j) + \sum_{j\in\mathcal{J}} \bar{\beta}_j (\kappa^{\mathrm{f}}_j - 1) + \sum_{j\in\mathcal{J}} \gamma_j \left[\kappa^{\mathrm{d}}_j \sum_{d\in\mathcal{D}} z_{j,d} - \sum_{d\in\mathcal{D}} (1 - a_d) z_{j,d} \right] \\ & - \sum_{i\in\mathcal{I}} \sum_{t\in\mathcal{T}} \iota_{i,t} \bar{q}_{i,t} + \psi \Gamma + \sum_{j\in\mathcal{J}} \phi_j + \sum_{j\in\mathcal{J}} \sum_{t\in\mathcal{T}} \sigma_{j,t}, \qquad (16a) \\ (\boldsymbol{\alpha}, \bar{\boldsymbol{\beta}}, \underline{\boldsymbol{\beta}}, \boldsymbol{\gamma}, \boldsymbol{\psi}, \boldsymbol{\phi}, \boldsymbol{\sigma}) \in & \mathcal{F}_{\mathrm{D}}(\boldsymbol{w}, \boldsymbol{z}, \boldsymbol{\pi}, \boldsymbol{\lambda}) = \{(\boldsymbol{\alpha}, \bar{\boldsymbol{\beta}}, \underline{\boldsymbol{\beta}}, \boldsymbol{\gamma}, \boldsymbol{\psi}, \boldsymbol{\phi}, \boldsymbol{\sigma}) \,|\, (15b)\text{–}(15f)\}. \qquad (16b) \end{aligned}$$

Algorithm 1 The column-and-constraint generation (C&CG) algorithm

Initialization: $\epsilon \geq 0$, $LB \leftarrow 0$, $UB \leftarrow \infty$, and $\widehat{\mathcal{S}} \leftarrow \emptyset$
Step 1. Solve the Master Problem.
- Solve the master problem (19). Record the optimal value $\mathfrak{v}_{MP}$ and solution $(\bar{\boldsymbol{x}}, \bar{\boldsymbol{w}}, \bar{\boldsymbol{z}}, \bar{\eta})$.
- Update $LB \leftarrow \mathfrak{v}_{MP}$.

Step 2. Solve the Subproblem.
- Solve the subproblem (20). Record the optimal value $\mathfrak{v}_{SP}$ and solution $(\bar{\boldsymbol{a}}, \bar{\boldsymbol{\mu}}, \bar{\boldsymbol{\pi}}, \bar{\boldsymbol{\lambda}})$.
- Update $UB \leftarrow \min\{UB, (\mathfrak{v}_{MP} - \bar{\eta}) + \mathfrak{v}_{SP}\}$.

Step 3. Optimality Check.
- If $(UB - LB)/UB \leq \epsilon$, terminate and return the best solution.
- Otherwise, enlarge the scenario set $\widehat{\mathcal{S}} \leftarrow \widehat{\mathcal{S}} \cup \{(\bar{\boldsymbol{a}}, \bar{\boldsymbol{\mu}}, \bar{\boldsymbol{\pi}}, \bar{\boldsymbol{\lambda}})\}$ and return to **Step 1**.

5.3. The C&CG algorithm

We are now ready to introduce our C&CG algorithm for solving (10) (equivalently, (8)). For notational convenience, we define $\mathcal{S} = \{0,1\}^{|\mathcal{D}|} \times \mathcal{G}^K$, where each element $\boldsymbol{s} \in \mathcal{S}$ is given by $\boldsymbol{s} = (\boldsymbol{a}, \boldsymbol{\mu}, \boldsymbol{\pi}, \boldsymbol{\lambda})$. Algorithm 1 summarizes the steps of the C&CG algorithm. We initialize the algorithm with a lower bound $LB \leftarrow 0$, an upper bound $UB \leftarrow \infty$, and an empty scenario set $\widehat{\mathcal{S}} \leftarrow \emptyset$. In each iteration, starting with a subset $\widehat{\mathcal{S}} \subseteq \mathcal{S}$, in step 1, we solve the following *master problem*

$$\underset{\substack{\boldsymbol{y},\boldsymbol{x},\boldsymbol{w},\boldsymbol{z},\,\eta \\ \boldsymbol{v}^k, k\in[K]}}{\text{minimize}} \quad \left\{ \sum_{j\in\mathcal{J}} \sum_{l\in\mathcal{L}} c_l^{\mathrm{f}} y_{j,l} + \sum_{j\in\mathcal{J}} \sum_{t\in\mathcal{T}} c_t^{\mathrm{a}} w_{j,t} + \sum_{j\in\mathcal{J}} \sum_{r\in\mathcal{R}} \sum_{d\in\mathcal{D}_r} c_r^{\mathrm{d}} z_{j,d} + \sum_{i\in\mathcal{I}} \sum_{j\in\mathcal{J}} \sum_{d\in\mathcal{D}} c_{i,j,d}^{\mathrm{m},1} x_{i,j,d} + \eta \right\} \tag{17a}$$

$$\text{subject to} \quad \text{(8b)–(8d)}, \tag{17b}$$

$$\eta \geq G\left(\boldsymbol{x}, \boldsymbol{w}, \boldsymbol{v}; \boldsymbol{a}, \boldsymbol{\mu}, \boldsymbol{\pi}, \boldsymbol{\lambda}\right), \quad \forall \boldsymbol{s} \in \widehat{\mathcal{S}}, \tag{17c}$$

and record an optimal solution $(\bar{\boldsymbol{y}}, \bar{\boldsymbol{x}}, \bar{\boldsymbol{w}}, \bar{\boldsymbol{z}}, \bar{\eta}, \{\bar{\boldsymbol{v}}^k\}_{k=1}^K)$ and optimal value $\mathfrak{v}_{MP}$. Problem (17) is a relaxation of problem (10) because we consider a finite subset $\widehat{\mathcal{S}} \subseteq \mathcal{S}$. Thus, it's optimal value $\mathfrak{v}_{MP}$ provides a lower bound on that of (10), i.e., $\mathfrak{v}_{MP} \leq \mathfrak{v}^*$. Accordingly, we update $LB \leftarrow \mathfrak{v}_{MP}$. In Step 2, given a solution to the master problem, we solve the following *subproblem*

$$\max_{(\boldsymbol{a},\boldsymbol{e},\boldsymbol{q})\in\mathcal{U}(\boldsymbol{z};\boldsymbol{\kappa},\Gamma)} \max_{(\boldsymbol{\mu}^k,\boldsymbol{\pi}^k,\boldsymbol{\lambda}^k)\in\mathcal{G},\, k\in[K]} \min_{k\in[K]} \left\{ \sum_{i\in\mathcal{I}} \sum_{j\in\mathcal{J}} \sum_{d\in\mathcal{D}} c_{i,j,d}^{\mathrm{m},2} v_{i,j,d}^k + \sum_{i\in\mathcal{I}} \sum_{t\in\mathcal{T}} q_{i,t} \lambda_{i,t}^k + \sum_{j\in\mathcal{J}} \sum_{t\in\mathcal{T}} w_{j,t}\, e_{j,t} \pi_{j,t}^k \right.$$
$$\left. - \sum_{i\in\mathcal{I}} \sum_{j\in\mathcal{J}} \sum_{r\in\mathcal{R}} \sum_{d\in\mathcal{D}_r} P_r\, a_d (x_{i,j,d} + v_{i,j,d}^k) \mu_{i,j,r,d}^k \right\}, \tag{18}$$

and record an optimal solution $\bar{\boldsymbol{s}} = (\bar{\boldsymbol{a}}, \bar{\boldsymbol{\mu}}, \bar{\boldsymbol{\pi}}, \bar{\boldsymbol{\lambda}})$ and optimal value $\mathfrak{v}_{SP}$. Since the solution $(\boldsymbol{y}, \boldsymbol{x}, \boldsymbol{w}, \boldsymbol{z}, \{\boldsymbol{v}^k\}_{k=1}^K)$ is feasible to (10), its objective value $UB = (\mathfrak{v}_{MP} - \bar{\eta}) + \mathfrak{v}_{SP}$ is a valid upper bound on the optimal value $\mathfrak{v}^*$ of (10). Finally, in Step 3, we first perform an optimality check. Specifically, if the relative gap $(UB - LB)/UB$ is less than or equal to the pre-specified

tolerance $\epsilon \geq 0$, we terminate and return the best planning decisions $(\boldsymbol{y}, \boldsymbol{x}, \boldsymbol{w}, \boldsymbol{z})$ along with the best K contingency plans for drones reassignment $\{\boldsymbol{v}^k\}_{k=1}^K$. Otherwise, we enlarge the scenario set $\widehat{\mathcal{S}} \leftarrow \widehat{\mathcal{S}} \cup \{\bar{\boldsymbol{s}}\}$ and return to Step 1 to re-solve the master problem (17) with the enlarged set $\widehat{\mathcal{S}}$.

In each iteration of our C&CG, we need to solve the master problem (17) and subproblem (18), which are not directly solvable in the presented forms. We use the equivalent reformulations of (17c) ((16a)–(16b)) to derive the following equivalent and solvable reformulation of the master problem.

$$
\begin{aligned}
\text{minimize} \quad & \sum_{j\in\mathcal{J}}\sum_{l\in\mathcal{L}} c^{\mathrm{f}}_{l} y_{j,l} + \sum_{j\in\mathcal{J}}\sum_{t\in\mathcal{T}} c^{\mathrm{a}}_{t} w_{j,t} + \sum_{j\in\mathcal{J}}\sum_{r\in\mathcal{R}}\sum_{d\in\mathcal{D}_r} c^{\mathrm{d}}_{r} z_{j,d} + \sum_{i\in\mathcal{I}}\sum_{j\in\mathcal{J}}\sum_{d\in\mathcal{D}} c^{\mathrm{m},1}_{i,j,d} x_{i,j,d} + \eta && \text{(19a)}\\
\text{subject to} \quad & \eta \geq \sum_{k\in[K]} \alpha^{\mathrm{i}}_{k} \left[\sum_{i\in\mathcal{I}}\sum_{j\in\mathcal{J}}\sum_{d\in\mathcal{D}} c^{\mathrm{m},2}_{i,j,d} v^{k}_{i,j,d} - \sum_{i\in\mathcal{I}}\sum_{j\in\mathcal{J}}\sum_{r\in\mathcal{R}}\sum_{d\in\mathcal{D}_r} P_r a_d (x_{i,j,d} + v^{k}_{i,j,d}) \mu^{k}_{i,j,d} \right] \\
& \qquad + \sum_{j\in\mathcal{J}} \underline{\beta}^{\mathrm{i}}_{j} (1+\kappa^{\mathrm{f}}_{j}) + \sum_{j\in\mathcal{J}} \bar{\beta}^{\mathrm{i}}_{j} (\kappa^{\mathrm{f}}_{j} - 1) + \sum_{j\in\mathcal{J}} \gamma^{\mathrm{i}}_{j} \left[\kappa^{\mathrm{d}}_{j} \sum_{d\in\mathcal{D}} z_{j,d} - \sum_{d\in\mathcal{D}} (1-a_d) z_{j,d} \right] \\
& \qquad - \sum_{i\in\mathcal{I}}\sum_{t\in\mathcal{T}} \iota^{\mathrm{i}}_{i,t} \bar{q}_{i,t} + \psi^{\mathrm{i}} \Gamma + \sum_{j\in\mathcal{J}} \phi^{\mathrm{i}}_{j} + \sum_{j\in\mathcal{J}}\sum_{t\in\mathcal{T}} \sigma^{\mathrm{i}}_{j,t}, \quad \forall s^{\mathrm{i}} \in \widehat{\mathcal{S}},\, \mathrm{i} \in [|\widehat{\mathcal{S}}|] && \text{(19b)}\\
& (\boldsymbol{\alpha}^{\mathrm{i}}, \bar{\boldsymbol{\beta}}^{\mathrm{i}}, \underline{\boldsymbol{\beta}}^{\mathrm{i}}, \boldsymbol{\gamma}^{\mathrm{i}}, \boldsymbol{\psi}^{\mathrm{i}}, \boldsymbol{\phi}^{\mathrm{i}}, \boldsymbol{\sigma}^{\mathrm{i}}) \in \mathcal{F}_{\mathrm{D}}(\boldsymbol{w}, \boldsymbol{\xi}^{\mathrm{i}}), \quad \forall \mathrm{i} \in [|\widehat{S}|], && \text{(19c)}\\
& \text{(8b)–(8d)}. && \text{(19d)}
\end{aligned}
$$

In Theorem 2, we derive an equivalent solvable reformulation of subproblem (18).

Theorem 2. For any feasible first-stage decision $(\boldsymbol{x}, \boldsymbol{w}, \boldsymbol{z})$ and $\{\boldsymbol{v}^k\}_{k=1}^K$, solving subproblem (18) is equivalent to solving the following problem

$$
\begin{aligned}
\underset{\boldsymbol{a},\boldsymbol{e},\boldsymbol{q},\boldsymbol{\mu},\boldsymbol{\pi},\boldsymbol{\lambda}}{\text{maximize}} \quad & \eta && \text{(20a)}\\
\text{subject to} \quad & \eta \leq \sum_{i\in\mathcal{I}}\sum_{j\in\mathcal{J}}\sum_{d\in\mathcal{D}} c^{\mathrm{m},2}_{i,j,d} v^{k}_{i,j,d} + \sum_{i\in\mathcal{I}}\sum_{j\in\mathcal{J}}\sum_{d\in\mathcal{D}}\sum_{t\in\mathcal{T}} c^{\mathrm{t}}_{i,j,d} n^{k}_{i,j,d,t} \\
& \qquad\qquad + \sum_{i\in\mathcal{I}}\sum_{t\in\mathcal{T}} c^{\mathrm{u}}_{t} u^{k}_{i,t} + \sum_{j\in\mathcal{J}}\sum_{t\in\mathcal{T}} c^{\mathrm{h}}_{t} h^{k}_{j,t}, \quad \forall k \in [K], && \text{(20b)}\\
& (\boldsymbol{n}^k, \boldsymbol{u}^k, \boldsymbol{h}^k, \boldsymbol{\lambda}^k, \boldsymbol{\pi}^k, \boldsymbol{\mu}^k, \boldsymbol{\alpha}^k, \boldsymbol{\beta}^k, \boldsymbol{\theta}^k, \boldsymbol{\iota}^k) \in \mathcal{O}(\boldsymbol{v}^k, \boldsymbol{\xi}), \quad \forall k \in [K], && \text{(20c)}\\
& (\boldsymbol{a}, \boldsymbol{e}, \boldsymbol{q}) \in \mathcal{U}_L(\boldsymbol{z}; \boldsymbol{\kappa}, \Gamma), && \text{(20d)}
\end{aligned}
$$

where the set $\mathcal{U}_L(\boldsymbol{z};\boldsymbol{\kappa},\Gamma)$ is defined as

$$\mathcal{U}_L(\boldsymbol{z};\boldsymbol{\kappa},\Gamma)=\left\{\begin{array}{l|l}\boldsymbol{e}\in[0,1]^{|\mathcal{J}|\times|\mathcal{T}|} & T(\tau_j-\kappa_j^{\mathrm{f}})\leq\sum_{t\in\mathcal{T}}(1-e_{j,t})\leq T(\tau_j+\kappa_j^{\mathrm{f}}),\quad\forall j\in\mathcal{J},\\ \boldsymbol{a}\in\{0,1\}^{|\mathcal{D}|} & \sum_{d\in\mathcal{D}}(1-a_d)z_{j,d}-\tau_j\sum_{d\in\mathcal{D}}z_{j,d}\leq\kappa_j^{\mathrm{d}}\sum_{d\in\mathcal{D}}z_{j,d},\quad\forall j\in\mathcal{J},\\ \boldsymbol{q}\in\mathbb{R}_+^{|\mathcal{I}|\times|\mathcal{T}|} & q_{i,t}=\bar{q}_{i,t}+\sum_{j\in\mathcal{J}}\tau_j\,\tilde{q}_{i,j,t},\quad\forall i\in\mathcal{I},\,t\in\mathcal{T},\\ & \sum_{j\in\mathcal{J}}\tau_j\leq\Gamma,\,\tau_j\in[0,1],\quad\forall j\in\mathcal{J}\end{array}\right\}$$

and the set $\mathcal{O}(\boldsymbol{v},\boldsymbol{\xi})$ is defined as

$$\mathcal{O}(\boldsymbol{v},\boldsymbol{\xi})=\left\{\begin{array}{ll|l}&&(\boldsymbol{n},\boldsymbol{u},\boldsymbol{h})\in\mathcal{H}(\boldsymbol{x},\boldsymbol{w},\boldsymbol{\xi};\boldsymbol{v}),\,(\boldsymbol{\lambda},\boldsymbol{\pi},\boldsymbol{\mu})\in\mathcal{G}\\ &&\mu_{i,j,r,d}\leq M^{\boldsymbol{\alpha}_1}_{i,j,r,d}\,\alpha_{i,j,r,d},\quad\forall i\in\mathcal{I},\,j\in\mathcal{J},\,r\in\mathcal{R},\,d\in\mathcal{D}_r\\ &&P_r\,a_d(\bar{x}_{i,j,d}+v_{i,j,d})-\sum_{t\in\mathcal{T}}n_{i,j,d,t}\leq M^{\boldsymbol{\alpha}_2}_{i,j,r,d}(1-\alpha_{i,j,r,d}),\quad\forall i\in\mathcal{I},\,j\in\mathcal{J},\,r\in\mathcal{R},\,d\in\mathcal{D}_r\\ \boldsymbol{n},\boldsymbol{u},\boldsymbol{h},&&u_{i,t}\leq M^{\boldsymbol{\theta}_1}_{i,t}\,\theta_{i,t},\quad c^{\mathrm{u}}_t-\lambda_{i,t}\leq M^{\boldsymbol{\theta}_2}_{i,t}(1-\theta_{i,t}),\quad\forall i\in\mathcal{I},\,t\in\mathcal{T}\\ \boldsymbol{\lambda},\boldsymbol{\pi},\boldsymbol{\mu},&&h_{j,t}\leq M^{\boldsymbol{\beta}_1}_{j,t}\,\beta_{j,t},\quad c^{\mathrm{h}}_t-\pi_{j,t}\leq M^{\boldsymbol{\beta}_2}_{j,t}\,(1-\beta_{j,t}),\quad\forall j\in\mathcal{J},\,t\in\mathcal{T}\\ \boldsymbol{\alpha},\boldsymbol{\beta},\boldsymbol{\theta},\boldsymbol{\iota}&&n_{i,j,d,t}\leq M^{\boldsymbol{\iota}_1}_{i,j,d,t}\,\iota_{i,j,d,t},\quad\forall i\in\mathcal{I},\,j\in\mathcal{J},\,d\in\mathcal{D},\,t\in\mathcal{T}\\ &&c^{\mathrm{t}}_{i,j,d}-(\lambda_{i,t}+\pi_{j,t}-\mu_{i,j,r,d})\leq M^{\boldsymbol{\iota}_2}_{i,j,d,t}(1-\iota_{i,j,d,t}),\quad\forall i\in\mathcal{I},\,j\in\mathcal{J},\,d\in\mathcal{D},\,t\in\mathcal{T}\\ &&\alpha_{i,j,r,d}\in\{0,1\},\beta_{j,t}\in\{0,1\},\theta_{i,t}\in\{0,1\},\iota_{i,j,r,d,t}\in\{0,1\},\quad\forall I\in\mathcal{I},\,j\in\mathcal{J},\,r\in\mathcal{R},\,d\in\mathcal{D}_r\end{array}\right\}\tag{21}$$

Note that constraints in (21) involve several big-M parameters. In Appendix C, we derive a suitable choice of these parameters for actual implementation. Finally, in Theorem 3, we show that our C&CG algorithm converges in a finite number of iterations.

Theorem 3. Algorithm 1 terminates in a finite number of iterations.

5.4. Warm-start mechanism

Recall that we initialize Algorithm 1 with an empty scenario set $\widehat{\mathcal{S}}$ and $LB=0$. As a result, it begins with a weak lower bound, which may converge slowly. To address this challenge, we develop an efficient warm-start mechanism for Algorithm 1 that produces a non-empty scenario set $\widehat{\mathcal{S}}^{\mathrm{ws}}$ and a tighter lower bound LB^{ws}. We then initialize Algorithm 1 with $\widehat{\mathcal{S}}\leftarrow\widehat{\mathcal{S}}^{\mathrm{ws}}$ and $LB\leftarrow LB^{\mathrm{ws}}$. Algorithm 2 summarizes the steps of our warm-start mechanism. We initialize this algorithm with $LB'=0$, $\widehat{\Xi}\leftarrow\{\boldsymbol{\xi}^0=(\boldsymbol{a}^0,\boldsymbol{e}^0,\boldsymbol{q}^0):=(\mathbf{1},\mathbf{1},\bar{\boldsymbol{q}})\}$, and *warm-start level* $\mathfrak{I}<|\mathcal{J}|$. Scenario $\boldsymbol{\xi}^0$ represents the case without any disaster—hence no disruptions to pre-positioned drones or relief items—and nominal demand. It is easy to verify that $\boldsymbol{\xi}^0\in\mathcal{U}(\boldsymbol{z};\boldsymbol{\kappa},\Gamma)$ for any feasible $\boldsymbol{z}$. The warm-start level $\mathfrak{I}$ controls the number of generated scenarios, i.e., the size of the set $\widehat{\mathcal{S}}^{\mathrm{ws}}$, when $\Gamma>0$. When $\Gamma=0$, the set $\widehat{\mathcal{S}}^{\mathrm{ws}}$ consists of one scenario. In Step 1, we construct an importance ranking of candidate facility locations. We use this ranking in Step 2 to generate effective scenarios for $\boldsymbol{\xi}$. In Step 3, we generate associated dual scenarios $(\boldsymbol{\mu},\boldsymbol{\pi},\boldsymbol{\lambda})$. The details of these steps are provided below.

Ideally, to minimize the transportation costs, a demand location should be served by a drone stored at the nearest open facility. We therefore assess the importance of a candidate location for establishing a facility by considering its distance to all demand nodes. Let $\mathsf{d}_{i,j}$ denote the (Euclidean) distance between facility $j \in \mathcal{J}$ and demand location $i \in \mathcal{I}$. We define the average distance $\mathsf{d}_j^{\text{avg}} = \sum_{i\in\mathcal{I}} \mathsf{d}_{i,j}/|\mathcal{I}|$ and interpret facilities with smaller $\mathsf{d}_j^{\text{avg}}$ values as more important, since they are, on average, closer to demand locations. Disruptions to such facilities are therefore more likely to increase the objective function value. In Step 1, we compute $\{\mathsf{d}_j^{\text{avg}}\}_{j\in\mathcal{J}}$ and reorder the elements of $\mathcal{J}$ in ascending order of these values, yielding ordered set of facilities $\mathcal{J}'$, representing a ranking from the most to least important facility locations.

The key idea of Step 2 is to distribute the disruption budget across facility locations based on their importance ranking from Step 1, and then construct feasible scenarios of $\boldsymbol{\xi}$ based on the resulting budget allocations. For each $p \in [\mathfrak{I}]$, we first (Step 2.1) assign as much of the budget Γ as possible to facility $j_p \in \mathcal{J}$, i.e., the pth facility location in $\mathcal{J}'$. Mathematically, we set $\tau^p_{j_p} \leftarrow \min\{\Gamma, 1\}$. We then allocate the remaining budget (if any) to the other facilities $\ell \in [|\mathfrak{I}|] \setminus \{p\}$ in order of importance. Formally, for each $\ell \in [|\mathfrak{I}|] \setminus \{p\}$, we set $\tau^p_{j_\ell} \leftarrow \min\left\{\Gamma - \tau^p_{j_p} - \sum_{\ell'<\ell} \tau^p_{j_{\ell'}}, 1\right\}$ iteratively until the budget Γ is fully allocated. The resulting budget allocation $\boldsymbol{\tau}^p = (\tau^p_1, \ldots, \tau^p_{|\mathcal{J}|})$ should satisfy $\sum_{j\in\mathcal{J}} \tau^p_j = \Gamma$. Then, for each allocation vector $\boldsymbol{\tau}^p$, we construct a scenario $\boldsymbol{\xi}^p = (\boldsymbol{a}^p, \boldsymbol{e}^p, \boldsymbol{q}^p)$ as follows (Step 2.2): $a^p_d = 1$, $e^p_{j,t} = \max\{1 - \tau^p_j - \kappa^{\text{f}}_j, 0\}$, and $q^p_{i,t} = \bar{q}_{i,t} + \sum_{j\in\mathcal{J}} \tau^p_j \tilde{q}_{i,j,t}$ for all $i \in \mathcal{I}$, $j \in \mathcal{J}$, $t \in \mathcal{T}$, and $d \in \mathcal{D}$. We set $a^p_d = 1$ for all $d \in \mathcal{D}$ so that $\boldsymbol{\xi}^p \in \mathcal{U}(\boldsymbol{z}; \boldsymbol{\kappa}, \Gamma)$ for any feasible first-stage decision $\boldsymbol{z}$. The following example illustrates Step 2.

Example 2. Consider an instance with $\mathcal{J} = \{1, 2, 3, 4, 5\}$ (five facility locations). Suppose that Step 1 produces the following ranking of facility locations: $\mathcal{J}' = \{2, 1, 5, 3, 4\}$. Let disruption budget $\Gamma = 2.2$ units and the warm-start level be $\mathfrak{I} = 3$. For $p = 1$ (facility $j_1 = 2$), we allocate one unit of budget to facility 2, leaving 1.2 units. The next most important facility is facility 1, which receives one unit, and the remaining 0.2 units are allocated to facility 5, producing $\boldsymbol{\tau}^1 = (1, 1, 0, 0, 0.2)$. For $p = 2$ (facility $j_2 = 1$), we allocate one unit to facility 1, then one unit to facility 2, and finally 0.2 units to facility 5, producing $\boldsymbol{\tau}^2 = (1, 1, 0, 0, 0.2)$. For $p = 3$ (facility $j_3 = 5$), we allocate one unit to facility 5, then one unit to facility 2, and the remaining 0.2 units to facility 1, producing $\boldsymbol{\tau}^3 = (0.2, 1, 0, 0, 1)$. These allocation vectors are subsequently used in Step 2.2 to construct the corresponding scenarios $\boldsymbol{\xi}^1$, $\boldsymbol{\xi}^2$, and $\boldsymbol{\xi}^3$.

In Step 3, we use the generated scenarios of $\boldsymbol{\xi}$ from Step 2 to obtain $(\boldsymbol{\mu}, \boldsymbol{\pi}, \boldsymbol{\lambda}) \in \mathcal{G}$. In Step 3.1, we solve the deterministic counterpart of the K-adaptability problem (8) with scenario $\boldsymbol{\xi}^p$ (i.e., problem (8) with $\mathcal{U}(\boldsymbol{z}; \boldsymbol{\kappa}, \Gamma) = \{\boldsymbol{\xi}^p\}$) for all $p \in \{0\} \cup [\mathfrak{I}]$ and feasible $\boldsymbol{z}$. We record an optimal first-stage solution $(\boldsymbol{y}^p, \boldsymbol{w}^p, \boldsymbol{z}^p, \boldsymbol{x}^p, \boldsymbol{v}^p)$ and the optimal value $\mathfrak{v}^p$ for all $p \in \{0\} \cup [\mathfrak{I}]$. Note that $\mathfrak{v}^p$ is a lower bound on the optimal value of our K-adaptability model since $\{\boldsymbol{\xi}^p\} \subseteq \mathcal{U}(\boldsymbol{z}; \boldsymbol{\kappa}, \Gamma)$ for all $p \in \{0\} \cup [\mathfrak{I}]$. Next, in Step 3.2, for each $p \in \{0\} \cup [\mathfrak{I}]$, we solve the dual of problem (9) with

Algorithm 2 Warm-Start Mechanism for Algorithm 1

Initialization: $\widehat{\Xi} \leftarrow \{\boldsymbol{\xi}^0 = (\boldsymbol{a}^0, \boldsymbol{e}^0, \boldsymbol{q}^0) := (\mathbf{1}, \mathbf{1}, \bar{\boldsymbol{q}})\}$, Warm-start level $\mathfrak{I} \leq |\mathcal{J}|$.
If $\Gamma > 0$, proceed to **Step 1**. Otherwise, if $\Gamma = 0$, set $\mathfrak{I} = 0$ and proceed to **Step 3**.

Step 1. Facility-Location Importance Ranking

1.1 For each candidate facility location $j \in \mathcal{J}$, compute $\mathsf{d}_j^{\text{avg}} = \sum_{i \in \mathcal{I}} \mathsf{d}_{i,j}/|\mathcal{I}|$.
1.2 Sort the facility locations in ascending order based on $\mathsf{d}_j^{\text{avg}}$, and denote the resulting ordered set as $\mathcal{J}'$.

Step 2. Scenario Generation for $\boldsymbol{\xi}$

2.1 `Budget Allocation`. Let $j_p \in \mathcal{J}$ be the pth facility in $\mathcal{J}'$.
for $p \in [\mathfrak{I}]$ **do**
  Set $\tau_{j_p}^p \leftarrow \min\{\Gamma, 1\}$.
  Set $\tau_{j_\ell}^p \leftarrow \min\left\{\Gamma - \tau_{j_p}^p - \sum_{\ell' < \ell} \tau_{j_{\ell'}}^p, 1\right\}$ iteratively for $\ell \in [|\mathcal{J}|] \setminus \{p\}$.
end
2.2 `Scenario Construction`
for $p \in [\mathfrak{I}]$ **do**
  Set $a_d^p \leftarrow 1$, $e_{j,t}^p \leftarrow \max\{1 - \tau_j^p - \kappa_j^{\text{f}}, 0\}$, and $q_{i,t}^p \leftarrow \bar{q}_{i,t} + \sum_{j \in \mathcal{J}} \tau_j^p \tilde{q}_{i,j,t}$ for all $i \in \mathcal{I}$, $j \in \mathcal{J}$, $d \in \mathcal{D}$, and $t \in \mathcal{T}$.
  Update $\widehat{\Xi} \leftarrow \widehat{\Xi} \cup \{(\boldsymbol{a}^p, \boldsymbol{e}^p, \boldsymbol{q}^p)\}$.
end

Step 3. Dual-Variable Scenario Generation

for $p \in \{0\} \cup [\mathfrak{I}]$ **do**
  3.1 Solve problem (8) with $\mathcal{U}(\boldsymbol{z}; \boldsymbol{\kappa}, \Gamma) = \{\boldsymbol{\xi}^p\}$.
  Record an optimal solution $(\boldsymbol{y}^p, \boldsymbol{w}^p, \boldsymbol{z}^p, \boldsymbol{x}^p, \boldsymbol{v}^p)$ and the optimal value $\mathfrak{v}^p$.
  3.2 Solve the dual of problem (9) with $(\boldsymbol{w}, \boldsymbol{x}, \boldsymbol{v})$ fixed to $(\boldsymbol{w}^p, \boldsymbol{x}^p, \boldsymbol{v}^p)$ under scenario $\boldsymbol{\xi}^p$.
  Record an optimal solution $(\boldsymbol{\mu}^p, \boldsymbol{\pi}^p, \boldsymbol{\lambda}^p)$.
end

Step 4. $\widehat{\mathcal{S}}^{\text{ws}}$ Assembly and LB^{ws} Update

Set $\widehat{\mathcal{S}}^{\text{ws}} \leftarrow \left\{(\boldsymbol{a}^p, \boldsymbol{\mu}^p, \boldsymbol{\pi}^p, \boldsymbol{\lambda}^p)\right\}_{p=0}^{\mathfrak{I}}$ and $LB^{\text{ws}} \leftarrow \max_{p \in [0, \mathfrak{I}]_{\mathbb{Z}}} \left\{\mathfrak{v}^p\right\}$

$(\boldsymbol{w}, \boldsymbol{x}, \boldsymbol{v})$ fixed to $(\boldsymbol{w}^p, \boldsymbol{x}^p, \boldsymbol{v}^p)$ and scenario $\boldsymbol{\xi}^p$ to obtain an optimal dual solution $(\boldsymbol{\mu}^p, \boldsymbol{\pi}^p, \boldsymbol{\lambda}^p)$. Finally, in Step 4, we update $\widehat{\mathcal{S}}^{\text{ws}} \leftarrow \left\{(\boldsymbol{a}^p, \boldsymbol{\mu}^p, \boldsymbol{\pi}^p, \boldsymbol{\lambda}^p)\right\}_{p=0}^{\mathfrak{I}}$ and $LB^{\text{ws}} \leftarrow \max_{p \in \{0,1,\ldots,\mathfrak{I}\}} \left\{\mathfrak{v}^p\right\}$.

5.5. Valid Inequalities

In this section, we derive a set of valid inequalities (VIs) to improve the solvability of the master problem. We first observe that allocating zero drones to an open facility is a feasible solution, i.e., a solution with $\sum_{l \in \mathcal{L}} y_{j,l} = 1$ and $\sum_{d \in D} z_{j,d} = 0$ for some $j \in \mathcal{J}$ satisfies constraints (2b)–(2i). However, it is easy to verify that such a solution is suboptimal, as relief items can only be delivered via drones. To eliminate such solutions, we add the following VIs to the master problem (19):

$$\sum_{l \in \mathcal{L}} y_{j,l} \leq \sum_{d \in \mathcal{D}} z_{j,d}, \quad \forall j \in \mathcal{J}. \tag{22}$$

Second, note that it is feasible to store a drone in an open facility without assigning that drone

to serve any demand node. For example, consider a facility $j \in \mathcal{J}$ and drone $d \in \mathcal{D}$. A solution with $\sum_{l\in\mathcal{L}} y_{j,l} = 1$ and $z_{j,d} = 1$, $\sum_{i\in\mathcal{I}} x_{i,j,d} = 0$ and $\sum_{i\in\mathcal{I}} v^k_{i,j,d} = 0$ for all $k \in [K]$, satisfies constraints (8b)–(8d). However, such a solution is suboptimal given the cost of renting or purchasing a drone. To avoid exploring such suboptimal solutions, we add the following VIs to the master problem (19):

$$\sum_{i\in\mathcal{I}} x_{i,j,d} + v^k_{i,j,d} \geq z_{j,d}, \quad \forall k \in [K],\, j \in \mathcal{J},\, d \in \mathcal{D}. \tag{23}$$

Finally, in Proposition 3, we identify a valid lower bound inequality on variable η in master problem (19).

Proposition 3. The following bound is valid for η in the master problem (19):

$$\eta \geq \sum_{i\in\mathcal{I}} \sum_{t\in\mathcal{T}} \min_{j\in\mathcal{J},d\in\mathcal{D}} \{c^{\mathrm{t}}_{i,j,d}\} \bar{q}_{i,t}. \tag{24}$$

5.6. Symmetry-Breaking Constraints

It is well known that symmetries in IP and MILP, such as those in our first-stage problem, lead to poor performance of numerical algorithms due to the costly duplication of computational effort in exploring equivalent solutions (Ostrowski, 2010; Liberti, 2012). In this section, we discuss practical situations leading to symmetry in the DDROP and present strategies to break these symmetries.

First, recall that we consider a set of $|\mathcal{R}|$ distinct drone types, with all drones of a given type having identical characteristics. Since drones of the same type are indistinguishable in terms of functionality and cost, any permutation of such drones among facilities, i.e., reassigning identical drones to different facilities while keeping the total number of drones per facility unchanged, yields equivalent solutions. For example, consider two facilities $\{j_1, j_2\}$ and three identical drones $\{d_1, d_2, d_3\}$. The following three solutions all correspond to the same facility-opening decision $\boldsymbol{y} = [1, 1]^\top$ are equivalent (i.e., yield the same objective value) in the sense that they all assign two identical drones to j_1 and one drone to j_2

$$\boldsymbol{z}_1 = \begin{bmatrix} 1 & 1 & 0 \\ 0 & 0 & 1 \end{bmatrix} \quad \boldsymbol{z}_2 = \begin{bmatrix} 1 & 0 & 1 \\ 0 & 1 & 0 \end{bmatrix} \quad \boldsymbol{z}_3 = \begin{bmatrix} 0 & 1 & 1 \\ 1 & 0 & 0 \end{bmatrix},$$

where each matrix $\boldsymbol{z}_k$ represents the assignment of drones $\{d_1, d_2, d_3\}$ (columns) to facilities j_1 and j_2 (rows). To prevent exploring such equivalent solutions, we introduce the following constraints

$$z_{1,d} \geq z_{1,d'}, \quad \forall r \in \mathcal{R},\, (d, d') \in \mathcal{D}_r \times \mathcal{D}_r,\, d' > d, \tag{25a}$$

$$z_{j,d'} \leq \sum_{j'\in\mathcal{J}:j'\leq j} z_{j',d}, \quad \forall j \in \mathcal{J},\, r \in \mathcal{R},\, (d, d') \in \mathcal{D}_r \times \mathcal{D}_r,\, d' > d. \tag{25b}$$

Constraints (25a) impose an ordering on the assignment of identical drones to facility 1: drone d'

(with a higher index) may only be assigned to facility 1 if all drones of the same type with lower indices $d < d'$ are also assigned to that facility. Constraints (25b) generalize this to enforce a consistent ordering on the assignment of identical drones to facilities. Specifically, a higher-index drone d' can be assigned to facility j only if all drones of the same type with lower indices (i.e., $d < d'$) have been assigned to facilities with indices less than or equal to j.

Second, recall that in the first stage, we decide the initial assignment of drones to gathering points using variables $x_{i,j,d}$. When multiple drones of the same type are deployed at the same facility, any permutation of those drones in their assignment to demand nodes results in an equivalent solution. Consider, for example, a facility j, two identical drones $\{d_1, d_2\}$, and five demand nodes $\{i_1, i_2, i_3, i_4, i_5\}$. The following drones-to-customers assignments, all corresponding to the same facility-opening decision $y_j = 1$ are equivalent:

$$\mathbf{x} = \begin{bmatrix} 1 & 1 & 0 & 1 & 0 \\ 0 & 0 & 1 & 0 & 1 \end{bmatrix} \quad \mathbf{x}' = \begin{bmatrix} 0 & 0 & 1 & 0 & 1 \\ 1 & 1 & 0 & 1 & 0 \end{bmatrix}$$

These solutions are equivalent because the drones are identical and assigned to serve $i_1, \ldots, i_5$ from the same facility. The second assignment x' is obtained by swapping the two rows of x, meaning the demand nodes assigned to each drone are exchanged. To eliminate such equivalent solutions, we introduce the following constraints

$$|\mathcal{I}| \times (1 - z_{j,d}) + \sum_{i \in \mathcal{I}} x_{i,j,d} \geq \sum_{i \in \mathcal{I}} x_{i,j,d'}, \quad \forall j \in \mathcal{J},\, r \in \mathcal{R},\, (d, d') \in \mathcal{D}_r \times \mathcal{D}_r,\, d' > d. \tag{26}$$

6. Computational Results

In this section, we present extensive computational results demonstrating the efficiency of our proposed approach and provide valuable practical insights. In Section 6.1, we discuss the experimental setup. In Section 6.2, we analyze the computational performance of our approach. We demonstrate the efficiency of the warm start mechanism, valid inequalities, and symmetry-breaking constraints in Section 6.3. Finally, in Section 6.4, we use two real-world case studies to compare the performance of optimal solutions to our proposed model and the model without drone reassignments.

6.1. Experimental Setup

To investigate the computational efficiency of our approach, we construct a diverse set of DDROP instances based on parameter settings reported in Zhu et al. (2022), Shehadeh and Tucker (2022), and Jin et al. (2024). We summarize these instances in Table 2. Each instance is characterized by a unique combination of the number of demand locations ($|\mathcal{I}|$), potential locations of establishing drone-supported facility ($|\mathcal{J}|$), and available drones ($|\mathcal{D}|$). These instances capture a

Table 2: Instances for CPU time test

Inst	1	2	3	4	5	6	7	8	9	10
$\lvert\mathcal{I}\rvert$	7	10	15	20	25	30	35	40	50	55
$\lvert\mathcal{J}\rvert$	2	3	4	4	5	6	6	6	7	7
$\lvert\mathcal{D}\rvert$	4	6	8	12	12	14	16	20	26	30

wide range of potential drone service regions, with problem size varying by $|\mathcal{I}| \times |\mathcal{J}| \times |\mathcal{D}|$. They reflect the compact service regions characteristic of drone-based delivery networks. In Section 6.4, we use real-world instances to compare the performance of our integrated approach with non-integrated approaches.

For each tested instance, we generate the locations of demand points and candidate facility sites using the same approach as described in Zhu et al. (2022); Jin et al. (2024) and Shehadeh (2023). Specifically, we assume that demand points and candidate facility sites are uniformly distributed over a square region (map) of size $X \times X$. For instances 1–8, we use a 10 km $\times$ 10 km map. For instances 9–10, we use a larger region of 30 km $\times$ 30 km. We compute the distance, $\mathsf{d}_{i,j}$, between each pair $(i, j) \in \mathcal{I} \times \mathcal{J}$ in the Euclidean sense as is common in the FL literature (Basciftci et al., 2021; Daskin, 2011; Jin et al., 2024; Zhu et al., 2022).

As in Jin et al. (2024), we consider a set of $|\mathcal{L}| = 3$ facility types: small ($l = 1$), medium ($l = 2$), and large ($l = 3$). The fixed costs of establishing these facilities are $c_1^{\mathrm{f}} = 200$, $c_2^{\mathrm{f}} = 300$, and $c_3^{\mathrm{f}} = 500$, respectively. The corresponding capacities for storing relief items are $W_1^{\mathrm{r}} = 50$, $W_2^{\mathrm{r}} = 80$, and $W_3^{\mathrm{r}} = 120$. The corresponding capacities for storing drones are $W_1^{\mathrm{d}} = 10$, $W_2^{\mathrm{d}} = 15$, and $W_3^{\mathrm{d}} = 20$. For illustrative purposes, in Sections 6.2, 6.3 and 6.4, we consider one type of relief item, medical kits. Following Jin et al. (2024) and Shehadeh and Tucker (2022), we set the unit acquisition cost to $c^{\mathrm{a}} = 140$, the unit penalty cost of unmet demand to $c^{\mathrm{u}} = 4c^{\mathrm{a}}$, and unit holding cost to $c^{\mathrm{h}} = 1.2c^{\mathrm{a}}$. We assume that relief items are pre-packaged with each package containing 20 units.

We consider two types of drones. The first type ($r = 1$) is DJI FlyCart 30, a long-distance heavy-lift drone equipped with a powerful communication system and advanced control intelligence. The second type ($r = 2$) is a hypothetical (and more powerful) variant constructed based on the DJI FlyCart 30's characteristics. In particular, we assume it has a larger mass, a larger battery mass, and a larger payload capacity than the DJI FlyCart 30 drone. We set the unit purchasing or renting costs to $c_1^{\mathrm{d}} = 20.5$ and $c_2^{\mathrm{d}} = 41$, respectively. We apply the power-consumption function proposed by Figliozzi (2017a) to estimate the total energy consumed by a drone during the delivery of an item from a facility to a demand location. A summary of the drones' specifications and the Figliozzi (2017a)'s model is provided in Appendix A. The transportation cost of delivering one unit of relief items from $j \in \mathcal{J}$ to $i \in \mathcal{I}$ is $0.01 \times \mathsf{d}_{i,j}$.

We use the following parameter settings for the uncertainty set. We set $\kappa_j^{\mathrm{d}} = \kappa_j^{\mathrm{f}} = 0.01$ for

all $j \in \mathcal{J}$. For each $i \in \mathcal{I}$, We generate the nominal demands for relief item $t \in \mathcal{T}$, $\bar{q}_{i,t}$ from a uniform distribution $U[20, 40]$ as in Jin et al. (2024). We implement an inexact version of our proposed C&CG method, which allows solutions to the master problem to be inexact; see Tsang et al. (2023). Additionally, we incorporate the following two sets of constraints into the master problem (19), ensuring that each demand node is visited by drones at least once, thereby mitigating the risk of severe shortages of relief items.

$$\sum_{j \in \mathcal{J}} \sum_{d \in \mathcal{D}} x_{i,j,d} \geq 1, \quad \forall i \in \mathcal{I}. \tag{27}$$

We use Gurobi 11.0.2 as the commercial solver and conduct all experiments on a computer with an M3 Pro processor and 18 GB of memory.

6.2. Computational Performance

In this section, we analyze the computational performance of the proposed C&CG algorithm. Similar to Lu and Cheng (2021), we define the disruption budget (Γ) as a fraction of the number of facility locations ($|\mathcal{J}|$), such that $\Gamma = \alpha \cdot |\mathcal{J}|$ with $\alpha \in \{0, 0.1, 0.2, 0.3, 0.4\}$. We set $K = 2$. For each test instance and value of Γ, we generate five random instances and solve each using Algorithm 1. Table 3 reports the average solution times (Time) in seconds and the average number of iterations (Iter) required by Algorithm 1 to solve the five randomly generated instances of each instance.

We observe the following from Table 3. First, we are able to solve all the generated instances quickly in a few iterations. The average solution times range from 0.4 seconds to 1847.8 seconds (about 18 minutes), and the average number of iterations ranges from 1.6 to 11.6. Second, solution times generally increase as the instance size increases. For example, solution times of relatively small instances (Instances 1–3) range from 0.39 to 26.1 seconds, medium-sized instances (Instances 4–7) range from 5.4 to 599.9 seconds, and large instances (Instances 8–10) range from 62 to 1847.8 seconds. This is reasonable because the master problem for larger instances contains more binary variables and constraints. As argued by Klotz and Newman (2013), such an increase in the size of an MIP model often leads to longer solution times. Third, solution times are generally larger when $\Gamma > 0$. This is reasonable because when $\Gamma > 0$, the uncertainty set introduces additional worst-case scenarios that must be considered, thereby increasing the complexity of the problem and the corresponding solution time. Solution times tend to increase as Γ becomes larger, although the trend is not strictly monotonic across all instances. For example, in Instance 5, solution times rise from 8.32 seconds ($\Gamma = 0$) to 102.18 seconds ($\Gamma = 0.4|\mathcal{J}|$). In contrast, in Instance 2, the solution time reaches 147.85 seconds at $\Gamma = 0.1|\mathcal{J}|$ but then decreases to 26.11 seconds when $\Gamma = 0.2|\mathcal{J}|$.

These results demonstrate the computational efficiency of our proposed algorithm for solving practical instances of the DDROP. As noted in Dukkanci et al. (2023a), solving FL problems for drone delivery with a cost-based objective is generally difficult, and existing studies often consider

Table 3: Computational time (in seconds) and number of iterations

	Inst 1		Inst 2		Inst 3		Inst 4		Inst 5	
Γ	Time	Iter	Time	Iter	Time	Iter	Time	Iter	Time	Iter
0	0.5	4.8	11.8	11.2	8.3	7.2	5.4	4.4	8.3	3.8
$0.1\|\mathcal{J}\|$	0.4	2.8	147.9	11.6	9.3	4.4	17.4	3.6	34.5	3.0
$0.2\|\mathcal{J}\|$	0.5	3.2	26.1	10.8	6.5	2.0	19.6	1.8	55.4	1.8
$0.3\|\mathcal{J}\|$	0.6	4.2	3.3	3.8	9.1	2.6	22.4	1.6	85.6	3.2
$0.4\|\mathcal{J}\|$	0.5	4.8	6.0	6.4	8.3	2.6	23.3	1.6	102.2	3.4
	Inst 6		Inst 7		Inst 8		Inst 9		Inst 10	
Γ	Time	Iter	Time	Iter	Time	Iter	Time	Iter	Time	Iter
0	9.7	2.8	17.0	3.4	64.5	5.4	62.0	3.6	170.2	4.8
$0.1\|\mathcal{J}\|$	182.8	6.0	224.2	3.6	370.2	5.2	655.5	2.6	1087.9	3.0
$0.2\|\mathcal{J}\|$	182.9	3.6	600.0	4.2	1253.8	6.8	1051.6	4.0	701.4	1.8
$0.3\|\mathcal{J}\|$	226.8	4.8	324.4	4.2	663.6	4.8	1714.9	3.6	1847.8	3.0
$0.4\|\mathcal{J}\|$	174.9	3.8	245.8	5.8	1044.7	7.4	1030.6	2.8	849.1	1.8

Table 4: Comparisons of the solution time (in seconds) and the number of iterations of Algorithm 1 with all enhancement strategies, w/o WS, w/o VIs, w/o SBCs, and without any enhancements (Plain).

	All Equipped		w/o WS		w/o VIs		w/o SBCs		Plain	
Γ	Time	Iter	Time	Iter	Time	Iter	Time	Iter	Time	Iter
$0.1\|\mathcal{J}\|$	223.85	3.80	2497.41	25.33	1252.23	9.40	163.43	1.60	24%	27.33
$0.2\|\mathcal{J}\|$	630.33	4.40	—	—	1266.77	6.00	737.03	3.80	65%	44.00
$0.3\|\mathcal{J}\|$	485.59	3.40	—	—	3321.35	11.60	706.47	4.00	99%	—
$0.4\|\mathcal{J}\|$	534.91	4.00	5940.43	21.00	2266.31	9.40	854.22	5.60	99%	—

smaller instances than our test instances, typically with a few nodes, one type of drone, and without considering fleet sizing, facility and drone disruption, decision-dependent uncertainty, or drone reassignment. Our model and test instances explicitly incorporate these additional complexities.

6.3. Efficiency of the warm start mechanism, VIs, and SBCs

In this section, we analyze the efficiency of the proposed warm-start (WS) mechanism, VIs, and symmetry-breaking constraints (SBCs). For illustrative purposes, we use Instance 8 in this experiment. We separately solve this instance with and without (w/o) the WS, VIs, and SBCs. We refer to Algorithm 1 without these enhancements as the *Plain* algorithm. Additionally, we separately solve Instance 8 using Algorithm 1 w/o WS, w/o VIs, and w/o SBCs. Table 4 reports the average solution time and number of iterations, computed across five randomly generated instances.

First, we observe that the Plain algorithm (i.e., Algorithm 1 without any enhancements) takes substantially longer times and requires more iterations to converge. In fact, the Plain algorithm fails to converge within two hours, terminating with a large relative optimality gap (i.e., the difference between the upper and lower bounds on the objective value) for most instances. For the instance with $\Gamma = 0.1|\mathcal{J}|$, $0.2|\mathcal{J}|$, $0.3|\mathcal{J}|$, and $0.4|\mathcal{J}|$, the associated termination gaps are 24%, 65%, 99%, and 99%, respectively. In contrast, when all enhancements are incorporated, the algorithm solves all instances relatively quickly, with average solution times ranging from 223.85 seconds (3.8 iterations) to 630.33 seconds (4.4 iterations).

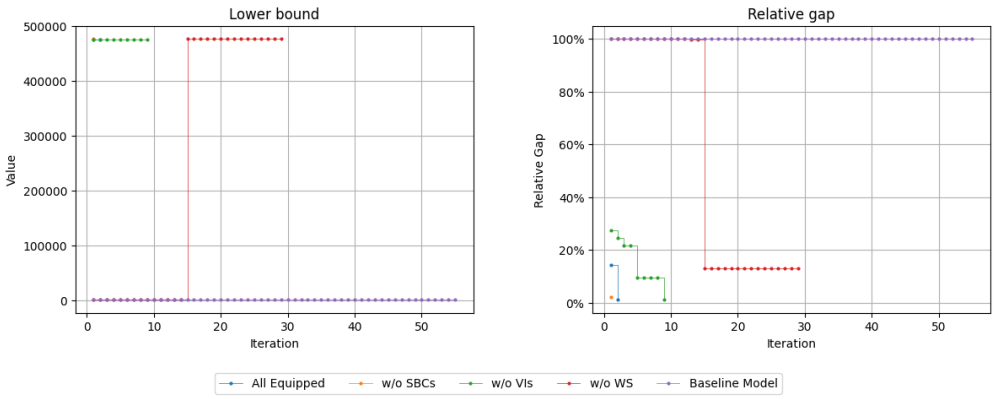

Figure 2: Comparisons of lower bound and gap values

Second, among the proposed strategies, the WS mechanism is the most effective. Without WS, solution times increase drastically and often exceed the two-hour limit. For example, when $\Gamma = 0.2|\mathcal{J}|$ and $\Gamma = 0.3|\mathcal{J}|$, the algorithm without WS fails to converge within two hours, whereas with WS the same instances are solved in 630.33 seconds (4.40 iterations) and 485.59 seconds (3.40 iterations), respectively. In contrast, the effects of removing VIs or SBCs are less severe, though still noticeable. In particular, the algorithm takes a longer time to converge without either VIs or SBCs. For example, when $\Gamma = 0.2|\mathcal{J}|$, the solution time increases from 630.33 seconds with all enhancements to 1266.77 seconds without VIs and 737.03 seconds without SBCs.

These results demonstrate that incorporating WS provides a stronger initial lower bound, thereby reducing the initial relative gap and accelerating convergence. As shown in Figure 2, the algorithm with all enhancements starts with a higher lower bound and converges within only a few iterations. In contrast, without WS, the initial lower bound is weak, leading to a larger gap and slower convergence. Although combining WS with either VIs or SBCs improves convergence—particularly by starting with a smaller gap—the algorithm converges more slowly than when all enhancements are included. This indicates that including all three strategies is most effective, with the warm-start mechanism playing a dominant role.

6.4. The Value of Incorporating Drones Reassignment

In this section, we demonstrate the benefits of allowing drone reassignment in the post-disaster phase, a novel feature of our DDROP model. We consider two real-world case studies. The first is based on the 2013 earthquake in the Lushan region of China (Section 6.4.1). The second is based on an earthquake that struck the Great Wenchuan in 2008 (Section 6.4.2).

For each case study, we investigate the performance of the proposed DDROP model and a no-reassignment variant (NRM), in which drone reassignment is not allowed in the second stage. Specifically, we solve each using the DDROP and NRM models and record the optimal planning (first-stage) decisions $(\boldsymbol{x}, \boldsymbol{w}, \boldsymbol{z}, \boldsymbol{v})$. (Note that $\boldsymbol{v} = 0$ in the optimal solution to the NRM Model

because it does not allow drone reassignment.) We then solve the recourse problem $\widetilde{Q}$ with fixed first-stage decisions under N' scenarios of $\boldsymbol{\xi} = (\boldsymbol{\tau}, \boldsymbol{a}, \boldsymbol{e}, \boldsymbol{q})$. We generate the N' simulation data as follows. We consider two realistic settings to generate facility-disruption levels. In the first, we consider a uniform budget split, where the disruption budget is distributed evenly across facilities, i.e., $\tau_j = \Gamma/|\mathcal{J}|$ for all $j \in \mathcal{J}$. In the second setting, we construct $\boldsymbol{\tau}$ by following the sample procedure described in Steps 1 and 2 of the warm-start mechanism. After generating $\boldsymbol{\tau}$, we compute the corresponding values of $(\boldsymbol{e}, \boldsymbol{q})$ as $e_{j,t} = \max\{1 - \tau_j - \kappa^{\mathrm{f}}_j, 0\}$ and $q_{i,t} = \bar{q}_{i,t} + \sum_{j\in\mathcal{J}} \tau_j \tilde{q}_{i,j,t}$ for all $i \in \mathcal{I}$, $j \in \mathcal{J}$, $t \in \mathcal{T}$, and $d \in \mathcal{D}$.

Recall that in our DDROP model (and similarly in the NRM model), the drone functionality indicator a_d depends on the initial assignment decisions $\boldsymbol{z}$ and facility disruption $\boldsymbol{\tau}$. Because DDROP and NRM produce different assignments, generating $\boldsymbol{\tau}$ conditional on those assignments would yield different simulation datasets. To ensure a fair comparison under a common set of scenarios, we introduce parameter $\tilde{a}_{j,d} \in \{0, 1\}$ to represent the functionality of drone if assigned to facility $j \in \mathcal{J}$, where $\tilde{a}_{j,d} = 0$ implies that a drone is disrupted. We generate $\tilde{a}_{j,d}$ from a Bernoulli distribution, $\tilde{a}_{j,d} \sim \text{Bernoulli}(1 - \tau_j)$, for all $j \in \mathcal{J}$ and $d \in \mathcal{D}$. We set N' to 300 and repeat the simulation procedure five times, each time generating new simulation data as described above. For illustrative purposes, we consider one type of facility, one type of drone (the pseudo-drone defined in Section 6.1), and one type of relief item (medical kits). We set the facility's inventory level to 200 and opening cost to 650. We assume the drone's range permits delivery between any origin–destination pair. This assumption is consistent with recent advances in long-range drone technology, such as Dronamics' Black Swan aircraft, which can cover substantial distances for logistics operations (Weitering, 2023). All other parameters are as described in Section 6.1.

6.4.1. Lushan Earthquake

The Lushan Region in Sichuan Province, China, is prone to earthquakes. On April 20, 2013, it was the epicenter of a major event that affected about 2.2 million people across multiple counties and cities, causing 176 deaths and over 12,000 injuries, with direct economic losses estimated at 85.17 billion CNY (Duan et al., 2022; Nunez-Ollero, 2024). The earthquake also triggered landslides and rockfalls, blocking numerous mountain roads, impeding rescue access and ground transportation. This case highlights the importance of employing drones into last-mile humanitarian logistics. Following Xu et al. (2016), who first introduced this case study, we construct an instance with 15 demand locations ($|\mathcal{I}| = 15$) and 3 candidate facility locations ($|\mathcal{J}| = 3$) within the disaster area; see Figure 3. We set $\Gamma = 0.2|\mathcal{J}|$ and generate the demand from a uniform distribution on $[20, 40]$.

We solve this instance with the DDROP and NRM models. Both solutions establish 3 facilities, deploy 8 drones, and preposition the same quantity of relief items at the open facilities. For each drone, Table 5 reports (i) the facility where it is stored and (ii) its initial assignments to demand nodes. For DDROP, we also report the post-disaster reassignment policies. Under policy $k \in \{1, 2\}$,

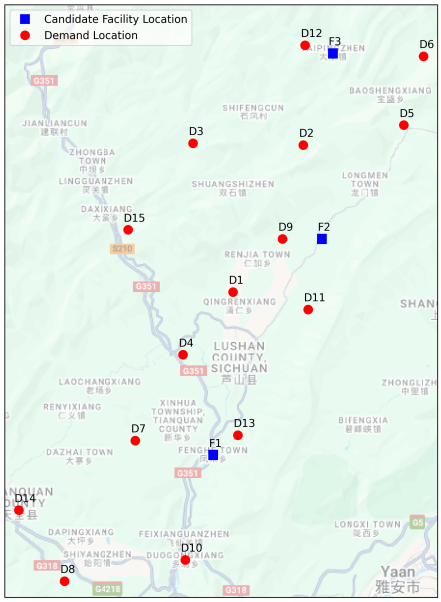

Figure 3: Lushan earthquake network

Table 5: Comparison of DDROP and NRM assignment decisions (Lushan case study)

	DDROP				NRM	
Drone	Facility	Initial Assignments	Policy 1	Policy 2	Facility	Assignments
1	F1	[1, 2, 3, 4, 8, 9, 11]	∅	∅	F1	[1, 2, 3, 4, 8, 9, 11]
2	F2	[2, 8, 10, 11, 12]	∅	∅	F1	[1, 4, 6, 9]
3	F2	[2, 5, 10, 12]	∅	[6]	F2	[5, 10, 11, 12, 14]
4	F2	[2, 10, 11, 12]	[3]	∅	F3	[5, 6, 7, 13, 15]
5	F2	[8, 10, 12, 13]	∅	∅	F3	[2, 5, 6, 7, 13]
6	F2	[10, 11, 14]	[8]	∅	F3	[3, 12, 13]
7	F3	[5, 6, 7, 13, 15]	∅	∅	F3	[7, 13, 15]
8	F3	[5, 6, 7, 10, 14]	∅	∅	F3	[7, 8, 14]

we present the set of nodes that drones are assigned to in the post-disaster stage, where the empty set ∅ indicates no reassignment. Note that if a drone is assigned to a node in the post-disaster phase, it serves that node in addition to its initial assignments. We observe the following from this table. While both models deploy eight drones, they differ in how they allocate drones across facilities. Specifically, DDROP deploy (1,5,2) in (F1, F2, F3), whereas NRM deploy (2,1,5) drones in (F1, F2, F3). Initial node-drone assignments also differ across models (with some overlap, e.g., drone 1). The DDROP post-disaster policies assign drones from facilities with more drones to cover nodes that were initially assigned to drones stored at facilities with fewer drones. Moreover, drones that receive additional post-disaster assignments are typically those with fewer initial assignments.

Next, we compare the performance of these solutions via simulation, as described in Section 6.4, under various disruption scenarios. Specifically, we consider two families for disruptions (a) uniform disruption level $\tau_j^E = \Gamma/|\mathcal{J}|$ applied to all $j \in \mathcal{J}$, and (b) targeted disruptions $\boldsymbol{\tau}^p$, where a single facility p is primarily affected. Table 6 reports the average relative difference, computed

Table 6: Average relative difference $\frac{\texttt{NRM}-\texttt{DDROP}}{\texttt{DDROP}} \times 100\%$ in second-stage, shortage, and holding costs (Lushan case study)

$\boldsymbol{\tau}$	Second-stage	Shortage	Holding
$\boldsymbol{\tau}^E$	12.3%	12.7%	11.3%
$\boldsymbol{\tau}^1$	474.1%	583.7%	321.7%
$\boldsymbol{\tau}^2$	13.5%	13.9%	12.7%
$\boldsymbol{\tau}^3$	29.7%	31.1%	26.7%

as $\frac{\texttt{NRM}-\texttt{DDROP}}{\texttt{DDROP}} \times 100\%$, over $N' = 300$ simulated scenarios for second-stage, shortage, and holding costs. It is clear that the DDROP consistently outperforms the NRM model across all disruption scenarios. In particular, the NRM solution incurs substantially higher shortage and holding costs. These results are reasonable because the NRM model fixes demand-to-drone assignments ex ante and does not account for the need to reassign after drone failures. When a drone is damaged, it cannot serve its assigned demand nodes, leading to shortages at those nodes and unused inventory elsewhere (reflected as higher shortage and holding costs). For example, consider the disruption scenario $\boldsymbol{\tau}^1$, where F1 is the only facility disrupted. If drone 1 is damaged, the NRM solution leaves nodes like 3 and 8 without aid. In contrast, the DDROP policy supports dynamic reassignment, allowing the decision-maker to reassign nodes 3 and 8 to drones 4 and 6 (stored at F2), thereby preventing excessive shortages at these nodes. These results are consistent with Theorem 1, further emphasizing that the `VoR` is positive.

6.4.2. Wenchuan Earthquake

Let us now consider another disaster based on the Great Wenchuan earthquake on May 12, 2008, along the Longmenshan fault, a thrust structure at the boundary between the Eurasian and Indo-Australian Plates. This 7-8 magnitude earthquake caused widespread devastation across Sichuan Province, including extensive landslides and road damage that isolated numerous communities. Almost 90,000 people were reported as dead or missing, and nearly 375,000 were injured. We construct an instance based on the disaster relief network used in Liu et al. (2019), which consists of eight demand locations ($|\mathcal{I}| = 8$) and three candidate facility locations ($|\mathcal{J}| = 3$); see Figure 4.

We solve these instances using the DDROP and NRM models. Both models establish 3 facilities, deploy seven drones, and preposition the same quantity of relief items. Table 7 reports drone assignments to facilities and demand nodes. We again observe that the two models produce different allocations of drones to facilities and demand nodes. Interestingly, unlike the results for the Lushan earthquake case study, in the DDROP solutions, some drones (4 and 5) are stored in F2 but are not assigned to any demand node in the pre-disaster phase. They are assigned to some demand nodes in the post-disaster phase under policies 1 and 2, which achieve significantly better performance; see Table 8. For example, in the NRM plan, dones 6 and 7 stored at F3 are assigned to serve demand nodes $(5, 7, 8)$ and $(6, 8)$, respectively. If a disruption damages one or both of these drones, as is likely under $\boldsymbol{\tau}^3$, their assigned nodes immediately lose service, producing significant shortages and

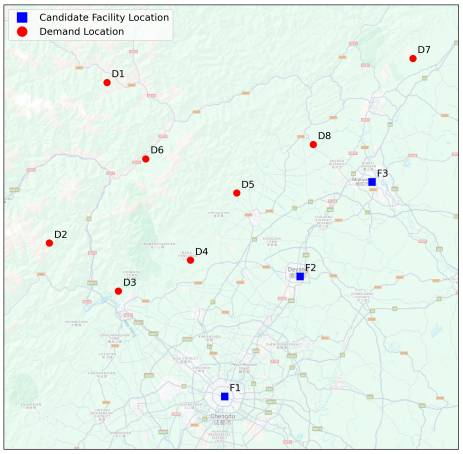

Figure 4: Wenchuan earthquake network

Table 7: Comparison of DDROP and NRM assignment decisions (Wenchuan case study)

	DDROP				NRM	
Drone	Facility	Initial Assignments	Policy 1	Policy 2	Facility	Assignments
1	F1	[3, 6]	∅	∅	F1	[2, 4]
2	F1	[2, 4]	∅	∅	F1	[3, 6]
3	F2	[1, 5]	∅	∅	F1	[2]
4	F2	∅	[1, 8]	[3, 4]	F2	[1, 5]
5	F2	∅	[4, 6]	[2]	F2	[3, 4]
6	F3	[7, 8]	∅	[5]	F3	[5, 7, 8]
7	F3	[8]	[5, 7]	[6]	F3	[6, 8]

Table 8: Average relative difference $\frac{\texttt{NRM}-\texttt{DDROP}}{\texttt{DDROP}} \times 100\%$ in second-stage, shortage, and holding (Wenchuan case study)

$\boldsymbol{\tau}$	Second Stage	Shortage	Holding
$\boldsymbol{\tau}^E$	38.77%	38.49%	42.70%
$\boldsymbol{\tau}^1$	12.16%	12.10%	13.56%
$\boldsymbol{\tau}^2$	1.36%	1.45%	1.67%
$\boldsymbol{\tau}^3$	130.90%	129.32%	147.85%

excess holding. In contrast, the DDROP solution keeps drones 4 and 5 at F2 unassigned to demand nodes pre-disaster, precisely so they can be deployed post-disaster. Under policy 1, the DDROP plan reassigns node 8 to drone 4 and node 6 to drone 5, while other functioning drones cover the remaining demand. Such adaptive assignment reduces the potential shortage at the nodes. The results in Table 8 show that under $\boldsymbol{\tau}^3$, the NRM plan has much worse outcomes: the average second-stage cost is 130.9% higher, the average unmet demand is 129.3% higher, and the average holding is 147.9% higher than DDROP. These results, along with the results in Section 6.4.1, demonstrate the benefits of our integrated approach in real-world disaster scenarios.

7. Conclusion

In this paper, we introduce a new two-stage RO framework for the integrated planning of drone-based disaster relief operations, which includes decisions related to drone-supported relief facilities, inventory prepositioning, and drone fleet deployment and operations. We present a new two-stage RO formulation with mixed-integer recourse and decision-dependent uncertainty set for the DDROP, incorporating the following novel, practically relevant elements. First, we explicitly account for the risk of facility disruptions and their impact on drone functionality, as well as their effect on demand and positioned inventory. Second, we explicitly capture, for the first time, the dependence of drone functionality on pre-disaster drone-to-facility assignment decisions, as is the case in real-world disaster scenarios. Third, unlike prior studies, we consider post-disaster drone reassignment to demand nodes. Such adaptability enhances the responsiveness and resilience of relief operations, as demonstrated both theoretically and numerically. We derive a K-adaptability approximation of the RO model that offers both practical and computational benefits. From a practical standpoint, it provides decision-makers with a set of contingency plans for drone-to-demand assignments that can be implemented in the aftermath of the disaster. Computationally, we derive an equivalent reformulation of the K-adaptability approximation amenable to a decomposition algorithm. We propose a C&CG algorithm to solve it and introduce several enhancement strategies that substantially improve computational performance. Our numerical results, based on diverse DDROP instances and two real-world disaster scenarios, demonstrate the computational efficiency of our approach and the superior operational performance of the disaster plans obtained using our framework compared to a non-integrated model.

We identify several promising directions for future research. Our results underscore the importance of considering practical aspects, such as dynamic post-disaster drone reassignment and the impact of disruptions on drone functionality. One can build upon and extend our framework to other last-mile drone delivery problems, including integrated operations with drones and trucks. While the K-adaptability approximation offers practical benefits in the context of DDROP, enabling us to address the challenges of integer recourse, it may not be the best approach in other drone applications. Thus, developing computationally efficient algorithmic strategies for solving RO problems with integer recourse and decision-dependent uncertainty is particularly relevant for drone-delivery problems, where these two challenges are particularly significant. Finally, it would be interesting to extend our framework by considering drones that can perform multiple functions in disaster and other contexts (e.g., surveillance and delivery of relief packages). This extension would require new formulations that capture multi-function capabilities, task coupling, and resource-sharing constraints, along with tailored algorithmic strategies, among others.

References

Agatz, N., Bouman, P., Schmidt, M., 2018. Optimization approaches for the traveling salesman problem with drone. Transportation Science 52, 965–981.

Ahmadi-Javid, A., Seyedi, P., Syam, S.S., 2017. A survey of healthcare facility location. Computers and Operations Research 79, 223–263.

Akbari, V., Shiri, D., Salman, F.S., 2021. An online optimization approach to post-disaster road restoration. Transportation Research Part B: Methodological 150, 1–25.

Álvarez-Miranda, E., Fernández, E., Ljubić, I., 2015. The recoverable robust facility location problem. Transportation Research Part B: Methodological 79, 93–120.

An, Y., Zeng, B., Zhang, Y., Zhao, L., 2014. Reliable p-median facility location problem: two-stage robust models and algorithms. Transportation Research Part B: Methodological 64, 54–72.

Anaya-Arenas, A.M., Renaud, J., Ruiz, A., 2014. Relief distribution networks: a systematic review. Annals of Operations Research 223, 53–79.

Basciftci, B., Ahmed, S., Shen, S., 2021. Distributionally robust facility location problem under decision-dependent stochastic demand. European Journal of Operational Research 292, 548–561.

Chauhan, D., Unnikrishnan, A., Figliozzi, M., 2019. Maximum coverage capacitated facility location problem with range constrained drones. Transportation Research Part C: Emerging Technologies 99, 1–18.

Cheng, C., Adulyasak, Y., Rousseau, L.M., 2021. Robust facility location under disruptions. INFORMS Journal on Optimization 3, 298–314.

Cheng, C., Qi, M., Zhang, Y., Rousseau, L.M., 2018. A two-stage robust approach for the reliable logistics network design problem. Transportation Research Part B: Methodological 111, 185–202.

Chung, S.H., Sah, B., Lee, J., 2020. Optimization for drone and drone-truck combined operations: A review of the state of the art and future directions. Computers & Operations Research 123, 105004.

Comes, T., Van de Walle, B., Van Wassenhove, L., 2020. The coordination-information bubble in humanitarian response: theoretical foundations and empirical investigations. Production and Operations Management 29, 2484–2507.

Correia, I., Saldanha-da Gama, F., 2019. Facility location under uncertainty. Location Science , 185–213.

CRED, 2024. 2023: Disasters in Numbers. Technical Report. Centre for Research on the Epidemiology of Disasters (CRED), UCLouvain. Brussels, Belgium. Maintained through the long-term support of USAID/BHA.

Cui, T., Ouyang, Y., Shen, Z.J.M., 2010. Reliable facility location design under the risk of disruptions. Operations Research 58, 998–1011.

Daskin, M.S., 2011. Network and Discrete Location: Models, Algorithms, and Applications. John Wiley & Sons.

Daskin, M.S., Dean, L.K., 2005. Location of health care facilities. Operations Research and Health Care , 43–76.

Dean, G., Entsie, B., 2020. Zipline drones deliver coronavirus supplies in Africa. Accessed: 2024-06-03.

Dönmez, Z., Kara, B.Y., Karsu, Ö., Saldanha-da Gama, F., 2021. Humanitarian facility location under uncertainty: Critical review and future prospects. Omega 102, 102393.

Döyen, A., Aras, N., Barbarosoğlu, G., 2012. A two-echelon stochastic facility location model for humanitarian relief logistics. Optimization Letters 6, 1123–1145.

Drezner, Z., 1987. Heuristic solution methods for two location problems with unreliable facilities. Journal of the Operational Research Society 38, 509–514.

Duan, H., Chen, J., Zhang, S., Wu, X., Chu, Z., 2022. Coseismic fault slip inversion of the 2013 lushan ms 7.0 earthquake based on the triangular dislocation model. Scientific Reports 12, 3514.

Dukkanci, O., Campbell, J.F., Kara, B.Y., 2023a. Facility location decisions for drone delivery: A literature review. European Journal of Operational Research .

Dukkanci, O., Campbell, J.F., Kara, B.Y., 2024. Facility location decisions for drone delivery with riding: A literature review. Computers & Operations Research , 106672.

Dukkanci, O., Koberstein, A., Kara, B.Y., 2023b. Drones for relief logistics under uncertainty after an earthquake. European Journal of Operational Research 310, 117–132.

Eiselt, H.A., Marianov, V., 2011. Foundations of Location Analysis. Springer.

Figliozzi, M.A., 2017a. Lifecycle modeling and assessment of unmanned aerial vehicles (drones) CO_2e emissions. Transportation Research Part D: Transport and Environment 57, 251–261.

Figliozzi, M.A., 2017b. Lifecycle modeling and assessment of unmanned aerial vehicles (drones) CO_2e emissions. Transportation Research Part D: Transport and Environment 57, 251–261.

Ghelichi, Z., Gentili, M., Mirchandani, P.B., 2022. Drone logistics for uncertain demand of disaster-impacted populations. Transportation Research Part C: Emerging Technologies 141, 103735.

Haidari, L.A., Brown, S.T., Ferguson, M., Bancroft, E., Spiker, M., Wilcox, A., Ambikapathi, R., Sampath, V., Connor, D.L., Lee, B.Y., 2016. The economic and operational value of using drones to transport vaccines. Vaccine 34, 4062–4067.

Hanasusanto, G.A., Kuhn, D., Wiesemann, W., 2015. K-adaptability in two-stage robust binary programming. Operations Research 63, 877–891.

Hassanalian, M., Abdelkefi, A., 2017. Classifications, applications, and design challenges of drones: A review. Progress in Aerospace sciences 91, 99–131.

Ishiwatari, M., 2024. Leveraging drones for effective disaster management: a comprehensive analysis of the 2024 noto peninsula earthquake case in Japan. Progress in Disaster Science , 100348.

Itatani, T., Kojima, M., Tanaka, J., Horiike, R., Sibata, K., Sasaki, R., 2024. Operational management and improvement strategies of evacuation centers during the 2024 Noto Peninsula Earthquake–a case study of wajima city. Safety 10, 62.

Jin, Z., Ng, K.K., Zhang, C., Liu, W., Zhang, F., Xu, G., 2024. A risk-averse distributionally robust optimisation approach for drone-supported relief facility location problem. Transportation Research Part E: Logistics and Transportation Review 186, 103538.

Kim, D., Lee, K., Moon, I., 2019. Stochastic facility location model for drones considering uncertain flight distance. Annals of Operations Research 283, 1283–1302.

Klibi, W., Ichoua, S., Martel, A., 2018. Prepositioning emergency supplies to support disaster relief: a case study using stochastic programming. INFOR: Information Systems and Operational Research 56, 50–81.

Klotz, E., Newman, A.M., 2013. Practical guidelines for solving difficult mixed integer linear programs. Surveys in Operations Research and Management Science 18, 18–32.

Kovács, G., Spens, K., 2009. Identifying challenges in humanitarian logistics. International Journal of Physical Distribution & Logistics Management 39, 506–528.

Küçükyavuz, S., Sen, S., 2017. An introduction to two-stage stochastic mixed-integer programming, in: Leading Developments from INFORMS Communities. INFORMS, pp. 1–27.

Li, X., Ouyang, Y., 2010. A continuum approximation approach to reliable facility location design under correlated probabilistic disruptions. Transportation Research Part B: Methodological 44, 535–548.

Liberti, L., 2012. Symmetry in mathematical programming, in: Mixed Integer Nonlinear Programming, Springer. pp. 263–283.

Liu, Y., Lei, H., Wu, Z., Zhang, D., 2019. A robust model predictive control approach for post-disaster relief distribution. Computers & Industrial Engineering 135, 1253–1270.

Lu, X., Cheng, C., 2021. Locating facilities with resiliency to capacity failures and correlated demand uncertainty. Transportation Research Part E: Logistics and Transportation Review 153, 102444.

Murray, C.C., Chu, A.G., 2015. The flying sidekick traveling salesman problem: Optimization of drone-assisted parcel delivery. Transportation Research Part C: Emerging Technologies 54, 86–109.

Murray, C.C., Raj, R., 2020. The multiple flying sidekicks traveling salesman problem: Parcel delivery with multiple drones. Transportation Research Part C: Emerging Technologies 110, 368–398.

Ni, W., Shu, J., Song, M., 2018. Location and emergency inventory pre-positioning for disaster response operations: Min-max robust model and a case study of yushu earthquake. Production and Operations Management 27, 160–183.

Noyan, N., 2012. Risk-averse two-stage stochastic programming with an application to disaster management. Computers & Operations Research 39, 541–559.

Nunez-Ollero, C., 2024. Implementation Completion Report (ICR) Review: Lushan Earthquake Reconstruction Project (P153548). Technical Report ICRR0024203. World Bank. Project ID: P153548; closing date: 31 December 2023.

OCHA, 2019. Bahamas: Hurricane Dorian - Situation Report No. 2. Technical Report 2. OCHA. Published 10 September 2019. Accessed via situation report issued by OCHA in collaboration with UN agencies and partners.

Ostrowski, J., 2010. Symmetry handling in mixed-integer programming. Wiley Encyclopedia of Operations Research and Management Science .

Otto, A., Agatz, N., Campbell, J., Golden, B., Pesch, E., 2018. Optimization approaches for civil applications of unmanned aerial vehicles (uavs) or aerial drones: A survey. Networks 72, 411–458.

Paul, J.A., Zhang, M., 2019. Supply location and transportation planning for hurricanes: A two-stage stochastic programming framework. European Journal of Operational Research 274, 108–125.

Rath, S., Gendreau, M., Gutjahr, W.J., 2016. Bi-objective stochastic programming models for determining depot locations in disaster relief operations. International Transactions in Operational Research 23, 997–1023.

Rawls, C.G., Turnquist, M.A., 2010. Pre-positioning of emergency supplies for disaster response. Transportation research part B: Methodological 44, 521–534.

Rejeb, A., Rejeb, K., Simske, S., Treiblmaier, H., 2021. Humanitarian drones: A review and research agenda. Internet of Things 16, 100434.

Rejeb, A., Rejeb, K., Simske, S.J., Treiblmaier, H., 2023. Drones for supply chain management and logistics: a review and research agenda. International Journal of Logistics Research and Applications 26, 708–731.

Ren, C., Wang, K., Han, J., Sun, L., Yang, C., 2024. Deterministic scenarios guided k-adaptability in multistage robust optimization for energy management and cleaning scheduling of heat transfer process. Energy 312, 133558.

Revelle, C.S., Eiselt, H.A., Daskin, M.S., 2008. A bibliography for some fundamental problem categories in discrete location science. European Journal of Operational Research 184, 817–848.

Sabbaghtorkan, M., Batta, R., He, Q., 2020. Prepositioning of assets and supplies in disaster operations management: Review and research gap identification. European Journal of Operational Research 284, 1–19.

Shakhatreh, H., Sawalmeh, A.H., Al-Fuqaha, A., Dou, Z., Almaita, E., Khalil, I., Othman, N.S., Khreishah, A., Guizani, M., 2019. Unmanned aerial vehicles (uavs): A survey on civil applications and key research challenges. Ieee Access 7, 48572–48634.

Shehadeh, K.S., 2023. Distributionally robust optimization approaches for a stochastic mobile facility fleet sizing, routing, and scheduling problem. Transportation Science 57, 197–229.

Shehadeh, K.S., Snyder, L.V., 2023. Equity in stochastic healthcare facility location, in: Uncertainty in Facility Location Problems. Springer, pp. 303–334.

Shehadeh, K.S., Tucker, E.L., 2022. Stochastic optimization models for location and inventory prepositioning of disaster relief supplies. Transportation Research Part C: Emerging Technologies 144, 103871.

Shen, Z.J.M., Zhan, R.L., Zhang, J., 2011. The reliable facility location problem: Formulations, heuristics, and approximation algorithms. INFORMS Journal on Computing 23, 470–482.

Snyder, L.V., 2006. Facility location under uncertainty: a review. IIE transactions 38, 547–564.

Snyder, L.V., Atan, Z., Peng, P., Rong, Y., Schmitt, A.J., Sinsoysal, B., 2016. Or/ms models for supply chain disruptions: A review. Iie Transactions 48, 89–109.

Snyder, L.V., Daskin, M.S., 2005. Reliability models for facility location: the expected failure cost case. Transportation science 39, 400–416.

Tsang, M.Y., Shehadeh, K.S., Curtis, F.E., 2023. An inexact column-and-constraint generation method to solve two-stage robust optimization problems. Operations Research Letters 51, 92–98.

UNICEF, 2017. Humanitarian drone corridor launched in malawi. Accessed on 3 May 2025.

UNICEF, 2018. Child given world's first drone-delivered vaccine in vanuatu – unicef. Accessed on 30 April 2025.

UNOCHA, 2024. Global Humanitarian Overview 2025. Technical Report. United Nations Office for the Coordination of Humanitarian Affairs (OCHA). Geneva & New York.

Vayanos, P., Georghiou, A., Yu, H., 2020. Robust optimization with decision-dependent information discovery. arXiv preprint arXiv:2004.08490 .

Velasquez, G.A., Mayorga, M.E., Özaltın, O.Y., 2020. Prepositioning disaster relief supplies using robust optimization. IISE Transactions 52, 1122–1140.

Wang, X., Zhao, J., Cheng, C., Qi, M., 2023. A multi-objective fuzzy facility location problem with congestion and priority for drone-based emergency deliveries. Computers & Industrial Engineering 179, 109167.

Wang, Z., Sheu, J.B., 2019. Vehicle routing problem with drones. Transportation Research Part B: Methodological 122, 350–364.

Weitering, H., 2023. Dronamics black swan cargo drone completes first flight test. Accessed: 2025-10-05.

Xie, S., An, K., Ouyang, Y., 2019. Planning facility location under generally correlated facility disruptions: Use of supporting stations and quasi-probabilities. Transportation Research Part B: Methodological 122, 115–139.

Xu, J., Wang, Z., Zhang, M., Tu, Y., 2016. A new model for a 72-h post-earthquake emergency logistics location-routing problem under a random fuzzy environment. Transportation Letters 8, 270–285.

Zhao, L., Zeng, B., 2012. An exact algorithm for two-stage robust optimization with mixed integer recourse problems.

Zheng, F., Wang, Z., Zhang, E., Liu, M., 2022. K-adaptability in robust container vessel sequencing problem with week-dependent demands of a service route. International Journal of Production Research 60, 2787–2801.

Zhu, T., Boyles, S.D., Unnikrishnan, A., 2022. Two-stage robust facility location problem with drones. Transportation Research Part C: Emerging Technologies 137, 103563.

Zokaee, S., Bozorgi-Amiri, A., Sadjadi, S.J., 2016. A robust optimization model for humanitarian relief chain design under uncertainty. Applied mathematical modelling 40, 7996–8016.

Supplementary Materials to "Integrated Planning of Drone-Based Disaster Relief: Facility Location, Inventory Prepositioning, and Fleet Operations under Uncertainty" Los Angeles, CA, USA

Appendix A. Drone Energy Consumption and Characteristics

As in Figliozzi (2017b), we use the following formula to compute the total energy consumed in delivery from facility $j \in \mathcal{J}$ to demand location $i \in \mathcal{I}$ with drones $d \in \mathcal{D}$:

$$b_{i,j,d} = \frac{(m_{uav} + m_{batt} + m_{payload})\, g}{\eta(s)\theta}\, \mathsf{d}_{i,j} + \frac{(m_{uav} + m_{batt})\, g}{\eta(s)\theta}\, \mathsf{d}_{j,i}. \tag{A.1}$$

We summarize the description and value of each parameter in Table A.1.

Table A.1: Attributes of Parameters

Notation	Description	DJI Flycart 30	Pseudo Drone
m_{uav}	UAV mass (kg)	42.5	85
m_{batt}	battery mass of type $r \in \mathcal{R}$ drones (kg)	22.5	45
P_r	payload mass of type $r \in \mathcal{R}$ drones (kg)	30	60
g	gravity acceleration (km/m^2)	9.81	
$\eta(s)\theta$	product of lift-to-drag ratio and power transfer efficiency	6.86	6.86
B_r	energy capacity of type $r \in \mathcal{R}$ drones (kWh)	3986.8	7973.6

Appendix B. Mathematical Proofs

Appendix B.1. Proof of Theorem 1

Proof. Proof. First, we prove the nonnegativity of `VoR`. Recall that problems (2) and (6) have the same first-stage variables and constraints. Hence, any feasible first-stage decision $(\boldsymbol{y}, \boldsymbol{w}, \boldsymbol{x}, \boldsymbol{z})$ for problem (2) is also feasible for problem (6). To show the desired result, we next show that the inequality $Q(\boldsymbol{x}, \boldsymbol{w}, \boldsymbol{z}, \boldsymbol{\xi}) \leq \widehat{Q}(\boldsymbol{x}, \boldsymbol{w}, \boldsymbol{z}, \boldsymbol{\xi})$ holds or any feasible first-stage decisions $(\boldsymbol{y}, \boldsymbol{w}, \boldsymbol{x}, \boldsymbol{z})$ and realization of $\boldsymbol{\xi} = (\boldsymbol{a}, \boldsymbol{e}, \boldsymbol{q}) \in \mathcal{U}(\boldsymbol{z}; \boldsymbol{\kappa}, \Gamma)$. To show this, we observe that $\boldsymbol{v} = 0$ (i.e., no reassignment) is a feasible solution for problem (3). Consider any scenario $\boldsymbol{\xi} \in \mathcal{U}(\boldsymbol{z}; \boldsymbol{\kappa}, \Gamma)$ and let $(\hat{\boldsymbol{n}}, \hat{\boldsymbol{u}}, \hat{\boldsymbol{h}})$ be an optimal solution to $\widehat{Q}(\boldsymbol{x}, \boldsymbol{w}, \boldsymbol{z}, \boldsymbol{\xi})$ defined in (7). Note that $(\boldsymbol{0}, \hat{\boldsymbol{n}}, \hat{\boldsymbol{u}}, \hat{\boldsymbol{h}})$ is a feasible solution to $Q(\boldsymbol{x}, \boldsymbol{w}, \boldsymbol{z}, \boldsymbol{\xi})$ defined in (3). Therefore, we have

$$\begin{aligned} Q(\boldsymbol{x}, \boldsymbol{w}, \boldsymbol{z}, \boldsymbol{\xi}) &\leq \sum_{i\in\mathcal{I}} \sum_{j\in\mathcal{J}} \sum_{d\in\mathcal{D}} c^{\mathrm{m},2}_{i,j,d}(0) + \sum_{i\in\mathcal{I}} \sum_{j\in\mathcal{J}} \sum_{d\in\mathcal{D}} \sum_{t\in\mathcal{T}} c^{\mathrm{t}}_{i,j,t} \hat{n}_{i,j,d,t} + \sum_{i\in\mathcal{I}} \sum_{t\in\mathcal{T}} c^{\mathrm{u}}_t \hat{u}_{i,t} + \sum_{j\in\mathcal{J}} c^{\mathrm{h}}_t \hat{h}_{j,t} \\ &= \sum_{i\in\mathcal{I}} \sum_{j\in\mathcal{J}} \sum_{d\in\mathcal{D}} \sum_{t\in\mathcal{T}} c^{\mathrm{t}}_{i,j,t} \hat{n}_{i,j,d,t} + \sum_{i\in\mathcal{I}} \sum_{t\in\mathcal{T}} c^{\mathrm{u}}_t \hat{u}_{i,t} + \sum_{j\in\mathcal{J}} c^{\mathrm{h}}_t \hat{h}_{j,t} \\ &= \widehat{Q}(\boldsymbol{x}, \boldsymbol{w}, \boldsymbol{z}, \boldsymbol{\xi}), \end{aligned} \tag{B.1}$$

where (B.1) follows from the assumption that $(\hat{\boldsymbol{n}}, \hat{\boldsymbol{u}}, \hat{\boldsymbol{h}})$ is an optimal solution to $\widehat{Q}(\boldsymbol{x}, \boldsymbol{w}, \boldsymbol{z}, \boldsymbol{\xi})$. Note that the the inequality $Q(\boldsymbol{x}, \boldsymbol{w}, \boldsymbol{z}, \boldsymbol{\xi}) \leq \widehat{Q}(\boldsymbol{x}, \boldsymbol{w}, \boldsymbol{z}, \boldsymbol{\xi})$ in (B.1) holds for any realization of $\boldsymbol{\xi} \in \mathcal{U}(\boldsymbol{z}; \boldsymbol{\kappa}, \Gamma)$. Taking the maximum over $\boldsymbol{\xi} \in \mathcal{U}(\boldsymbol{z}; \boldsymbol{\kappa}, \Gamma)$ on both sides of the inequality, we obtain

$$\max_{\boldsymbol{\xi} \in \mathcal{U}(\boldsymbol{z}; \boldsymbol{\kappa}, \Gamma)} Q(\boldsymbol{x}, \boldsymbol{w}, \boldsymbol{z}, \boldsymbol{\xi}) \leq \max_{\boldsymbol{\xi} \in \mathcal{U}(\boldsymbol{z}; \boldsymbol{\kappa}, \Gamma)} \widehat{Q}(\boldsymbol{x}, \boldsymbol{w}, \boldsymbol{z}, \boldsymbol{\xi}).$$

It follows that the objective function of problem (2) is always less than or equal to that of problem (6) for any feasible first-stage decision $(\boldsymbol{y}, \boldsymbol{w}, \boldsymbol{x}, \boldsymbol{z})$. This implies that the optimal value η of problem (2) is always less than or equal to the optimal value $\hat{\eta}$ of problem (6). Therefore, we have $\texttt{VoR} = \hat{\eta} - \eta \geq 0$.

Next, we prove the following lower bound for VoR: $\texttt{VoR} \geq \varphi(\bar{\boldsymbol{n}}, \hat{\boldsymbol{n}}, \bar{\boldsymbol{v}})$. For notational convenience, define

$$\mathfrak{f}(\boldsymbol{y}, \boldsymbol{x}, \boldsymbol{w}, \boldsymbol{z}) = \sum_{j \in \mathcal{J}} \sum_{l \in \mathcal{L}} c_l^{\mathrm{f}} y_{j,l} + \sum_{j \in \mathcal{J}} \sum_{t \in \mathcal{T}} c_t^{\mathrm{a}} w_{j,t} + \sum_{j \in \mathcal{J}} \sum_{r \in \mathcal{R}} \sum_{d \in \mathcal{D}_r} c_r^{\mathrm{d}} z_{j,d} + \sum_{i \in \mathcal{I}} \sum_{j \in \mathcal{J}} \sum_{d \in \mathcal{D}} c_{i,j,d}^{\mathrm{m},1} x_{i,j,d}. \quad \text{(B.2)}$$

as the first-stage objective value associated with a feasible first-stage solution $(\boldsymbol{y}, \boldsymbol{x}, \boldsymbol{w}, \boldsymbol{z})$ to (2). Let $(\bar{\boldsymbol{y}}, \bar{\boldsymbol{x}}, \bar{\boldsymbol{w}}, \bar{\boldsymbol{z}})$ and $(\hat{\boldsymbol{y}}, \hat{\boldsymbol{x}}, \hat{\boldsymbol{w}}, \hat{\boldsymbol{z}})$ be optimal first-stage solutions to (2) and (6), respectively. Note that

$$\begin{aligned}
\texttt{VoR} &= \widehat{\eta} - \eta && \text{(B.3a)}\\
&= \Big\{\mathfrak{f}(\hat{\boldsymbol{y}}, \hat{\boldsymbol{x}}, \hat{\boldsymbol{w}}, \hat{\boldsymbol{z}}) + \max_{\boldsymbol{\xi} \in \mathcal{U}(\hat{\boldsymbol{z}}; \boldsymbol{\kappa}, \Gamma)} \widehat{Q}(\hat{\boldsymbol{x}}, \hat{\boldsymbol{w}}, \hat{\boldsymbol{z}}, \boldsymbol{\xi})\Big\} - \Big\{\mathfrak{f}(\bar{\boldsymbol{y}}, \bar{\boldsymbol{x}}, \bar{\boldsymbol{w}}, \bar{\boldsymbol{z}}) + \max_{\boldsymbol{\xi} \in \mathcal{U}(\bar{\boldsymbol{z}}; \boldsymbol{\kappa}, \Gamma)} Q(\bar{\boldsymbol{x}}, \bar{\boldsymbol{w}}, \bar{\boldsymbol{z}}, \boldsymbol{\xi})\Big\} && \text{(B.3b)}\\
&\geq \Big\{\mathfrak{f}(\hat{\boldsymbol{y}}, \hat{\boldsymbol{x}}, \hat{\boldsymbol{w}}, \hat{\boldsymbol{z}}) + \max_{\boldsymbol{\xi} \in \mathcal{U}(\hat{\boldsymbol{z}}; \boldsymbol{\kappa}, \Gamma)} \widehat{Q}(\hat{\boldsymbol{x}}, \hat{\boldsymbol{w}}, \hat{\boldsymbol{z}}, \boldsymbol{\xi})\Big\} - \Big\{\mathfrak{f}(\hat{\boldsymbol{y}}, \hat{\boldsymbol{x}}, \hat{\boldsymbol{w}}, \hat{\boldsymbol{z}}) + \max_{\boldsymbol{\xi} \in \mathcal{U}(\hat{\boldsymbol{z}}; \boldsymbol{\kappa}, \Gamma)} Q(\hat{\boldsymbol{x}}, \hat{\boldsymbol{w}}, \hat{\boldsymbol{z}}, \boldsymbol{\xi})\Big\} && \text{(B.3c)}\\
&= \max_{\boldsymbol{\xi} \in \mathcal{U}(\hat{\boldsymbol{z}}; \boldsymbol{\kappa}, \Gamma)} \Big\{\widehat{Q}(\hat{\boldsymbol{x}}, \hat{\boldsymbol{w}}, \hat{\boldsymbol{z}}, \boldsymbol{\xi})\Big\} - \max_{\boldsymbol{\xi} \in \mathcal{U}(\hat{\boldsymbol{z}}; \boldsymbol{\kappa}, \Gamma)} \Big\{Q(\hat{\boldsymbol{x}}, \hat{\boldsymbol{w}}, \hat{\boldsymbol{z}}, \boldsymbol{\xi})\Big\}, && \text{(B.3d)}
\end{aligned}$$

where (B.3b) holds from the definitions of η and $\widehat{\eta}$, and (B.3c) follows from the fact that $(\hat{\boldsymbol{y}}, \hat{\boldsymbol{w}}, \hat{\boldsymbol{z}}, \hat{\boldsymbol{x}})$ is a feasible solution to (2).

Now, let $\boldsymbol{\xi}^* = (\boldsymbol{a}^*, \boldsymbol{e}^*, \boldsymbol{q}^*)$ be an optimal solution to the problem $\max_{\boldsymbol{\xi} \in \mathcal{U}(\hat{\boldsymbol{z}}; \kappa, \Gamma)} Q(\hat{\boldsymbol{x}}, \hat{\boldsymbol{w}}, \hat{\boldsymbol{z}}, \boldsymbol{\xi})$. Note that $\boldsymbol{\xi}^*$ is a feasible solution to $\max_{\boldsymbol{\xi} \in \mathcal{U}(\hat{\boldsymbol{z}}; \boldsymbol{\kappa}, \Gamma)} \widehat{Q}(\hat{\boldsymbol{x}}, \hat{\boldsymbol{w}}, \hat{\boldsymbol{z}}, \boldsymbol{\xi})$. Let $(\hat{\boldsymbol{n}}, \hat{\boldsymbol{u}}, \hat{\boldsymbol{h}})$ and $(\bar{\boldsymbol{v}}, \bar{\boldsymbol{n}}, \bar{\boldsymbol{u}}, \bar{\boldsymbol{h}})$ be optimal solutions to the problems $\widehat{Q}(\hat{\boldsymbol{x}}, \hat{\boldsymbol{w}}, \hat{\boldsymbol{z}}, \boldsymbol{\xi}^*)$ and $Q(\hat{\boldsymbol{x}}, \hat{\boldsymbol{w}}, \hat{\boldsymbol{z}}, \boldsymbol{\xi}^*)$, respectively. It follows from (B.3d) that

$$\begin{aligned}
&\texttt{VoR}\\
&\geq \max_{\boldsymbol{\xi} \in \mathcal{U}(\hat{\boldsymbol{z}}; \boldsymbol{\kappa}, \Gamma)} \Big\{\widehat{Q}(\hat{\boldsymbol{x}}, \hat{\boldsymbol{w}}, \hat{\boldsymbol{z}}, \boldsymbol{\xi})\Big\} - \max_{\boldsymbol{\xi} \in \mathcal{U}(\hat{\boldsymbol{z}}; \boldsymbol{\kappa}, \Gamma)} \Big\{Q(\hat{\boldsymbol{x}}, \hat{\boldsymbol{w}}, \hat{\boldsymbol{z}}, \boldsymbol{\xi})\Big\} && \text{(B.4a)}\\
&\geq \widehat{Q}(\hat{\boldsymbol{x}}, \hat{\boldsymbol{w}}, \hat{\boldsymbol{z}}, \boldsymbol{\xi}^*) - Q(\hat{\boldsymbol{x}}, \hat{\boldsymbol{w}}, \hat{\boldsymbol{z}}, \boldsymbol{\xi}^*) && \text{(B.4b)}
\end{aligned}$$

$$= \left\{ \sum_{i\in\mathcal{I}} \sum_{j\in\mathcal{J}} \sum_{d\in\mathcal{D}} \sum_{t\in\mathcal{T}} c^{\mathrm{t}}_{i,j,d} \hat{n}_{i,j,d,t} + \sum_{i\in\mathcal{I}} \sum_{t\in\mathcal{T}} c^{\mathrm{u}}_{t} \hat{u}_{i,t} + \sum_{j\in\mathcal{J}} \sum_{t\in\mathcal{T}} c^{\mathrm{h}}_{t} \hat{h}_{j,t} \right\}$$

$$- \left\{ \sum_{i\in\mathcal{I}} \sum_{j\in\mathcal{J}} \sum_{d\in\mathcal{D}} c^{\mathrm{m},2}_{i,j,d} \bar{v}_{i,j,d} + \sum_{i\in\mathcal{I}} \sum_{j\in\mathcal{J}} \sum_{d\in\mathcal{D}} \sum_{t\in\mathcal{T}} c^{\mathrm{t}}_{i,j,d} \bar{n}_{i,j,d,t} + \sum_{i\in\mathcal{I}} \sum_{t\in\mathcal{T}} c^{\mathrm{u}}_{t} \bar{u}_{i,t} + \sum_{j\in\mathcal{J}} \sum_{t\in\mathcal{T}} c^{\mathrm{h}}_{t} \bar{h}_{j,t} \right\} \quad \text{(B.4c)}$$

$$= \sum_{i\in\mathcal{I}} \sum_{j\in\mathcal{J}} \sum_{d\in\mathcal{D}} \sum_{t\in\mathcal{T}} c^{\mathrm{t}}_{i,j,d} (\hat{n}_{i,j,d,t} - \bar{n}_{i,j,d,t}) + \sum_{i\in\mathcal{I}} \sum_{t\in\mathcal{T}} c^{\mathrm{u}}_{t} (\hat{u}_{i,t} - \bar{u}_{i,t}) + \sum_{j\in\mathcal{J}} \sum_{t\in\mathcal{T}} c^{\mathrm{h}}_{t} (\hat{h}_{j,t} - \bar{h}_{j,t})$$
$$- \sum_{i\in\mathcal{I}} \sum_{j\in\mathcal{J}} \sum_{d\in\mathcal{D}} c^{\mathrm{m},2}_{i,j,d} \bar{v}_{i,j,d} \quad \text{(B.4d)}$$

$$= \sum_{i\in\mathcal{I}} \sum_{j\in\mathcal{J}} \sum_{d\in\mathcal{D}} \sum_{t\in\mathcal{T}} c^{\mathrm{t}}_{i,j,d} (\hat{n}_{i,j,d,t} - \bar{n}_{i,j,d,t})$$
$$+ \sum_{i\in\mathcal{I}} \sum_{t\in\mathcal{T}} c^{\mathrm{u}}_{t} \left[\left(q^{*}_{i,t} - \sum_{j\in\mathcal{J}} \sum_{d\in\mathcal{D}} \hat{n}_{i,j,d,t} \right) - \left(q^{*}_{i,t} - \sum_{j\in\mathcal{J}} \sum_{d\in\mathcal{D}} \bar{n}_{i,j,d,t} \right) \right]$$
$$+ \sum_{j\in\mathcal{J}} \sum_{t\in\mathcal{T}} c^{\mathrm{h}}_{t} \left[\left(\hat{w}_{j,t} e^{*}_{j,t} - \sum_{i\in\mathcal{I}} \sum_{d\in\mathcal{D}} \hat{n}_{i,j,d,t} \right) - \left(\hat{w}_{j,t} e^{*}_{j,t} - \sum_{i\in\mathcal{I}} \sum_{d\in\mathcal{D}} \bar{n}_{i,j,d,t} \right) \right]$$
$$- \sum_{i\in\mathcal{I}} \sum_{j\in\mathcal{J}} \sum_{d\in\mathcal{D}} c^{\mathrm{m},2}_{i,j,d} \bar{v}_{i,j,d} \quad \text{(B.4e)}$$

$$= \sum_{i\in\mathcal{I}} \sum_{j\in\mathcal{J}} \sum_{d\in\mathcal{D}} \sum_{t\in\mathcal{T}} (c^{\mathrm{u}}_{t} + c^{\mathrm{h}}_{t} - c^{\mathrm{t}}_{i,j,d}) (\bar{n}_{i,j,d,t} - \hat{n}_{i,j,d,t}) - \sum_{i\in\mathcal{I}} \sum_{j\in\mathcal{J}} \sum_{d\in\mathcal{D}} c^{\mathrm{m},2}_{i,j,d} \bar{v}_{i,j,d} \quad \text{(B.4f)}$$

$$= \varphi(\bar{\boldsymbol{n}}, \hat{\boldsymbol{n}}, \bar{\boldsymbol{v}}). \quad \text{(B.4g)}$$

Here, (B.4b) follows from the fact that $\boldsymbol{\xi}^{*}$ is a feasible solution to $\max_{\boldsymbol{\xi}\in\mathcal{U}(\hat{\boldsymbol{z}};\kappa,\Gamma)} \widehat{Q}(\hat{\boldsymbol{x}}, \hat{\boldsymbol{w}}, \hat{\boldsymbol{z}}, \boldsymbol{\xi})$; (B.4c) follows from the definitions of Q and $\widehat{Q}$ in (3) and (7), respectively; (B.4e) follows from constraints (3b)–(3c) and the definition that $(\hat{\boldsymbol{n}}, \hat{\boldsymbol{u}}, \hat{\boldsymbol{h}})$ and $(\bar{\boldsymbol{v}}, \bar{\boldsymbol{n}}, \bar{\boldsymbol{u}}, \bar{\boldsymbol{h}})$ are optimal solutions to $\widehat{Q}(\hat{\boldsymbol{x}}, \hat{\boldsymbol{w}}, \hat{\boldsymbol{z}}, \boldsymbol{\xi}^{*})$ and $Q(\hat{\boldsymbol{x}}, \hat{\boldsymbol{w}}, \hat{\boldsymbol{z}}, \boldsymbol{\xi}^{*})$, respectively.

Finally, combining the two lower bounds, i.e., $\texttt{VoR} \geq 0$ and $\texttt{VoR} \geq \varphi(\bar{\boldsymbol{n}}, \hat{\boldsymbol{n}}, \bar{\boldsymbol{v}})$, we obtain the desired inequality $\texttt{VoR} \geq \max\{\varphi(\bar{\boldsymbol{n}}, \hat{\boldsymbol{n}}, \bar{\boldsymbol{v}}),\, 0\}$. This completes the proof. □

Appendix B.2. Proof of Proposition 1

Proof. Proof. First, suppose that the set $\mathcal{U}(\boldsymbol{z}; \boldsymbol{\kappa}, \Gamma)$ is empty, i.e., $\mathcal{U}(\boldsymbol{z}; \boldsymbol{\kappa}, \Gamma) = \emptyset$. It follows from the definition of $\mathcal{U}(\boldsymbol{z}; \boldsymbol{\kappa}, \Gamma)$ that there do not exist $\boldsymbol{\tau} \in \Pi := \{\tau \in [0,1]^{|\mathcal{J}|} \mid \sum_{j\in\mathcal{J}} \tau_j \leq \Gamma\}$ and $(\boldsymbol{a}, \boldsymbol{e}, \boldsymbol{q}) \in \Xi$ satisfying the following constraints:

$$\left| \frac{1}{T} \sum_{t\in\mathcal{T}} (1 - e_{j,t}) - \tau_j \right| \leq \kappa^{\mathrm{f}}_{j}, \quad \forall j \in \mathcal{J}, \quad \text{(B.5a)}$$

$$\sum_{d\in\mathcal{D}} (1 - a_d) z_{j,d} - \tau_j \sum_{d\in\mathcal{D}} z_{j,d} \leq \kappa^{\mathrm{d}}_{j} \sum_{d\in\mathcal{D}} z_{j,d}, \quad \forall j \in \mathcal{J}, \quad \text{(B.5b)}$$

$$q_{i,t} = \bar{q}_{i,t} + \sum_{j\in\mathcal{J}} \tau_j \, \tilde{q}_{i,j,t}, \quad \forall i \in \mathcal{I},\, t \in \mathcal{T}. \quad \text{(B.5c)}$$

In other words, there does not exist $\boldsymbol{a} \in \{0,1\}^{|\mathcal{D}|}$ such that $\mathcal{U}(\boldsymbol{z}, \boldsymbol{a}; \boldsymbol{\kappa}, \Gamma) \neq \emptyset$. Hence, we have $\bigcup_{\boldsymbol{a} \in \{0,1\}^{|\mathcal{D}|}} (\{\boldsymbol{a}\} \times \mathcal{U}(\boldsymbol{z}, \boldsymbol{a}; \boldsymbol{\kappa}, \Gamma)) = \emptyset$.

Now, suppose that the uncertainty set $\mathcal{U}(\boldsymbol{z}; \boldsymbol{\kappa}, \Gamma)$ is non-empty, i.e., $\mathcal{U}(\boldsymbol{z}; \boldsymbol{\kappa}, \Gamma) \neq \emptyset$. Let $(\boldsymbol{a}, \boldsymbol{e}, \boldsymbol{q}) \in \mathcal{U}(\boldsymbol{z}; \boldsymbol{\kappa}, \Gamma)$. It follows from the definition of $\mathcal{U}(\boldsymbol{z}; \boldsymbol{\kappa}, \Gamma)$ that there exists $\boldsymbol{\tau} \in \Pi$ such that (B.5a)–(B.5c) are satisfied. This in turn implies that $(\boldsymbol{e}, \boldsymbol{q}) \in \mathcal{U}(\boldsymbol{z}, \boldsymbol{a}; \boldsymbol{\kappa}, \Gamma)$. Hence, we have $(\boldsymbol{a}, \boldsymbol{e}, \boldsymbol{q}) \in \{\boldsymbol{a}\} \times \mathcal{U}(\boldsymbol{z}, \boldsymbol{a}; \boldsymbol{\kappa}, \Gamma) \subseteq \bigcup_{\boldsymbol{a}' \in \{0,1\}^{|\mathcal{D}|}} (\{\boldsymbol{a}'\} \times \mathcal{U}(\boldsymbol{z}, \boldsymbol{a}'; \boldsymbol{\kappa}, \Gamma))$. Next, let $(\boldsymbol{a}, \boldsymbol{e}, \boldsymbol{q}) \in \bigcup_{\boldsymbol{a}' \in \{0,1\}^{|\mathcal{D}|}} (\{\boldsymbol{a}'\} \times \mathcal{U}(\boldsymbol{z}, \boldsymbol{a}'; \boldsymbol{\kappa}, \Gamma))$. Then, we have $(\boldsymbol{e}, \boldsymbol{q}) \in \mathcal{U}(\boldsymbol{z}, \boldsymbol{a}; \boldsymbol{\kappa}, \Gamma)$. If follows from the definition of $\mathcal{U}(\boldsymbol{z}, \boldsymbol{a}; \boldsymbol{\kappa}, \Gamma)$ that there exists $\boldsymbol{\tau} \in \Pi$ such that $(\boldsymbol{a}, \boldsymbol{e}, \boldsymbol{q})$ satisfies (B.5a)–(B.5c). This shows that $(\boldsymbol{a}, \boldsymbol{e}, \boldsymbol{q}) \in \mathcal{U}(\boldsymbol{z}; \boldsymbol{\kappa}, \Gamma)$. Hence, we have $\mathcal{U}(\boldsymbol{z}; \boldsymbol{\kappa}, \Gamma) = \bigcup_{\boldsymbol{a} \in \{0,1\}^{|\mathcal{D}|}} (\{\boldsymbol{a}\} \times \mathcal{U}(\boldsymbol{z}, \boldsymbol{a}; \boldsymbol{\kappa}, \Gamma))$. □

Appendix B.3. Proof of Proposition 2

Proof. Proof. For a fixed $\boldsymbol{a} \in \{0,1\}^{|\mathcal{D}|}$, the inner problem in (12), $\max\limits_{(\boldsymbol{e}, \boldsymbol{q}) \in \mathcal{U}(\boldsymbol{z}, \boldsymbol{a}; \boldsymbol{\kappa}, \Gamma)} \min\limits_{k \in [K]} \widetilde{Q}(\boldsymbol{x}, \boldsymbol{w}, \boldsymbol{\xi}; \boldsymbol{v}^k)$, is equivalent to

$$\begin{aligned}
\underset{\chi, \boldsymbol{e}, \boldsymbol{q}}{\text{maximize}} \quad & \chi && \text{(B.6a)}\\
\text{subject to} \quad & \chi \leq \widetilde{Q}(\boldsymbol{x}, \boldsymbol{w}, \boldsymbol{\xi}; \boldsymbol{v}^k), \quad \forall k \in [K], && \text{(B.6b)}\\
& (\boldsymbol{e}, \boldsymbol{q}) \in \mathcal{U}(\boldsymbol{z}, \boldsymbol{a}; \boldsymbol{\kappa}, \Gamma). && \text{(B.6c)}
\end{aligned}$$

Next, we derive an equivalent reformulation of (B.6). Recall that $\widetilde{Q}(\boldsymbol{x}, \boldsymbol{w}, \boldsymbol{\xi}; \boldsymbol{v}^k)$ defined in (9) is an LP. The dual of this LP is as follows.

$$\begin{aligned}
\underset{\boldsymbol{\mu}, \boldsymbol{\pi}, \boldsymbol{\lambda}}{\text{maximize}} \quad & \Bigg\{ \sum_{i \in \mathcal{I}} \sum_{j \in \mathcal{J}} \sum_{d \in \mathcal{D}} c^{\mathrm{m},2}_{i,j,d} v^k_{i,j,d} + \sum_{i \in \mathcal{I}} \sum_{t \in \mathcal{T}} q_{i,t} \lambda_{i,t} + \sum_{j \in \mathcal{J}} \sum_{t \in \mathcal{T}} w_{j,t}\, e_{j,t} \pi_{j,t} \\
& \quad - \sum_{i \in \mathcal{I}} \sum_{j \in \mathcal{J}} \sum_{r \in \mathcal{R}} \sum_{d \in \mathcal{D}_r} P_r\, a_d (x_{i,j,d} + v^k_{i,j,d}) \mu_{i,j,r,d} \Bigg\} && \text{(B.7a)}\\
\text{subject to} \quad & \lambda_{i,t} \leq c^{\mathrm{u}}_t, \quad \forall i \in \mathcal{I},\, t \in \mathcal{T}, && \text{(B.7b)}\\
& \pi_{j,t} \leq c^{\mathrm{h}}_t, \quad \forall j \in \mathcal{J},\, t \in \mathcal{T}, && \text{(B.7c)}\\
& \lambda_{i,t} + \pi_{j,t} - \mu_{i,j,r,d} \leq c^{\mathrm{t}}_{i,j,d}, \quad \forall i \in \mathcal{I},\, j \in \mathcal{J},\, r \in \mathcal{R},\, d \in \mathcal{D}_r,\, t \in \mathcal{T}, && \text{(B.7d)}\\
& \mu_{i,j,r,d} \geq 0, \quad \forall i \in \mathcal{I},\, j \in \mathcal{J},\, r \in \mathcal{R},\, d \in \mathcal{D}_r. && \text{(B.7e)}
\end{aligned}$$

We define $\mathcal{G} := \{(\boldsymbol{\mu}, \boldsymbol{\pi}, \boldsymbol{\lambda}) \mid \text{(B.7b)–(B.7e)}\}$ as the feasible set of the dual problem (B.7). Replacing $\widetilde{Q}(\boldsymbol{x}, \boldsymbol{w}, \boldsymbol{\xi}; \boldsymbol{v}^k)$ in constraints (B.6b) with its dual (B.7), we derive the following equivalent reformulation of (B.6).

$$\begin{aligned}
\underset{\chi, \boldsymbol{e}, \boldsymbol{q}}{\text{maximize}} \quad & \chi && \text{(B.8a)}\\
\text{subject to} \quad & \chi \leq \max_{(\boldsymbol{\pi}^k, \boldsymbol{\mu}^k, \boldsymbol{\lambda}^k) \in \mathcal{G}} \Bigg\{ \sum_{i \in \mathcal{I}} \sum_{j \in \mathcal{J}} \sum_{d \in \mathcal{D}} c^{\mathrm{m},2}_{i,j,d} v^k_{i,j,d} + \sum_{i \in \mathcal{I}} \sum_{t \in \mathcal{T}} q_{i,t} \lambda^k_{i,t} + \sum_{j \in \mathcal{J}} \sum_{t \in \mathcal{T}} w_{j,t}\, e_{j,t} \pi^k_{j,t}
\end{aligned}$$

$$- \sum_{i\in\mathcal{I}} \sum_{j\in\mathcal{J}} \sum_{r\in\mathcal{R}} \sum_{d\in\mathcal{D}_r} P_r\, a_d (x_{i,j,d} + v^k_{i,j,d}) \mu^k_{i,j,r,d} \Bigg\}, \quad \forall k \in [K], \tag{B.8b}$$

$$(\boldsymbol{e}, \boldsymbol{q}) \in \mathcal{U}(\boldsymbol{z}, \boldsymbol{a}; \boldsymbol{\kappa}, \Gamma). \tag{B.8c}$$

Note that the maximization problem in constraints (B.8b) is LP for each $k \in [K]$. Thus, the optimal value is always attained by some feasible solution, and (B.8b) holds if and only if there exists $(\boldsymbol{\mu}^k, \boldsymbol{\pi}^k, \boldsymbol{\lambda}^k) \in \mathcal{G}$ such that

$$\chi \le \sum_{i\in\mathcal{I}} \sum_{j\in\mathcal{J}} \sum_{d\in\mathcal{D}} c^{\mathrm{m},2}_{i,j,d} v^k_{i,j,d} + \sum_{i\in\mathcal{I}} \sum_{t\in\mathcal{T}} q_{i,t} \lambda^k_{i,t} + \sum_{j\in\mathcal{J}} \sum_{t\in\mathcal{T}} w_{j,t}\, e_{j,t} \pi^k_{j,t} - \sum_{i\in\mathcal{I}} \sum_{j\in\mathcal{J}} \sum_{r\in\mathcal{R}} \sum_{d\in\mathcal{D}_r} P_r\, a_d (x_{i,j,d} + v^k_{i,j,d}) \mu^k_{i,j,r,d}$$

holds. Consequently, we can reformulate (B.8) by introducing decision variables $(\boldsymbol{\mu}, \boldsymbol{\pi}, \boldsymbol{\lambda})$ and incorporating the constraints of the maximization problem in (B.8b) into (B.8) as follows:

$$\underset{\chi, \boldsymbol{e}, \boldsymbol{q}, \boldsymbol{\pi}, \boldsymbol{\mu}, \boldsymbol{\lambda}}{\text{maximize}} \quad \chi \tag{B.9a}$$

$$\text{subject to} \quad \chi \le \sum_{i\in\mathcal{I}} \sum_{j\in\mathcal{J}} \sum_{d\in\mathcal{D}} c^{\mathrm{m},2}_{i,j,d} v^k_{i,j,d} + \sum_{i\in\mathcal{I}} \sum_{t\in\mathcal{T}} q_{i,t} \lambda^k_{i,t} + \sum_{j\in\mathcal{J}} \sum_{t\in\mathcal{T}} w_{j,t}\, e_{j,t} \pi^k_{j,t}$$

$$- \sum_{i\in\mathcal{I}} \sum_{j\in\mathcal{J}} \sum_{r\in\mathcal{R}} \sum_{d\in\mathcal{D}_r} P_r\, a_d (x_{i,j,d} + v^k_{i,j,d}) \mu^k_{i,j,r,d}, \quad \forall k \in [K], \tag{B.9b}$$

$$(\boldsymbol{\mu}^k,\, \boldsymbol{\pi}^k,\, \boldsymbol{\lambda}^k) \in \mathcal{G}, \quad \forall k \in [K], \tag{B.9c}$$

$$(\boldsymbol{e}, \boldsymbol{q}) \in \mathcal{U}(\boldsymbol{z}, \boldsymbol{a}; \boldsymbol{\kappa}, \Gamma). \tag{B.9d}$$

Note that (B.9) is equivalent to

$$\underset{(\boldsymbol{\pi}^k, \boldsymbol{\mu}^k, \boldsymbol{\lambda}^k) \in \mathcal{G},\, k\in[K]}{\text{maximize}} \quad G\left(\boldsymbol{x}, \boldsymbol{w}, \boldsymbol{z}, \boldsymbol{v}; \boldsymbol{a}, \boldsymbol{\mu}, \boldsymbol{\pi}, \boldsymbol{\lambda}\right),$$

where $G\left(\boldsymbol{x}, \boldsymbol{w}, \boldsymbol{z}, \boldsymbol{v}; \boldsymbol{a}, \boldsymbol{\mu}, \boldsymbol{\pi}, \boldsymbol{\lambda}\right)$ is the optimal value of the following maximization problem

$$\underset{\chi, \boldsymbol{e}, \boldsymbol{q}}{\text{maximize}} \quad \chi \tag{B.10a}$$

$$\text{subject to} \quad \chi \le \sum_{i\in\mathcal{I}} \sum_{j\in\mathcal{J}} \sum_{d\in\mathcal{D}} c^{\mathrm{m},2}_{i,j,d} v^k_{i,j,d} + \sum_{i\in\mathcal{I}} \sum_{t\in\mathcal{T}} q_{i,t} \lambda^k_{i,t} + \sum_{j\in\mathcal{J}} \sum_{t\in\mathcal{T}} w_{j,t}\, e_{j,t} \pi^k_{j,t}$$

$$- \sum_{i\in\mathcal{I}} \sum_{j\in\mathcal{J}} \sum_{r\in\mathcal{R}} \sum_{d\in\mathcal{D}_r} P_r\, a_d (x_{i,j,d} + v^k_{i,j,d}) \mu^k_{i,j,r,d}, \quad \forall k \in [K], \tag{B.10b}$$

$$(\boldsymbol{e}, \boldsymbol{q}) \in \mathcal{U}(\boldsymbol{z}, \boldsymbol{a}; \boldsymbol{\kappa}, \Gamma). \tag{B.10c}$$

Finally, we can rewrite (B.10) as the following LP:

$$\underset{\chi, \boldsymbol{e}, \boldsymbol{q}, \boldsymbol{\tau}}{\text{maximize}} \quad \chi \tag{B.11a}$$

$$
\begin{aligned}
\text{subject to}\quad \chi \le{}& \sum_{i\in\mathcal{I}}\sum_{j\in\mathcal{J}}\sum_{d\in\mathcal{D}} c^{\mathrm{m},2}_{i,j,d} v^k_{i,j,d} + \sum_{i\in\mathcal{I}}\sum_{t\in\mathcal{T}} q_{i,t}\lambda^k_{i,t} + \sum_{j\in\mathcal{J}}\sum_{t\in\mathcal{T}} w_{j,t}\, e_{j,t}\pi^k_{j,t} \\
&- \sum_{i\in\mathcal{I}}\sum_{j\in\mathcal{J}}\sum_{r\in\mathcal{R}}\sum_{d\in\mathcal{D}_r} P_r\, a_d(x_{i,j,d}+v^k_{i,j,d})\mu^k_{i,j,r,d}, \quad \forall k\in[K], && \text{(B.11b)}\\
& T(\tau_j - \kappa^{\mathrm{f}}_j) \le \sum_{t\in\mathcal{T}}(1-e_{j,t}) \le T(\tau_j + \kappa^{\mathrm{f}}_j), \quad \forall j\in\mathcal{J}, && \text{(B.11c)}\\
& \sum_{d\in\mathcal{D}}(1-a_d)z_{j,d} - \tau_j \sum_{d\in\mathcal{D}} z_{j,d} \le \kappa^{\mathrm{d}}_j \sum_{d\in\mathcal{D}} z_{j,d}, \quad \forall j\in\mathcal{J}, && \text{(B.11d)}\\
& q_{i,t} = \bar{q}_{i,t} + \sum_{j\in\mathcal{J}} \tau_j\, \tilde{q}_{i,j,t}, \quad \forall i\in\mathcal{I},\, t\in\mathcal{T}, && \text{(B.11e)}\\
& \sum_{j\in\mathcal{J}} \tau_j \le \Gamma, && \text{(B.11f)}\\
& e_{j,t}\in[0,1], \quad \forall j\in\mathcal{J},\, t\in\mathcal{T}, && \text{(B.11g)}\\
& \tau_j \in [0,1], \quad \forall j\in\mathcal{J}, && \text{(B.11h)}\\
& q_{i,t}\ge 0, \quad \forall i\in\mathcal{I},\, t\in\mathcal{T}. && \text{(B.11i)}
\end{aligned}
$$

By LP duality, $G(\boldsymbol{x},\boldsymbol{w},\boldsymbol{z},\boldsymbol{v};\boldsymbol{a},\boldsymbol{\mu},\boldsymbol{\pi},\boldsymbol{\lambda})$ equals the optimal value of the dual of (B.11), which is (15). This completes the proof. □

Appendix B.4. Proof of Theorem 2

Proof. Proof. Consider the optimization problem $\widetilde{Q}(\boldsymbol{x},\boldsymbol{w},\boldsymbol{\xi};\boldsymbol{v})$ defined in (9) and its dual formulation (B.7). Let $(\boldsymbol{n},\boldsymbol{u},\boldsymbol{h})$ be a primal feasible solution to (9) and $(\boldsymbol{\mu},\boldsymbol{\pi},\boldsymbol{\lambda})$ be a dual feasible solution to (B.7). These solutions are optimal if and only if they satisfy the following complementary slackness conditions:

$$
\begin{aligned}
& \mu_{i,j,r,d}\cdot\left(P_r\, a_d(x_{i,j,d}+v_{i,j,d}) - \sum_{t\in\mathcal{T}} n_{i,j,d,t}\right) = 0, \quad \forall r\in\mathcal{R},\, d\in\mathcal{D}_r,\, j\in\mathcal{J},\, i\in\mathcal{I}, && \text{(B.12a)}\\
& u_{i,t}\cdot(c^{\mathrm{u}}_t - \lambda_{i,t}) = 0, \quad \forall i\in\mathcal{I},\, t\in\mathcal{T}, && \text{(B.12b)}\\
& h_{j,t}\cdot\left(c^{\mathrm{h}}_t - \pi_{j,t}\right) = 0, \quad \forall j\in\mathcal{J},\, t\in\mathcal{T}, && \text{(B.12c)}\\
& n_{i,j,d,t}\cdot\left(c^{\mathrm{t}}_{i,j,d} - (\lambda_{i,t}+\pi_{j,t}-\mu_{i,j,r,d})\right) = 0, \quad \forall r\in\mathcal{R}, d\in\mathcal{D}_r\, j\in\mathcal{J},\, i\in\mathcal{I},\, t\in\mathcal{T}. && \text{(B.12d)}
\end{aligned}
$$

Accordingly, we define the set

$$
\widehat{\mathcal{O}}(\boldsymbol{v},\boldsymbol{\xi}) = \Big\{(\boldsymbol{n},\boldsymbol{u},\boldsymbol{h},\boldsymbol{\mu},\boldsymbol{\pi},\boldsymbol{\lambda}) \;\Big|\; (\boldsymbol{n},\boldsymbol{u},\boldsymbol{h})\in\mathcal{H}(\boldsymbol{x},\boldsymbol{w},\boldsymbol{\xi};\boldsymbol{v}),\, (\boldsymbol{\mu},\boldsymbol{\pi},\boldsymbol{\lambda})\in\mathcal{G},\, \text{(B.12a)–(B.12d)}\Big\},
$$

which consists of primal feasibility constraints, dual feasibility constraints, and complementary slackness conditions, characterizing the set of optimal primal and dual solutions to $\widetilde{Q}(\boldsymbol{x},\boldsymbol{w},\boldsymbol{\xi};\boldsymbol{v})$.

Therefore, we can reformulate (B.7) into

$$\underset{\boldsymbol{n},\boldsymbol{u},\boldsymbol{h},\boldsymbol{\mu},\boldsymbol{\pi},\boldsymbol{\lambda}}{\text{maximize}} \quad \left\{ \sum_{i\in\mathcal{I}}\sum_{j\in\mathcal{J}}\sum_{d\in\mathcal{D}} c^{\mathrm{m},2}_{i,j,d} v_{i,j,d} + \sum_{i\in\mathcal{I}}\sum_{j\in\mathcal{J}}\sum_{d\in\mathcal{D}}\sum_{t\in\mathcal{T}} c^{\mathrm{t}}_{i,j,d} n_{i,j,d,t} + \sum_{i\in\mathcal{I}}\sum_{t\in\mathcal{T}} c^{\mathrm{u}}_{t} u_{i,t} + \sum_{j\in\mathcal{J}}\sum_{t\in\mathcal{T}} c^{\mathrm{h}}_{t} h_{j,t} \right\} \tag{B.13a}$$

$$\text{subject to} \quad (\boldsymbol{n},\boldsymbol{u},\boldsymbol{h},\boldsymbol{\mu},\boldsymbol{\pi},\boldsymbol{\lambda}) \in \widehat{\mathcal{O}}(\boldsymbol{v},\boldsymbol{\xi}). \tag{B.13b}$$

Next, we derive an equivalent reformulation of subproblem (18) using the equivalent reformulation (B.13) of $\widetilde{Q}(\boldsymbol{x},\boldsymbol{w},\boldsymbol{\xi};\boldsymbol{v})$. First, we rewrite (18) as

$$\underset{\boldsymbol{a},\boldsymbol{e},\boldsymbol{q}}{\text{maximize}} \quad \eta \tag{B.14a}$$

$$\text{subject to} \quad \eta \le \widetilde{Q}(\boldsymbol{x},\boldsymbol{w},\boldsymbol{\xi};\boldsymbol{v}^k), \quad \forall k \in [K], \tag{B.14b}$$

$$(\boldsymbol{a},\boldsymbol{e},\boldsymbol{q}) \in \mathcal{U}_L(\boldsymbol{z};\boldsymbol{\kappa},\Gamma). \tag{B.14c}$$

Note that for a fixed reassignment decisions $\{\boldsymbol{v}^k\}_{k=1}^K$, constraint (B.14b) holds if and only if there exists $(\boldsymbol{n},\boldsymbol{u},\boldsymbol{h},\boldsymbol{\mu},\boldsymbol{\pi},\boldsymbol{\lambda}) \in \widehat{\mathcal{O}}(\boldsymbol{v},\boldsymbol{\xi})$ such that η is less than or equal to the objective function (B.13a) evaluated at $(\boldsymbol{n},\boldsymbol{u},\boldsymbol{h},\boldsymbol{\mu},\boldsymbol{\pi},\boldsymbol{\lambda})$. That is, (B.14) is equivalent to

$$\underset{\substack{\boldsymbol{\tau},\boldsymbol{a},\boldsymbol{e},\boldsymbol{q},\eta \\ \boldsymbol{n},\boldsymbol{u},\boldsymbol{h},\boldsymbol{\mu},\boldsymbol{\pi},\boldsymbol{\lambda}}}{\text{maximize}} \quad \eta \tag{B.15a}$$

$$\text{subject to} \quad \eta \le \sum_{i\in\mathcal{I}}\sum_{j\in\mathcal{J}}\sum_{d\in\mathcal{D}} c^{\mathrm{m},2}_{i,j,d} v^k_{i,j,d} + \sum_{i\in\mathcal{I}}\sum_{j\in\mathcal{J}}\sum_{d\in\mathcal{D}}\sum_{t\in\mathcal{T}} c^{\mathrm{t}}_{i,j,d} n^k_{i,j,d,t} + \sum_{i\in\mathcal{I}}\sum_{t\in\mathcal{T}} c^{\mathrm{u}}_{t} u^k_{i,t} + \sum_{j\in\mathcal{J}}\sum_{t\in\mathcal{T}} c^{\mathrm{h}}_{t} h^k_{j,t}, \quad \forall k \in [K], \tag{B.15b}$$

$$(\boldsymbol{n}^k,\boldsymbol{u}^k,\boldsymbol{h}^k,\boldsymbol{\mu}^k,\boldsymbol{\pi}^k,\boldsymbol{\lambda}^k) \in \widehat{\mathcal{O}}(\boldsymbol{v}^k,\boldsymbol{\xi}), \quad \forall k \in [K], \tag{B.15c}$$

$$(\boldsymbol{a},\boldsymbol{e},\boldsymbol{q}) \in \mathcal{U}_L(\boldsymbol{z};\boldsymbol{\kappa},\Gamma). \tag{B.15d}$$

Note that (B.15) is non-linear due to the complementary slackness constraints (B.12a)–(B.12d) in $\widehat{\mathcal{O}}(\boldsymbol{v},\boldsymbol{\xi})$. To linearize constraints (B.12a)–(B.12d), we introduce binary variables $\alpha_{i,j,r,d}$, $\beta_{j,t}$, $\theta_{i,t}$, and $\iota_{i,j,d,t}$ and the following constraints

$$\mu_{i,j,r,d} \le M^{\boldsymbol{\alpha}_1}_{i,j,r,d}\, \alpha_{i,j,r,d}, \quad \forall i \in \mathcal{I},\, j \in \mathcal{J},\, r \in \mathcal{R},\, d \in \mathcal{D}_r, \tag{B.16a}$$

$$P_r\, a_d(x_{i,j,d} + v_{i,j,d}) - \sum_{t\in\mathcal{T}} n_{i,j,d,t} \le M^{\boldsymbol{\alpha}_2}_{i,j,r,d}(1-\alpha_{i,j,r,d}), \quad \forall i \in \mathcal{I},\, j \in \mathcal{J},\, r \in \mathcal{R},\, d \in \mathcal{D}_r, \tag{B.16b}$$

$$u_{i,t} \le M^{\boldsymbol{\theta}_1}_{i,t}\, \theta_{i,t}, \quad \forall i \in \mathcal{I},\, t \in \mathcal{T}, \tag{B.16c}$$

$$c^{\mathrm{u}}_t - \lambda_{i,t} \le M^{\boldsymbol{\theta}_2}_{i,t}(1-\theta_{i,t}), \quad \forall i \in \mathcal{I},\, t \in \mathcal{T}, \tag{B.16d}$$

$$h_{j,t} \le M^{\boldsymbol{\beta}_1}_{j,t}\, \beta_{j,t}, \quad \forall j \in \mathcal{J},\, t \in \mathcal{T}, \tag{B.16e}$$

$$c^{\mathrm{h}}_t - \pi_{j,t} \le M^{\boldsymbol{\beta}_2}_{j,t}\, (1-\beta_{j,t}), \quad \forall j \in \mathcal{J},\, t \in \mathcal{T}, \tag{B.16f}$$

$$n_{i,j,d,t} \le M^{\boldsymbol{\iota}_1}_{i,j,d,t}\, \iota_{i,j,d,t}, \quad \forall i \in \mathcal{I},\, j \in \mathcal{J},\, d \in \mathcal{D},\, t \in \mathcal{T}, \tag{B.16g}$$

$$c^{\mathrm{t}}_{i,j,d} - (\lambda_{i,t} + \pi_{j,t} - \mu_{i,j,r,d}) \le M^{\boldsymbol{\iota}_2}_{i,j,d,t}(1-\iota_{i,j,d,t}), \quad \forall i \in \mathcal{I},\, j \in \mathcal{J},\, r \in \mathcal{R},\, d \in \mathcal{D}_r,\, t \in \mathcal{T}, \tag{B.16h}$$

$$\alpha_{i,j,r,d} \in \{0,1\}, \quad \forall i \in \mathcal{I},\, j \in \mathcal{J},\, r \in \mathcal{R},\, d \in \mathcal{D}_r, \tag{B.16i}$$

$$\beta_{j,t} \in \{0,1\}, \quad \forall j \in \mathcal{J},\, t \in \mathcal{T}, \tag{B.16j}$$

$$\theta_{i,t} \in \{0,1\}, \quad \forall i \in \mathcal{I}, t \in \mathcal{T}, \tag{B.16k}$$

$$\iota_{i,j,r,d,t} \in \{0,1\}, \quad \forall i \in \mathcal{I}, j \in \mathcal{J},\, r \in \mathcal{R},\, d \in \mathcal{D}_r,\, t \in \mathcal{T}, \tag{B.16l}$$

where $M^{\alpha_\ell}_{i,j,r,d}$, $M^{\theta_\ell}_{i,t}$, $M^{\beta_\ell}_{j,t}$, and $M^{\iota_\ell}_{i,j,r,d}$ are sufficiently large constants for $\ell \in \{1,2\}$. Accordingly, we can replace $\widehat{\mathcal{O}}(\boldsymbol{v},\boldsymbol{\xi})$ in (B.15c) by the set

$$\mathcal{O}(\boldsymbol{v},\boldsymbol{\xi}) = \Big\{(\boldsymbol{n},\boldsymbol{u},\boldsymbol{h},\boldsymbol{\mu},\boldsymbol{\pi},\boldsymbol{\lambda},\boldsymbol{\alpha},\boldsymbol{\beta},\boldsymbol{\theta},\boldsymbol{\iota}) \;\Big|\; (\boldsymbol{n},\boldsymbol{u},\boldsymbol{h}) \in \mathcal{H}(\boldsymbol{x},\boldsymbol{w},\boldsymbol{\xi};\boldsymbol{v}),\, (\boldsymbol{\mu},\boldsymbol{\pi},\boldsymbol{\lambda}) \in \mathcal{G},\, \text{(B.16a)–(B.16l)}\Big\}.$$

In summary, an equivalent formulation of subproblem (18) is shown as (20). □

Appendix B.5. Proof of Theorem 3

Proof. Proof. Let $\widehat{\mathcal{S}}^{\mathfrak{k}}$ be the set of scenarios used in the master problem (Step 1) in iteration $\mathfrak{k} \in \mathbb{N}$. Also, let $LB^{\mathfrak{k}}$ and $UB^{\mathfrak{k}}$ be the lower and upper bounds updated in iteration $\mathfrak{k} \in \mathbb{N}$. First, we show that if a scenario $\boldsymbol{s}^{\mathfrak{k}} = (\boldsymbol{\xi}^{\mathfrak{k}}, \boldsymbol{\mu}^{\mathfrak{k}}, \boldsymbol{\pi}^{\mathfrak{k}}, \boldsymbol{\lambda}^{\mathfrak{k}})$ identified (in Step 2) in iteration $\mathfrak{k}$ belongs to the current scenario set $\widehat{\mathcal{S}}^{\mathfrak{k}}$, i.e., $\boldsymbol{s}^{\mathfrak{k}} \in \widehat{\mathcal{S}}$, the algorithm will terminate in iteration $\mathfrak{k}$. Let $(\boldsymbol{y}^{\mathfrak{k}}, \boldsymbol{x}^{\mathfrak{k}}, \boldsymbol{w}^{\mathfrak{k}}, \boldsymbol{z}^{\mathfrak{k}}, \boldsymbol{v}^{\mathfrak{k}}, \eta^{\mathfrak{k}})$ be the optimal solution to the master problem obtained in Step 1. For notational simplicity, also let $f(\boldsymbol{y},\boldsymbol{x},\boldsymbol{w},\boldsymbol{z}) = \sum_{j\in\mathcal{J}}\sum_{l\in\mathcal{L}} c^{\mathrm{f}}_l y_{j,l} + \sum_{j\in\mathcal{J}}\sum_{t\in\mathcal{T}} c^{\mathrm{a}}_t w_{j,t} + \sum_{j\in\mathcal{J}}\sum_{r\in\mathcal{R}}\sum_{d\in\mathcal{D}_r} c^{\mathrm{d}}_r z_{j,d} + \sum_{i\in\mathcal{I}}\sum_{j\in\mathcal{J}}\sum_{d\in\mathcal{D}} c^{\mathrm{m},1}_{i,j,d} x_{i,j,d}$ be the first-stage cost. Then,

$$LB^{\mathfrak{k}} = f(\boldsymbol{y}^{\mathfrak{k}}, \boldsymbol{x}^{\mathfrak{k}}, \boldsymbol{w}^{\mathfrak{k}}, \boldsymbol{z}^{\mathfrak{k}}) + \eta^{\mathfrak{k}} \ge f(\boldsymbol{y}^{\mathfrak{k}}, \boldsymbol{x}^{\mathfrak{k}}, \boldsymbol{w}^{\mathfrak{k}}, \boldsymbol{z}^{\mathfrak{k}}) + \max_{\boldsymbol{s}\in\widehat{\mathcal{S}}^{\mathfrak{k}}} \left\{ \min_{k\in[K]} \widetilde{Q}(\boldsymbol{x}^{\mathfrak{k}}, \boldsymbol{z}^{\mathfrak{k}}, \boldsymbol{\xi}; \boldsymbol{v}^{\mathfrak{k},k}) \right\} \tag{B.17a}$$

$$\ge f(\boldsymbol{y}^{\mathfrak{k}}, \boldsymbol{x}^{\mathfrak{k}}, \boldsymbol{w}^{\mathfrak{k}}, \boldsymbol{z}^{\mathfrak{k}}) + \min_{k\in[K]} \widetilde{Q}(\boldsymbol{x}^{\mathfrak{k}}, \boldsymbol{z}^{\mathfrak{k}}, \boldsymbol{\xi}^{\mathfrak{k}}; \boldsymbol{v}^{\mathfrak{k},k}). \tag{B.17b}$$

Here, (B.17a) follows from (10c) and (B.17b) follows from the fact that $\boldsymbol{s}^{\mathfrak{k}} \in \widehat{\mathcal{S}}$, i.e., $\boldsymbol{\xi}^{\mathfrak{k}} \in \mathcal{U}(\boldsymbol{z}^{\mathfrak{k}}; \boldsymbol{\kappa}, \Gamma)$. Next, note that

$$\begin{aligned} UB^{\mathfrak{k}} &\le f(\boldsymbol{y}^{\mathfrak{k}}, \boldsymbol{x}^{\mathfrak{k}}, \boldsymbol{w}^{\mathfrak{k}}, \boldsymbol{z}^{\mathfrak{k}}) + \max_{(\boldsymbol{a},\boldsymbol{e},\boldsymbol{q})\in\mathcal{U}(\boldsymbol{z}^{\mathfrak{k}};\boldsymbol{\kappa},\Gamma)} \min_{k\in[K]} \widetilde{Q}(\boldsymbol{x}^{\mathfrak{k}}, \boldsymbol{w}^{\mathfrak{k}}, \boldsymbol{\xi}; \boldsymbol{v}^{\mathfrak{k},k}) \\ &= f(\boldsymbol{y}^{\mathfrak{k}}, \boldsymbol{x}^{\mathfrak{k}}, \boldsymbol{w}^{\mathfrak{k}}, \boldsymbol{z}^{\mathfrak{k}}) + \min_{k\in[K]} \widetilde{Q}(\boldsymbol{x}^{\mathfrak{k}}, \boldsymbol{z}^{\mathfrak{k}}, \boldsymbol{\xi}^{\mathfrak{k}}; \boldsymbol{v}^{\mathfrak{k},k}), \end{aligned} \tag{B.18}$$

where (B.18) follows from the fact that scenario $\boldsymbol{s}^{\mathfrak{k}}$ is optimal to the subproblem. Combining (B.17) and (B.18), we have $UB^{\mathfrak{k}} - LB^{\mathfrak{k}} \leq 0$. Thus, the algorithm will terminate in iteration $\mathfrak{k}$.

Next, we show that there is at most a finite number of new scenarios identified from solving the subproblem. It suffices to show that, without loss of optimality, we can optimize the subproblem (18) over a finite number of $\boldsymbol{s} = (\boldsymbol{a}, \boldsymbol{\mu}, \boldsymbol{\pi}, \boldsymbol{\lambda})$. First, note that for any feasible first-stage decision, the recourse function $\widetilde{Q}(\boldsymbol{x}, \boldsymbol{z}, \boldsymbol{\xi}; \boldsymbol{v}^k)$ is always finite for all $k \in [K]$. Thus, there always exists an dual optimal solution $(\boldsymbol{\mu}^k, \boldsymbol{\pi}^k, \boldsymbol{\lambda}^k) \in \mathcal{G}$ which is an extreme point of $\mathcal{G}$. Therefore, without loss of optimality, we can maximize $(\boldsymbol{\mu}^k, \boldsymbol{\pi}^k, \boldsymbol{\lambda}^k)$ over the finite set $\mathrm{ext}(\mathcal{G})$, the set of extreme points of $\mathcal{G}$. Note that a_d is binary for all $d \in \mathcal{D}$. Thus, there are only a finite number of combinations $\{\boldsymbol{a}\} \times (\boldsymbol{\mu}^k, \boldsymbol{\pi}^k, \boldsymbol{\lambda}^k) \in \{0,1\}^{|\mathcal{D}|} \times \mathrm{ext}(\mathcal{G})$. Hence, the C&CG algorithm terminates in a finite number of iterations.

□

Appendix B.6. Proof of Proposition 3

Proof. Proof. Consider a first-stage decision $(\boldsymbol{y}, \boldsymbol{w}, \boldsymbol{x}, \boldsymbol{z}, \boldsymbol{v}, \eta)$ to formulation (10). Suppose $\boldsymbol{\xi}^* = (\boldsymbol{a}^*, \boldsymbol{e}^*, \boldsymbol{q}^*)$ denotes the worst-case realization of uncertainty in (10c), $\boldsymbol{v}^{k^*}$ represents the corresponding optimal reassignment policy, and $(\boldsymbol{n}^*, \boldsymbol{u}^*, \boldsymbol{h}^*)$ denotes the associated optimal second-stage decisions to $\widetilde{Q}(\boldsymbol{x}, \boldsymbol{w}, \boldsymbol{\xi}^*; \boldsymbol{v}^{k^*})$. Note that

$$\eta \geq \max_{\boldsymbol{\xi} \in \mathcal{U}(\boldsymbol{z}; \boldsymbol{\kappa}, \Gamma)} \min_{k \in [K]} \widetilde{Q}(\boldsymbol{x}, \boldsymbol{w}, \boldsymbol{\xi}; \boldsymbol{v}^k) \tag{B.19a}$$

$$\geq \min_{k \in [K]} \widetilde{Q}(\boldsymbol{x}, \boldsymbol{w}, \boldsymbol{\xi}^*; \boldsymbol{v}^k) \tag{B.19b}$$

$$= \sum_{i \in \mathcal{I}} \sum_{j \in \mathcal{J}} \sum_{d \in \mathcal{D}} c^{\mathrm{m},2}_{i,j,d} \, v^{k^*}_{i,j,d} + \sum_{i \in \mathcal{I}} \sum_{j \in \mathcal{J}} \sum_{d \in \mathcal{D}} \sum_{t \in \mathcal{T}} c^{\mathrm{t}}_{i,j,d} n^*_{i,j,d,t} + \sum_{i \in \mathcal{I}} \sum_{t \in \mathcal{T}} c^{\mathrm{u}}_t u^*_{i,t} + \sum_{j \in \mathcal{J}} \sum_{t \in \mathcal{T}} c^{\mathrm{h}}_t h^*_{j,t} \tag{B.19c}$$

$$\geq \sum_{i \in \mathcal{I}} \sum_{j \in \mathcal{J}} \sum_{d \in \mathcal{D}} \sum_{t \in \mathcal{T}} c^{\mathrm{t}}_{i,j,d} n^*_{i,j,d,t} + \sum_{i \in \mathcal{I}} \sum_{t \in \mathcal{T}} c^{\mathrm{u}}_t u^*_{i,t}. \tag{B.19d}$$

Here, (B.19a) follows from constraints (10c), (B.19b) follows from the definition of $\boldsymbol{\xi}^*$, (B.19c) holds based on the definition of recourse objective function $\widetilde{Q}$, and (B.19d) is valid because of the nonnegativity of decisions $\boldsymbol{v}^{k^*}$ and $\boldsymbol{h}^*$. Furthermore, deriving from (B.19d), we have

$$\sum_{i \in \mathcal{I}} \sum_{j \in \mathcal{J}} \sum_{d \in \mathcal{D}} \sum_{t \in \mathcal{T}} c^{\mathrm{t}}_{i,j,d} n^*_{i,j,d,t} + \sum_{i \in \mathcal{I}} \sum_{t \in \mathcal{T}} c^{\mathrm{u}}_t u^*_{i,t} \tag{B.20a}$$

$$= \sum_{i \in \mathcal{I}} \sum_{t \in \mathcal{T}} \left(c^{\mathrm{u}}_t u^*_{i,t} + \sum_{j \in \mathcal{J}} \sum_{d \in \mathcal{D}} c^{\mathrm{t}}_{i,j,d} n^*_{i,j,d,t} \right) \tag{B.20b}$$

$$\geq \sum_{i \in \mathcal{I}} \sum_{t \in \mathcal{T}} \min \left\{ c^{\mathrm{u}}_t, \min_{j \in \mathcal{J}, d \in \mathcal{D}} \{ c^{\mathrm{t}}_{i,j,d} \} \right\} \left(u^*_{i,t} + \sum_{j \in \mathcal{J}} \sum_{d \in \mathcal{D}} n^*_{i,j,d,t} \right) \tag{B.20c}$$

$$= \sum_{i \in \mathcal{I}} \sum_{t \in \mathcal{T}} \min_{j \in \mathcal{J}, d \in \mathcal{D}} \{ c^{\mathrm{t}}_{i,j,d} \} \, q^*_{i,t} \tag{B.20d}$$

$$= \sum_{i\in\mathcal{I}} \sum_{t\in\mathcal{T}} \min_{j\in\mathcal{J},d\in\mathcal{D}} \{c^{\mathrm{t}}_{i,j,d}\} \left(\bar{q}_{i,t} + \sum_{j\in\mathcal{J}} \tau^*_j \, \tilde{q}_{i,j,t} \right) \tag{B.20e}$$

$$\geq \sum_{i\in\mathcal{I}} \sum_{t\in\mathcal{T}} \min_{j\in\mathcal{J},d\in\mathcal{D}} \{c^{\mathrm{t}}_{i,j,d}\} \, \bar{q}_{i,t}, \tag{B.20f}$$

where $\boldsymbol{\tau}^*$ is the value of $\boldsymbol{\tau}$ corresponding to the worst-case scenario $\boldsymbol{\xi}^* = (\boldsymbol{a}^*, \boldsymbol{e}^*, \boldsymbol{q}^*)$ in (5). Here, (B.20d) holds since $\max_{i\in\mathcal{I},j\in\mathcal{J},d\in\mathcal{D}}\{c^{\mathrm{t}}_{i,j,d}\} < c^{\mathrm{h}}_t < c^{\mathrm{u}}_t$, and $(\boldsymbol{n}^*, \boldsymbol{u}^*, \boldsymbol{h}^*)$ satisfy constraints (3b). (B.20e) is derived based on the definition of uncertain demand $\boldsymbol{q}$ in (5), and (B.20f) holds because of the nonnegativity of terms $\sum_{j\in\mathcal{J}} \tau^*_j \, \tilde{q}_{i,j,t}$ for all $i \in \mathcal{I}, j \in \mathcal{J}$ and $t \in \mathcal{T}$. This shows that inequality (24) is valid for (10). Therefore, without loss of optimality, we can impose (24) to the master problem (19).

□

Appendix C. Choice of Big-M Parameters

In formulation (20), we have eight big-M parameters involved in constraints (21). In this appendix, we derive a suitable choice of these parameters for actual implementation. First, in the following proposition, we derive valid lower bounds on variables $\boldsymbol{\lambda}$ and $\boldsymbol{\pi}$ of the dual problem of $\widetilde{Q}(\boldsymbol{x}, \boldsymbol{w}, \boldsymbol{\xi}; \boldsymbol{v})$.

Proposition 4. For any value of parameters $\{c^{\mathrm{t}}_{i,j,d}\}_{i\in\mathcal{I},d\in\mathcal{D},t\in\mathcal{T}}$, $\{c^{\mathrm{h}}_t\}_{t\in\mathcal{T}}$, and $\{c^{\mathrm{u}}_t\}_{t\in\mathcal{T}}$, we have

(a) $\lambda_{i,t} \geq \min_{j\in\mathcal{J},d\in\mathcal{D}_r} \{c^{\mathrm{t}}_{i,j,d} - c^{\mathrm{h}}_t\}$ for all $i \in \mathcal{I}$ and $t \in \mathcal{T}$;

(b) $\pi_{j,t} \geq \min_{i\in\mathcal{I},d\in\mathcal{D}_r} \{c^{\mathrm{t}}_{i,j,d} - c^{\mathrm{u}}_t\}$ for all $j \in \mathcal{J}$ and $t \in \mathcal{T}$.

Proof. Proof. We first prove part (a). Consider the optimization problem $\widetilde{Q}(\boldsymbol{x}, \boldsymbol{w}, \boldsymbol{\xi}; \boldsymbol{v})$ in (B.7). Constraints (B.7d) and (B.7e) ensure that $\mu_{i,j,r,d} \geq \max_{t\in\mathcal{T}} \{\lambda_{i,t} + \pi_{j,t} - c^{\mathrm{t}}_{i,j,d}\}$ and $\mu_{i,j,r,d} \geq 0$, respectively, for all $i \in \mathcal{I}$, $j \in \mathcal{J}$, $r \in \mathcal{R}$, and $d \in \mathcal{D}_r$. Since $P_r a_d(x_{i,j,d} + v_{i,j,d}) \geq 0$ and we maximize $-P_r a_d(x_{i,j,d} + v_{i,j,d})\mu_{i,j,r,d}$ in the objective (B.7a), at optimality, we have

$$\mu_{i,j,r,d} = \left(\max \left\{ \max_{t''\in\mathcal{T}\setminus\{t\}} \{\lambda_{i,t''} + \pi_{j,t''} - c^{\mathrm{t}}_{i,j,d}\}, \, \lambda_{i,t} + \pi_{j,t} - c^{\mathrm{t}}_{i,j,d} \right\} \right)^+. \tag{C.1}$$

Now, let $(\boldsymbol{\mu}^*, \boldsymbol{\pi}^*, \boldsymbol{\lambda}^*) \in \mathcal{G}$ be a feasible to (B.7) with $\lambda^*_{i,t} < \min_{j\in\mathcal{J},r\in\mathcal{R},d\in\mathcal{D}_r} \{c^{\mathrm{t}}_{i,j,d} - c^{\mathrm{h}}_t\} < 0$ for some $i \in \mathcal{I}$ and $t \in \mathcal{T}$. Consider another solution $(\widetilde{\boldsymbol{\mu}}, \widetilde{\boldsymbol{\pi}}, \widetilde{\boldsymbol{\lambda}})$, where $\widetilde{\boldsymbol{\pi}} = \boldsymbol{\pi}^*$, $\widetilde{\boldsymbol{\mu}} = \boldsymbol{\mu}^*$, and for all $i' \in \mathcal{I}, t' \in \mathcal{T}$, we define $\widetilde{\lambda}_{i',t'}$ as

$$\widetilde{\lambda}_{i',t'} = \begin{cases} \lambda^*_{i',t'} & \text{if } (i',t') \neq (i,t), \\ \min_{j\in\mathcal{J},r\in\mathcal{R},d\in\mathcal{D}_r} \{c^{\mathrm{t}}_{i,j,d} - c^{\mathrm{h}}_t\} & \text{if } (i',t') = (i,t). \end{cases} \tag{C.2}$$

We claim that $(\widetilde{\boldsymbol{\mu}}, \widetilde{\boldsymbol{\pi}}, \widetilde{\boldsymbol{\lambda}}) \in \mathcal{G}$. It is trivial that $(\widetilde{\boldsymbol{\mu}}, \widetilde{\boldsymbol{\pi}}, \widetilde{\boldsymbol{\lambda}})$ satisfies (B.7b)–(B.7c) and (B.7e). Note that if $(i', t') \neq (i, t)$, it is trivial that (B.7d) holds for all $j \in \mathcal{J}$, $r \in \mathcal{R}$, and $d \in \mathcal{D}_r$. If $(i', t') = (i, t)$, then

$$\begin{aligned}
\widetilde{\mu}_{i,j,r,d} &= \mu^*_{i,j,r,d} \\
&= \left(\max \left\{ \max_{t'' \in \mathcal{T} \setminus \{t\}} \{\lambda^*_{i,t''} + \pi^*_{j,t''} - c^{\mathrm{t}}_{i,j,d}\},\ \lambda^*_{i,t} + \pi^*_{j,t} - c^{\mathrm{t}}_{i,j,d} \right\} \right)^+ && \text{(C.3a)} \\
&= \left(\max \left\{ \max_{t'' \in \mathcal{T} \setminus \{t\}} \{\widetilde{\lambda}_{i,t''} + \widetilde{\pi}_{j,t''} - c^{\mathrm{t}}_{i,j,d}\},\ \lambda^*_{i,t} + \pi^*_{j,t} - c^{\mathrm{t}}_{i,j,d} \right\} \right)^+ && \text{(C.3b)} \\
&= \left(\max \left\{ \max_{t'' \in \mathcal{T} \setminus \{t\}} \{\widetilde{\lambda}_{i,t''} + \widetilde{\pi}_{j,t''} - c^{\mathrm{t}}_{i,j,d}\},\ \widetilde{\lambda}_{i,t} + \widetilde{\pi}_{j,t} - c^{\mathrm{t}}_{i,j,d} \right\} \right)^+ && \text{(C.3c)} \\
&\geq \widetilde{\lambda}_{i,t} + \widetilde{\pi}_{j,t} - c^{\mathrm{t}}_{i,j,d}
\end{aligned}$$

for all $j \in \mathcal{J}$, $r \in \mathcal{R}$, and $d \in \mathcal{D}_r$. Here, (C.3a) follows from (C.1), and (C.3b) follows from the construction of $(\widetilde{\boldsymbol{\mu}}, \widetilde{\boldsymbol{\pi}}, \widetilde{\boldsymbol{\lambda}})$ that $\widetilde{\boldsymbol{\pi}} = \boldsymbol{\pi}^*$ and $\widetilde{\boldsymbol{\lambda}}_{i',t'} = \boldsymbol{\lambda}^*_{i',t'}$ if $(i', t') \neq (i, t)$. Furthermore, (C.3c) follows from

$$\lambda^*_{i,t} + \pi^*_{j,t} - c^{\mathrm{t}}_{i,j,d} \leq \widetilde{\lambda}_{i,t} + \widetilde{\pi}_{j,t} - c^{\mathrm{t}}_{i,j,d} \leq (c^{\mathrm{h}}_t - c^{\mathrm{t}}_{i,j,d}) - \max_{j \in \mathcal{J}, r \in \mathcal{R}, d \in \mathcal{D}_r} \{c^{\mathrm{h}}_t - c^{\mathrm{t}}_{i,j,d}\} \leq 0,$$

where the first inequality is derived from the construction $(\widetilde{\boldsymbol{\mu}}, \widetilde{\boldsymbol{\pi}}, \widetilde{\boldsymbol{\lambda}})$, and the second inequality is derived based on constraints (B.7b)–(B.7c). Therefore, if $(i', t') = (i, t)$, (B.7d) still holds for all $j \in \mathcal{J}$, $r \in \mathcal{R}$, and $d \in \mathcal{D}_r$. This proves the claim that $(\widetilde{\boldsymbol{\mu}}, \widetilde{\boldsymbol{\pi}}, \widetilde{\boldsymbol{\lambda}}) \in \mathcal{G}$. Since $q_{i,t} \geq 0$, it is straightforward to verify that the objective function (B.7a) evaluated at $(\widetilde{\boldsymbol{\mu}}, \widetilde{\boldsymbol{\pi}}, \widetilde{\boldsymbol{\lambda}})$ is greater than or equal to that of $(\boldsymbol{\mu}^*, \boldsymbol{\pi}^*, \boldsymbol{\lambda}^*)$. Thus, the lower bound $\lambda_{i,t} \geq \min_{j \in \mathcal{J}, r \in \mathcal{R}, d \in \mathcal{D}_r} \{c^{\mathrm{t}}_{i,j,d} - c^{\mathrm{h}}_t\}$ is valid for all $i \in \mathcal{I}$ and $t \in \mathcal{T}$.

We now prove part (b). Following the same idea as in the proof of part (a), let $(\boldsymbol{\mu}^*, \boldsymbol{\pi}^*, \boldsymbol{\lambda}^*) \in \mathcal{G}$ be a feasible solution to (B.7) with $\pi^*_{j,t} < \min_{i \in \mathcal{I}, r \in \mathcal{R}, d \in \mathcal{D}_r} \{c^{\mathrm{t}}_{i,j,d} - c^{\mathrm{u}}_t\} < 0$ for some $j \in \mathcal{J}$ and $t \in \mathcal{T}$. Consider another feasible solution $(\widetilde{\boldsymbol{\mu}}, \widetilde{\boldsymbol{\pi}}, \widetilde{\boldsymbol{\lambda}})$, where $\widetilde{\boldsymbol{\lambda}} = \boldsymbol{\lambda}^*$, $\widetilde{\boldsymbol{\mu}} = \boldsymbol{\mu}^*$, and $\widetilde{\boldsymbol{\pi}}$ is defined as

$$\widetilde{\pi}_{j',t'} = \begin{cases} \pi^*_{j',t'} & \text{if } (i', t') \neq (i, t), \\ \min_{i \in \mathcal{I}, r \in \mathcal{R}, d \in \mathcal{D}_r} \{c^{\mathrm{t}}_{i,j,d} - c^{\mathrm{u}}_t\} & \text{if } (i', t') = (i, t). \end{cases} \tag{C.4}$$

We claim that $(\widetilde{\boldsymbol{\mu}}, \widetilde{\boldsymbol{\pi}}, \widetilde{\boldsymbol{\lambda}}) \in \mathcal{G}$. It is trivial that $(\widetilde{\boldsymbol{\mu}}, \widetilde{\boldsymbol{\pi}}, \widetilde{\boldsymbol{\lambda}})$ satisfies (B.7b)–(B.7c) and (B.7e). Note that if $(j', t') \neq (j, t)$, it is trivial that (B.7d) holds for all $i \in \mathcal{I}$, $r \in \mathcal{R}$, and $d \in \mathcal{D}_r$. If $(j', t') = (j, t)$, then

$$\widetilde{\mu}_{i,j,r,d} = \mu^*_{i,j,r,d}$$

$$= \left(\max \left\{ \max_{t'' \in \mathcal{T} \setminus \{t\}} \{\lambda^*_{i,t''} + \pi^*_{j,t''} - c^{\mathrm{t}}_{i,j,d}\},\ \lambda^*_{i,t} + \pi^*_{j,t} - c^{\mathrm{t}}_{i,j,d} \right\} \right)^+ \tag{C.5a}$$

$$= \left(\max \left\{ \max_{t'' \in \mathcal{T} \setminus \{t\}} \{\widetilde{\lambda}_{i,t''} + \widetilde{\pi}_{j,t''} - c^{\mathrm{t}}_{i,j,d}\},\ \lambda^*_{i,t} + \pi^*_{j,t} - c^{\mathrm{t}}_{i,j,d} \right\} \right)^+ \tag{C.5b}$$

$$= \left(\max \left\{ \max_{t'' \in \mathcal{T} \setminus \{t\}} \{\widetilde{\lambda}_{i,t''} + \widetilde{\pi}_{j,t''} - c^{\mathrm{t}}_{i,j,d}\},\ \widetilde{\lambda}_{i,t} + \widetilde{\pi}_{j,t} - c^{\mathrm{t}}_{i,j,d} \right\} \right)^+ \tag{C.5c}$$

$$\geq \widetilde{\lambda}_{i,t} + \widetilde{\pi}_{j,t} - c^{\mathrm{t}}_{i,j,d}$$

for all $i \in \mathcal{I}$, $r \in \mathcal{R}$, and $d \in \mathcal{D}_r$. Here, (C.5a) follows from (C.1), and (C.5b) follows from the construction of $(\widetilde{\boldsymbol{\mu}}, \widetilde{\boldsymbol{\pi}}, \widetilde{\boldsymbol{\lambda}})$ Additionally, (C.5c) follows from

$$\lambda^*_{i,t} + \pi^*_{j,t} - c^{\mathrm{t}}_{i,j,d} \leq \widetilde{\lambda}_{i,t} + \widetilde{\pi}_{j,t} - c^{\mathrm{t}}_{i,j,d} \leq (c^{\mathrm{u}}_t - c^{\mathrm{t}}_{i,j,d}) - \max_{i \in \mathcal{I}, r \in \mathcal{R}, d \in \mathcal{D}_r} \{c^{\mathrm{u}}_t - c^{\mathrm{t}}_{i,j,d}\} \leq 0,$$

where the first inequality is derived from the construction $(\widetilde{\boldsymbol{\mu}}, \widetilde{\boldsymbol{\pi}}, \widetilde{\boldsymbol{\lambda}})$, and the second inequality is derived based on constraints (B.7b)–(B.7c). Therefore, if $(j', t') = (j, t)$, (B.7d) still holds for all $i \in \mathcal{I}$, $r \in \mathcal{R}$, and $d \in \mathcal{D}_r$. This proves the claim that $(\widetilde{\boldsymbol{\mu}}, \widetilde{\boldsymbol{\pi}}, \widetilde{\boldsymbol{\lambda}}) \in \mathcal{G}$. Since $w_{j,t} e_{j,t} \geq 0$, it is straightforward to verify that the objective function (B.7a) evaluated at $(\widetilde{\boldsymbol{\mu}}, \widetilde{\boldsymbol{\pi}}, \widetilde{\boldsymbol{\lambda}})$ is greater than or equal to that of $(\boldsymbol{\mu}^*, \boldsymbol{\pi}^*, \boldsymbol{\lambda}^*)$. Thus, the lower bound $\pi_{j,t} \geq \min_{i \in \mathcal{I}, d \in \mathcal{D}} \{c^{\mathrm{t}}_{i,j,d} - c^{\mathrm{u}}_t\}$ is valid for any $j \in \mathcal{J}$ and $t \in \mathcal{T}$. □

Next, in Proposition 5, we derive tight bounds on the big-M parameters. We leverage the results of Proposition 4 in deriving some of these bounds.

Proposition 5. The following are valid choices for the big-Mconstants in (21):

$$M^{\boldsymbol{\alpha}_1}_{i,j,r,d} = \max_{t \in \mathcal{T}} \{c^{\mathrm{u}}_t + c^{\mathrm{h}}_t - c^{\mathrm{t}}_{i,j,d}\},$$
$$M^{\boldsymbol{\alpha}_2}_{i,j,r,d} = P_r,$$
$$M^{\boldsymbol{\theta}_1}_{i,t} = \bar{q}_{i,t} + \sum_j \tilde{q}_{i,j,t},$$
$$M^{\boldsymbol{\theta}_2}_{i,t} = c^{\mathrm{u}}_t - \min_{j \in \mathcal{J}, d \in \mathcal{D}} \{c^{\mathrm{t}}_{i,j,d} - c^{\mathrm{h}}_t\},$$
$$M^{\boldsymbol{\beta}_1}_{j,t} = w_{j,t},$$
$$M^{\boldsymbol{\beta}_2}_{j,t} = c^{\mathrm{h}}_t - \min_{i \in \mathcal{I}, d \in \mathcal{D}} \{c^{\mathrm{t}}_{i,j,d} - c^{\mathrm{u}}_t\},$$
$$M^{\boldsymbol{\iota}_1}_{i,j,d,t} = P_r,$$
$$M^{\boldsymbol{\iota}_2}_{i,j,r,d,t} = c^{\mathrm{t}}_{i,j,d} + \max_{t \in \mathcal{T}} \{c^{\mathrm{u}}_t + c^{\mathrm{h}}_t - c^{\mathrm{t}}_{i,j,d}\} - \min_{j \in \mathcal{J}, d \in \mathcal{D}} \{c^{\mathrm{t}}_{i,j,d} - c^{\mathrm{h}}_t\} - \min_{i \in \mathcal{I}, d \in \mathcal{D}} \{c^{\mathrm{t}}_{i,j,d} - c^{\mathrm{u}}_t\}$$

Proof. Proof. We derive tight bounds on the big-M parameters, $M^{\alpha_\ell}_{i,j,r,d}$, $M^{\theta_\ell}_{i,t}$, $M^{\beta_\ell}_{j,t}$, and $M^{\iota_\ell}_{i,j,r,d}$ for all $i \in \mathcal{I}$, $j \in \mathcal{J}$, $r \in \mathcal{R}$, and $d \in \mathcal{D}_r$.

- For constraint (B.16a) to hold for all feasible values of $\mu_{i,j,r,d}$, parameter $M^{\boldsymbol{\alpha}_1}_{i,j,r,d}$ should be greater than or equal to the maximum possible value of variable $\mu_{i,j,r,d}$. Note that the value of the objective function (B.7a) decreases as the value of $\boldsymbol{\mu}$ increases. Given that (B.7) is a maximization problem, the variable $\boldsymbol{\mu}$ will attain its lower bound in any optimal solution to problem (B.7). Specifically, by constraints (B.7d)–(B.7e), we have $\mu_{i,j,r,d} = \max\{(c^{\mathrm{u}}_t + c^{\mathrm{h}}_t - c^{\mathrm{t}}_{i,j,d}), 0\}$. Since we assume that $\max_{i\in\mathcal{I},j\in\mathcal{J},d\in\mathcal{D}}\{c^{\mathrm{t}}_{i,j,d}\} < c^{\mathrm{h}}_t < c^{\mathrm{u}}_t$, we have $\mu_{i,j,r,d} = c^{\mathrm{u}}_t + c^{\mathrm{h}}_t - c^{\mathrm{t}}_{i,j,d}$. It follows that the following is a valid value for $M^{\boldsymbol{\alpha}_1}_{i,j,r,d}$:

$$M^{\boldsymbol{\alpha}_1}_{i,j,r,d} = \max_{t\in\mathcal{T}} \left\{c^{\mathrm{u}}_t + c^{\mathrm{h}}_t - c^{\mathrm{t}}_{i,j,d}\right\}, \quad \forall i \in \mathcal{I},\, j \in \mathcal{J},\, d \in \mathcal{D}.$$

- For constraints (B.16b) to hold, parameter $M^{\boldsymbol{\alpha}_2}_{i,j,r,d}$ should be greater than or equal to the maximum possible value of $P_r a_d(x_{i,j,d} + v_{i,j,d}) - \sum_{t\in\mathcal{T}} n_{i,j,d,t}$. Since $\sum_{t\in\mathcal{T}} n_{i,j,d,t} \geq 0$ for each $i \in \mathcal{I}, j \in \mathcal{J}$, and $d \in \mathcal{D}$, we can set $\boldsymbol{M}^{\boldsymbol{\alpha}_2}$ as

$$M^{\boldsymbol{\alpha}_2}_{i,j,r,d} = P_r, \quad \forall i \in \mathcal{I},\, j \in \mathcal{J},\, r \in \mathcal{R},\, d \in \mathcal{D}_r.$$

- For constraints (B.16c) to hold for all feasible values of $u_{i,t}$, parameter $M^{\boldsymbol{\theta}_1}_{i,t}$ should be greater than or equal to the maximum possible value of variable $u_{i,t}$. In any optimal solution, the value of unsatisfied demand $u_{i,t}$ is less than or equal to $q_{i,t}$. Thus, by the third constraints in (5), we have

$$M^{\boldsymbol{\theta}_1}_{i,t} = \bar{q}_{i,t} + \sum_j \tilde{q}_{i,j,t}, \quad \forall i \in \mathcal{I},\, t \in \mathcal{T}.$$

- For constraints (B.16d) to hold, parameter $M^{\boldsymbol{\theta}_2}_{i,t}$ should be greater than or equal to the maximum value of $(c^{\mathrm{u}}_t - \lambda_{i,t})$. From Proposition 4, we have $\lambda_{i,t} \geq \min_{j\in\mathcal{J},d\in\mathcal{D}}\{c^{\mathrm{t}}_{i,j,d} - c^{\mathrm{h}}_t\}$ for all $i \in \mathcal{I}, t \in \mathcal{T}$. It follows that we can set $M^{\boldsymbol{\theta}_2}_{i,t}$ as

$$M^{\boldsymbol{\theta}_2}_{i,t} = c^{\mathrm{u}}_t - \min_{j\in\mathcal{J},d\in\mathcal{D}}\{c^{\mathrm{t}}_{i,j,d} - c^{\mathrm{h}}_t\}, \quad \forall i \in \mathcal{I},\, t \in \mathcal{T}.$$

- For constraints (B.16e) to hold, parameter $\boldsymbol{M}^{\boldsymbol{\beta}_1}$ should be greater than or equal to the maximum possible value of variable $h_{j,t}$. For every $j \in \mathcal{J}$ and $t \in \mathcal{T}$, the value of holding inventory $h_{j,t}$ is always upper bounded by the amount of prepositioned relief items $w_{j,t}$. Thus, we can set $\boldsymbol{M}^{\boldsymbol{\beta}_1}$ as

$$M^{\boldsymbol{\beta}_1}_{j,t} = w_{j,t}, \quad \forall j \in \mathcal{J},\, t \in \mathcal{T}.$$

- For constraints (B.16f) to hold, parameter $\boldsymbol{M}^{\boldsymbol{\beta}_2}$ should be greater than or equal to the maximum possible value of $c^{\mathrm{h}}_t - \pi_{j,t}$. From Proposition 4, we have $\pi_{j,t} \geq \min_{i\in\mathcal{I},d\in\mathcal{D}}\{c^{\mathrm{t}}_{i,j,d} - c^{\mathrm{u}}_t\}$ for all

$j \in \mathcal{J}$ and $t \in \mathcal{T}$. Therefore, we can set $\boldsymbol{M}^{\boldsymbol{\beta}_2}$ as

$$M^{\boldsymbol{\beta}_2}_{j,t} = c^{\mathrm{h}}_t - \min_{i\in\mathcal{I},d\in\mathcal{D}}\{c^{\mathrm{t}}_{i,j,d} - c^{\mathrm{u}}_t\}, \quad \forall j \in \mathcal{J},\, t \in \mathcal{T}.$$

- For constraints (B.16g) to hold, parameter $\boldsymbol{M}^{\iota_1}$ should be greater than or equal to the maximum possible value of variable $n_{i,j,d,t}$. Similar to the parameter $\boldsymbol{M}^{\boldsymbol{\alpha}_2}$, since value of $n_{i,j,d,t}$ is always upper bounded by the value of P_r for every $i \in \mathcal{I}, j \in \mathcal{J}$, $r \in \mathcal{R}, d \in \mathcal{D}_r, t \in \mathcal{T}$, we can set $\boldsymbol{M}^{\iota_1}$ as

$$M^{\iota_1}_{i,j,d,t} = P_r, \quad \forall i \in \mathcal{I},\, j \in \mathcal{J},\, r \in \mathcal{R},\, d \in \mathcal{D}_r,\, t \in \mathcal{T}.$$

- For constraints (B.16g) to hold, parameter $\boldsymbol{M}^{\iota_1}$ should be greater than or equal to the maximum possible value of variable $c^{\mathrm{t}}_{i,j,d} - \lambda_{i,t} - \pi_{j,t} + \mu_{i,j,r,d}$. For every $i \in \mathcal{I}$, $j \in \mathcal{J}$, $r \in \mathcal{R}$, $d \in \mathcal{D}_r$, and $t \in \mathcal{T}$, with the lower-bound values on $\lambda_{i,t}$ and $\pi_{j,t}$, and the upper-bound values on $\mu_{i,j,r,d}$, we can set the value of $\boldsymbol{M}^{\boldsymbol{\beta}_2}$ as

$$M^{\boldsymbol{\beta}_2}_{i,j,r,d,t} = c^{\mathrm{t}}_{i,j,d} + \max_{t\in\mathcal{T}}\left\{c^{\mathrm{u}}_t + c^{\mathrm{h}}_t - c^{\mathrm{t}}_{i,j,d}\right\} - \min_{j\in\mathcal{J},d\in\mathcal{D}}\{c^{\mathrm{t}}_{i,j,d} - c^{\mathrm{h}}_t\} - \min_{i\in\mathcal{I},d\in\mathcal{D}}\{c^{\mathrm{t}}_{i,j,d} - c^{\mathrm{u}}_t\},$$

  for every $i \in \mathcal{I}$, $j \in \mathcal{J}$, $r \in \mathcal{R}$, $d \in \mathcal{D}_r$ and $t \in \mathcal{T}$.

This completes the proof. □